ISSN 1023-9855

Thoracic Medicine

Volume 37 • Number 3 • September 2022

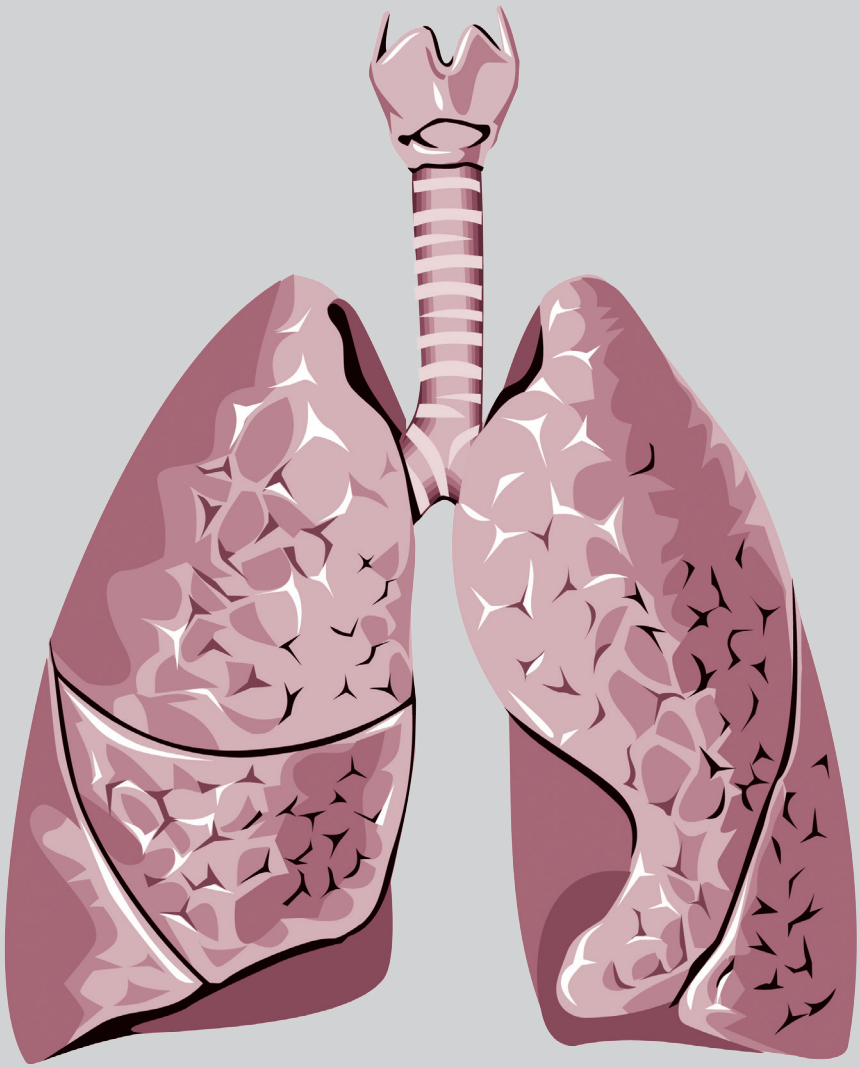

The Official Journal of

Taiwan Society of Pulmonary and Critical Care Medicine

Taiwan Society of Sleep Medicine

Taiwan Society for Respiratory Therapy

Taiwan Society of Tuberculosis and Lung Diseases

Thoracic Medicine

The Official Journal of
Taiwan Society of Pulmonary and Critical Care Medicine
Taiwan Society for Respiratory Therapy
Taiwan Society of Sleep Medicine
Taiwan Society of Tuberculosis and Lung Diseases

Publisher

Hao-Chien Wang, M.D., Ph.D., President
Taiwan Society of Pulmonary and Critical Care Medicine

Chia-Chen Chu, Ph.D., RRT, FAARC President
Taiwan Society for Respiratory Therapy

Yi-Wen Huang, M.D., President
Taiwan Society of Tuberculosis and Lung Diseases

Hsueh-Yu Li, M.D., President
Taiwan Society of Sleep Medicine

Editor-in-Chief

Kang-Yun Lee, M.D., Ph.D., Professor
Taipei Medical University-Shuang Ho Hospital, Taiwan

Deputy Editors-in-Chief

Shang-Gin Wu, M.D., Ph.D.
National Taiwan University Hospital, Taiwan

Editorial Board

Section of Pulmonary and Critical Care Medicine

Jin-Yuan Shih, M.D., Professor
National Taiwan University Hospital, Taiwan

Gee-Chen Chang, M.D., Professor
Chung Shan Medical University Hospital, Taiwan

Chung-Chi Huang, M.D., Professor
Linkou Chang Gung Memorial Hospital, Taiwan

Kuang-Yao Yang, M.D., Ph.D., Professor
Taipei Veterans General Hospital, Taiwan

Chi-Li Chung, M.D., Ph.D., Associate Professor
Taipei Medical University Hospital, Taiwan

Section of Respiratory Therapy

Hue-Ling Lin, Ph.D. RRT, RN, FAARC, Associate Professor
Chang Gung University, Taiwan

I- Chun Chuang, Ph.D., Assistant Professor
Kaohsiung Medical University College of Medicine, Taiwan

Jia-Jhen Lu, Ph.D., Professor
Fu Jen Catholic University, Taiwan

Shih-Hsing Yang, Ph.D., Associate Professor
Fu Jen Catholic University, Taiwan

Chin-Jung Liu, Ph.D., Associate Professor
China Medical University, Taiwan

Section of Tuberculosis and Lung Diseases

Jann-Yuan Wang, M.D., Professor
National Taiwan University Hospital, Taiwan

Chen-Yuan Chiang, M.D., Associate Professor
Taipei Municipal Wanfang Hospital, Taiwan

Ming-Chi Yu, M.D., Professor
Taipei Municipal Wanfang Hospital, Taiwan

Yi-Wen Huang, M.D., Professor
Changhua Hospital, Ministry of Health & Welfare, Taiwan

Wei-Juin Su, M.D., Professor
Taipei Veterans General Hospital, Taiwan

Section of Sleep Medicine

Li- Ang Lee, M.D., Associate Professor
Linkou Chang Gung Memorial Hospital, Taiwan

Pei-Lin Lee, M.D., Assistant Professor
National Taiwan University Hospital, Taiwan

Hsin-Chien Lee, M.D., Associate Professor
Taipei Medical University-Shuang-Ho Hospital, Taiwan

Kun-Ta Chou, M.D., Associate Professor
Taipei Veterans General Hospital, Taiwan

Li-Pang Chuang, M.D., Assistant Professor
Linkou Chang Gung Memorial Hospital, Taiwan

International Editorial Board

Charles L. Daley, M.D., Professor
National Jewish Health Center, Colorado, USA

Chi-Chiu Leung, MBBS, FFPH, FCCP, Professor
Stanley Ho Centre for Emerging Infectious Diseases, Hong Kong, China

Daniel D. Rowley, MSc, RRT-ACCS, RRT-NPS, RPFT, FAARC
University of Virginia Medical Center, Charlottesville, Virginia, U.S.A.

Fang Han, M.D., Professor
Peking University People's Hospital Beijing, China

Huiqing Ge, Ph.D.
Sir Run Run Shaw Hospital, School of Medicine, Zhejiang University Hangzhou, China

J. Brady Scott, Ph.D., RRT-ACCS, AE-C, FAARC, FCCP, Associate Professor
Rush University, Chicago, Illinois, USA

Kazuhiro Ito, Ph.D., DVM, Honorary Professor
Imperial College London, UK

Kazuo Chin (HWA BOO JIN), M.D., Professor
Graduate School of Medicine, Kyoto University

Masaki Nakane, M.D., Ph.D., Professor
Yamagata University Hospital, Japan

Naricha Chirakalwasan, M.D., FAASM, FAPSR, Associate Professor
Faculty of Medicine, Chulalongkorn University, Thailand

Petros C. Karakousis, M.D., Professor
The Johns Hopkins University School of Medicine, USA

Thoracic Medicine

The Official Journal of
Taiwan Society of Pulmonary and Critical Care Medicine
Taiwan Society for Respiratory Therapy
Taiwan Society of Sleep Medicine
Taiwan Society of Tuberculosis and Lung Diseases

Volume 37
Number 3
September 2022

CONTENTS

Clinician and Pharmacist Participation in a Multidisciplinary Team-Care Model to Improve the Rate of Correct Inhaler Usage and Medication Adherence in COPD Patients

Pei-Chia Mai[1], Chia-Chen Huang[1], Ho-Shen Lee[1], Yu-Feng Wei[3,4], Jung-Yueh Chen[1,2]

Introduction: Inhaler therapy is a cornerstone of treatment for patients with chronic obstructive pulmonary disease (COPD), and symptomatic patients always need long-term inhaler usage. However, poor therapeutic adherence and poor inhaler usage techniques are challenges to treatment efficacy. The participation of a clinician and a pharmacist in COPD management has been discussed in recent years. Some previous studies have provided evidence that such models could have positive effects on medication adherence and correct inhaler usage.

Methods: This was a single-center study conducted in southern Taiwan. The COPD care service was provided by a multidisciplinary team, including a clinician, a pharmacist and a case manager as the core members. Patients with COPD (group B, C or D) were enrolled into the intervention group (clinician and pharmacist care service model) or the control group (standard care). We evaluated the patients' inhaler use technique and medication adherence by assessing the percentage of inhalation steps performed correctly and using the Morisky Medication Adherence Scale (MMAS-8), respectively, at both baseline and 12 months after study enrollment.

Results: A total of 692 patients with stable COPD were recruited for our study; 118 patients (17%) were enrolled into the intervention group and 574 patients (83%) into the standard care group. The intervention group showed significant improvement in their inhaler technique total score compared with the standard care group (92.7±10.4 vs 88.5±13.4, P<0.01). Medication adherence was also improved in the intervention group (percentage of high adherence patients increased from 22 (18.6%) to 26 (22%)). However, there was no significant improvement in the rate of correct inhaler usage after a 12-month interval in both groups.

Conclusion: The multidisciplinary team-care model, with clinician and pharmacist participation, may result in improvement in inhaler usage and medication adherence in patients with COPD. In the intervention group, there was similar correct inhaler usage with all of the different devices. ***(Thorac Med 2022; 37: 154-165)***

Key words: Chronic obstructive pulmonary disease; multidisciplinary team-care model; inhaler technique; inhaler adherence

Introduction

Chronic obstructive pulmonary disease (COPD), a systemic inflammatory disease that presents with chronic airway obstruction, is the 4th leading cause of death worldwide [1]. In Taiwan, the trend line of COPD-associated death is decreasing, but it remains the 8th leading cause of death [2]. It has not only been a major global public health problem but also carries a high economic burden for all countries.

Inhaler therapy is a cornerstone of treatment for patients with COPD [3]. Compared with systemic therapy, inhaler therapy has advantages such as rapid onset of action, higher local concentrations in the lung tissue, and a lower rate of adverse events [3]. Inhaler therapy is not only for symptom control, it also reduces the risk of complications, prevents exacerbations, improves quality of life, and slows disease progression [4-5].

However, adherence to inhaler therapy by patients with COPD is a real challenge in clinical practice [6]. Many previous studies have reported associations between low adherence to inhaler therapy and poor patient outcomes (mortality, hospitalization rate), and an increased economic impact (higher healthcare costs) [7]. Only 40–60% of patients with COPD adhere to the prescribed regimen and only 1 out of every 10 patients with a metered dose inhaler performs all essential steps correctly [8-9].

Pharmacists play a critical role in educating COPD patients on appropriate inhaler use and ensuring correct medication adherence [10]. A previous meta-analysis revealed that pharmacist-led interventions had a positive effect on medication adherence and inhaler technique among COPD patients [11].

Therefore, the aim of this study was to evaluate whether a multidisciplinary team-care model, with clinician and pharmacist cooperation, improved inhaler usage and medication adherence among COPD patients, compared with standard care.

Methods

Patient eligibility and recruitment

A total of 881 subjects with stable COPD were recruited from E-Da Hospital (Kaohsiung City, Taiwan) between January 1, 2019 and December 31, 2020. All recruited patients were from the outpatient department or general ward. Pulmonary medicine specialists assessed and confirmed the diagnosis of COPD, based on the clinical symptoms and pulmonary function test criteria of a post-bronchodilator ratio of forced expiratory volume in 1 second to forced vital capacity (FEV_1/FVC) lower than 0.70.

These clinically diagnosed COPD patients were enrolled in the study if they fulfilled the following inclusion criteria: (1) age ≥40 years, and (2) COPD classification in group B, C, or D. The classification of COPD was based on the Global Initiative for Chronic Obstructive Lung

[1]Department of Internal Medicine, E-Da Hospital, Kaohsiung, Taiwan, [2]College of Medicine, I-Shou University, Kaohsiung, Taiwan, [3]Department of Internal Medicine, E-Da Cancer Hospital, Kaohsiung, Taiwan, [4]School of Medicine for International Students, College of Medicine, and Institute of Biotechnology and Chemical Engineering, I-Shou University, Kaohsiung, Taiwan, [5]Department of Pharmacy, E-Da Hospital, Kaohsiung, Taiwan.
Address reprint requests to: Dr. Jung-Yueh Chen, Department of Internal Medicine, E-Da Hospital, No. 1, E-Da road, Kaohsiung 824, Taiwan

Disease (GOLD) 2021 guidelines [1]. A total of 110 patients did not meet the above inclusion criteria and were excluded from the study. An additional 79 patients were excluded from the study for the following reasons: (1) unable to use inhalers independently, (2) long-term bedridden status, and (3) impaired cognitive function. Following an explanation by the pulmonary medicine specialists, 118 patients accepted the multidisciplinary team-care model, while the remaining 574 patients chose to receive standard care (Figure 1).

Multidisciplinary team-care model

The core members of the multidisciplinary team-care model included the pulmonary medicine specialist, the COPD case manager and the pharmacist. Other team-care members included dietitians, nurses, respiratory therapists, physical therapists, and clinical psychologists, all of whom actively participated in the team operation as required. This 1-year service consisted of a face-to-face meeting every 3 months for 9 months after the patient was enrolled (at baseline, and at 3 and 6 months post-baseline) and 1 annual assessment (at 12 months post-baseline).

The initial action was led by the pulmonary medicine specialist, the pharmacist and the COPD case manager at the first meeting (baseline). The pharmacist assessed the patient's inhaler device technique and medication adherence, and reviewed current medication usage

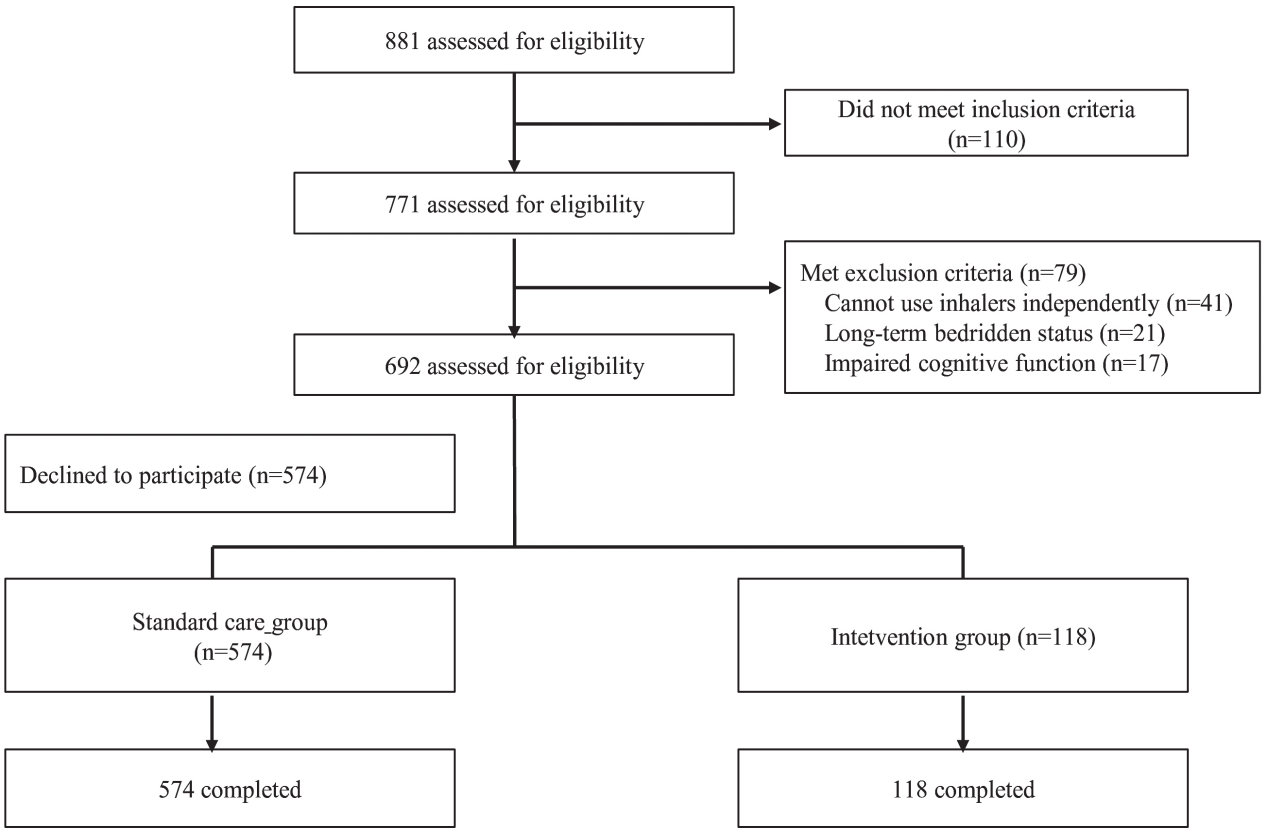

Fig. 1. Flow chart for COPD patients multidisciplinary care model enrollment

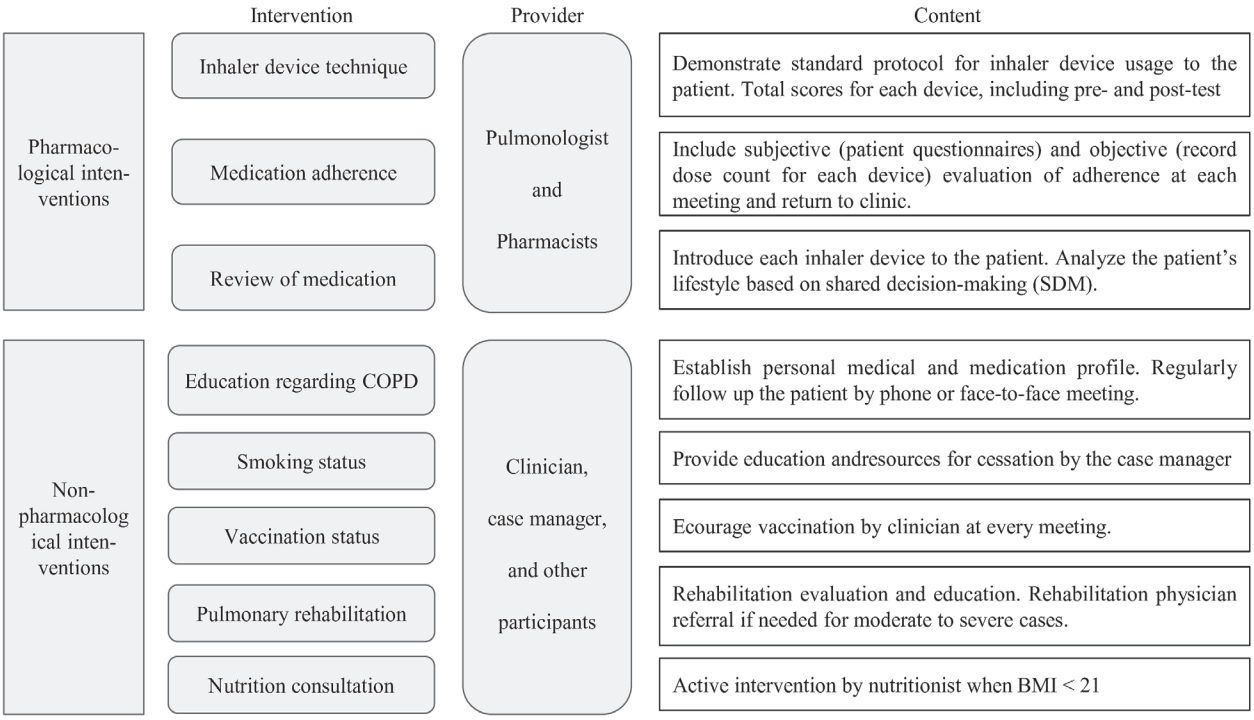

Fig. 2. COPD multidisciplinary team-care model.

based on individual pharmacological needs. COPD case managers recorded the patient's demographic characteristics, including smoking status, vaccination status, pulmonary rehabilitation attendance, and medical and medication profile (pulmonary function test, chest radiography and laboratory tests). Other non-pharmacologic interventions, including smoking cessation, nutritional consultation, and pulmonary and physical rehabilitation, were also evaluated and performed by other team members (Figure 2).

Education on inhaler device usage for COPD patients was different in the 2 groups. In the standard care group, a pharmacists' referral was only required for patients newly diagnosed with COPD or for those changing inhaler medications as directed by their pulmonary medicine specialist. Such referrals occurred periodically and without regular monitoring of the patient's condition. In the intervention group, patient education was provided by the new multidisciplinary team. Pharmacists were highly involved in this service model and cooperated with the other team members. The pharmacists actively analyzed and demonstrated the advantages and disadvantages of each available inhaler device to the COPD patients. Patient decision aids were then used to help the patient choose an appropriate inhaler device via shared decision-making. The results of this education were fed back through computerized communication systems. To improve the patient's medication adherence, instruction manuals (including important disease information, common questions and answers, public resources, and social and psychological support) were provided. The pharmacists also aggressively followed up the

patients' inhaler technique and adherence during each regular pulmonary outpatient department visit.

Measurements

Assessments of the patients' demographic characteristics, including age, gender, body mass index (BMI), smoking status, comorbidities (including cardiovascular diseases, lung cancer, gastroesophageal reflux [GERD], osteoporosis, and depression/anxiety – the most common comorbidities of COPD [1]), blood eosinophil count, inhaler usage number, and inhaler medications and devices, were conducted. Disease severity, including COPD grouping, and pulmonary function tests as measured by spirometry (including FVC predicted and FEV_1% predicted) were also measured and recorded. Scores on the COPD Assessment Test (CAT) and Modified Medical Research Council (mMRC) dyspnea scale self-assessment questionnaires were used to assess the symptom severity of COPD [1]. The CAT score was established using 8 different items, including cough, sputum amount of phlegm, chest tightness, shortness of breath, limited activities at home, confidence leaving home, sleep quality, and personal vitality. Each item had a score ranging from 0 to 5, with the total score ranging from 0 to 40 [1]. Higher total CAT scores correlated with more severe COPD symptoms. The mMRC consisted of grades 0 to 4 (5 grades). Higher mMRC grades indicated more severe dyspnea.

Medication adherence was evaluated using the Morisky Medication Adherence Scale (MMAS-8) in the multidisciplinary team-care model group. MMAS-8 is one of the most widely used tools for assessing medication adherence in patients with COPD [12]. It is an 8-item self-report questionnaire, where each item describes a reason for low adherence. The total score ranges from 0 to 8. Higher total scores reflect higher medication adherence. MMAS-8 total scores of 8 indicate high adherence, 7 or 6 means medium adherence, and scores lower than 6 indicate low adherence.

Four types of inhalers were used in this study, including the Breezhaler®, Ellipta®, Evohaler® and Respimat®. Each inhaler device has its own standard number of steps which should be completed (Breezhaler® and Ellipta®: 8 steps, Evohaler®: 9 steps, Respimat®: 11 steps). The patients' inhalation technique was evaluated for their respective inhaler.

In the intervention group, the pharmacist showed the patient the correct step-by-step inhalation technique, based on the standard protocol for their inhaler, in their first meeting (baseline). Patients then needed to demonstrate the inhalation technique for their devices. The pharmacist scored the percentage of total correct steps using a checklist. After 12 months of follow-up (end of study), the pharmacist again scored the percentage of total correct steps.

For study consistency, experienced pharmacists were necessary. The pharmacists participating in this study needed to have more than 2 years of clinical work experience, or, they needed to complete inhaler therapy education and other conscientious face-to-face training courses offered by COPD experts. To minimize the impact of subjective bias, only 2 pharmacists were recruited based on their years of clinical practice experience.

Based on previous studies [13] [14] [15], we assumed that 50% of recruited COPD patients used inhaler devices correctly and that the intervention would enhance this to at least 80%. So, using a significance level of 0.05, a power

of 90%, and assuming a 20% dropout rate, at least 25 patients were required to participate in the study.

Statistical analysis

All data were recorded on and analyzed using Statistical Product and Service Solutions (SPSS, version 28). Nominal or ordinal variables were presented as numbers (N) and percentages (%). Continuous variables were presented as the mean ± standard deviation (SD). Before statistical analysis, the data were tested for normality. A chi-squared test or Fisher's exact test was used for comparisons of categorical variables. A t-test or analysis of variance (ANOVA) was used for continuous variables with a normal distribution, and a Mann–Whitney U-test or Kruskal–Wallis test was used for continuous variables without a normal distribution. Regression analysis was adopted to determine factors that affected the correct inhaler use rate and medication adherence. All tests were 2-tailed, and a p-value <0.05 was considered to indicate a significant difference.

Results

A total of 692 patients with stable COPD were enrolled in the current study. After completing prescreening, 118 patients (17%) were enrolled into the multidisciplinary team-care (intervention) group. A total of 574 patients (83%) were enrolled into the standard care group because they declined to participate in the team-care project. Table 1 details the baseline characteristics of the enrolled COPD patients. Most patients were elderly males. The mean age of the study population was 74.6±7.9 years in the standard care group and 75.2±7.1 years in the intervention group. The mean BMI was 23.2 kg/m^2 in the standard care group and 21.9 kg/m^2 in the intervention group. Most of the participants in this study were moderate COPD cases, with a mean FEV_1 of 61.8% in the standard care group and 62.5% in the intervention group. Most cases were in COPD group B or group C, and most were current smokers (75.8% in the standard care group; 68.6% in the intervention group). As for baseline characteristics, there was no significant difference between the 2 groups.

The most-used devices were Ellipta® (32.8%) and Evohaler® (31.2%). The least-used device was Breezhaler® (5.9%). Most patients used 2 inhalers (57.3%) (average: 1.62±0.53). The most common inhaler medication combinations were inhaled corticosteroids (ICS) + long-acting beta-agonists (LABA) (32.4%), and LABA + long-acting muscarinic antagonist (LAMA) (31.9%).

The number of operation steps in the checklist and the rate of correct inhaler usage for different devices are shown in Table 2. Respimat® had the greatest number of operation steps compared with other devices. The lowest rate of correct usage for a device was with Evohaler® in the standard care group (85.7%). The highest rate of correct usage for a device was with Breezhaler® in the intervention group (94.6%). The most common patient "critical error" steps among all inhaler devices were (1) insufficient complete exhalation before use of the inhaler and (2) an inability to hold their breath for 5 to 10 seconds after use of the inhaler.

Table 3 shows a comparison of the overall rate of correct inhaler usage between the standard care and intervention groups. The intervention group had a significantly higher rate of correct inhaler usage than the standard group (92.7% vs. 88.5%, p<0.001).

Table 1. Baseline Characteristics of the Enrolled COPD Patients

	Standard care group (n=574)	**Intervention group (n=118)**	***P value***
Age (years), mean (SD)	74.6 (7.9)	75.2 (7.1)	0.439
Gender, N (%)			0.455
Male	545 (94.9)	114 (96.6)	
Female	29 (5.1)	4 (3.4)	
Mean BMI (kg/m2), mean (SD)	23.2 (9.1)	21.9 (3.9)	0.114
BMI < 21, N (%)	232 (40)	49 (41.9)	
BMI ≥ 21, N (%)	342 (60)	68 (58.1)	
mMRC, N (%)			0.439
0-1	141 (24.6)	31 (26.3)	
2-4	433 (45.4)	87 (73.7)	
Lung function testing, mean (SD)			
FVC% predicted (%)	80.4	79.5	0.532
FEV_1% predicted (%)	61.8	62.5	0.200
ABCD group, N (%)			0.824
B	310 (54.0)	63 (53.4)	
C	229 (39.9)	46 (38.9)	
D	35 (6.1)	9 (7.7)	
Smoking status, N (%)			0.229
Current smoker	435 (75.8)	81 (68.6)	
Ever-smoker	61 (10.6)	18 (22.2)	
Never-smoker	78 (13.6)	19 (23.5)	
Comorbidities, N (%)	450 (78.4%)	99 (83.4%)	0.179
Blood eosinophil count (cells/μL)			0.680
< 300	374 (65.3)	80 (69.6)	
≥ 300	35 (6.1)	6 (5.2)	
no data	164 (28.6)	30 (25.4)	
Inhaler numbers, N (%)			0.946
1	235 (40.9)	46 (39.0)	
2	325 (56.7)	71 (60.2)	
≥ 3	14 (2.4)	1 (0.8)	
Inhaler medication, N (%)			0.070
LABA	94 (16.4)	13 (11.0)	
LAMA	94 (16.4)	23 (19.5)	
LABA+LAMA	173 (30.1)	48 (40.7)	
ICS+LABA	195 (34.0)	29 (24.6)	
ICS+LABA+LAMA	18 (3.1)	5 (4.2)	
Inhaler device, N (%)			0.111
Breezhaler®	30 (5.3)	7 (5.9)	
Ellipta®	190 (33.1)	37 (31.4)	
Evohaler®	193 (33.6)	23 (19.5)	
Respimat®	161 (28.0)	51 (43.2)	

Acronyms: BMI: body mass index; COPD: chronic obstructive pulmonary disease; mMRC: Modified Medical Research Council Dyspnea scale; FEV_1: forced expiratory volume in 1 second; FVC: forced vital capacity; LABA: long-acting beta-agonists; LAMA: long-acting muscarinic antagonist; ICS: inhaled corticosteroid.

Table 2. Mean Correct Rate for Different Inhaler Devices after 12 Months of Follow-up

Inhaler device	Device type	Operating Steps	Standard care groupe		Intervention group	
			n (%)	Mean (%)	n (%)	Mean (%)
Breezhaler®	DPI	8	30 (5.3%)	92.5	7 (5.9%)	94.6
Ellipta®	DPI	8	190 (33.1%)	90.5	37 (31.4%)	92.3
Evohaler®	MDI	9	193 (33.6%)	85.7	23 (19.5%)	92.3
Respimat®	SMI	11	161 (28.0%)	88.1	51 (43.2%)	93.0

Acronyms: DPI: dry powder inhaler; MDI: metered dose inhaler; SMI: soft mist inhaler

Table 3. Comparison of Overall Correct Inhaler Usage Rates (mean (%)) Between the Standard Care and Intervention Groups

	Standard care group	Intervention group	*P value*
n	574	118	
Mean (%)	88.5	92.7	<0.001
SD	13.4	10.4	
Minimum	25	60	
Maximum	100	100	

Table 4. Improvement in the Inhaler Usage Rate (mean (%)) from Baseline to end of Study (12 months) Between the Standard Care and Intervention Groups

Group	Baseline			End of study (12 months)			
	mean	SD	Coefficient of Variation (%)	mean	SD	Coefficient of Variation (%)	*P value*
Intervention group	91.4%	11.4	12.5	93.0%	11.5	12.4	0.538
Standard care group	88.9%	12.8	14.4	89.7%	12.7	14.2	0.720

Improvement in the rate of correct inhaler usage was determined by comparing baseline and end-of-study (12 months) findings among both the standard care and intervention groups. Even though the trend line of correct usage improved in both groups, there was no statistically significant increase in the rate of correct inhaler usage in either group (p=0.720 in the standard care group; p=0.538 in the intervention group) (Table 4).

Medication adherence was improved in the intervention group. The number of patients with high adherence (MMAS-8 score = 8) increased from 22 (18.6%) to 26 (22%) (Table 5). Paired t-test analysis revealed that the MMAS score increased significantly after intervention (p=0.045, <0.05). However, there was no meaningful improvement in the low adherence group (baseline MMAS-8 score <6). The most common reasons for low adherence included: symptoms seemed

Table 5. Morisky Medication Adherence Scale (MMAS-8) Scores in the Intervention Group

	Before intervention (n=118) (%)	**After intervention (n=118) (%)**	***P value***
High adherence (score 8) n (%)	22 (18.6)	26 (22.0)	0.045*
Medium adherence (score 7 or 6) n (%)	88 (74.6)	84 (71.2)	
Low adherence (score <6) n (%)	8 (6.8)	8 (6.8)	

* $P< 0.05$

to improve, so the patient stopped taking medication by themselves, and the patients forgot to take their medications.

Finally, the correlation between the overall rate of correct inhaler usage and all categorical variables is shown in Supplementary Table 1. No patient demographic characteristics (including age, gender, BMI, smoking status or comorbidities) influenced the overall rate of correct inhaler usage. Even though the overall rate was lower in the older patient group (age ≥65 years) than in the younger patient group (age <65 years) (mean 89.6% vs 90.34%), there was no significant difference. Disease characteristics (including CAT severity, mMRC severity, and COPD group), number of inhalers used and inhaler device types were not factors that influenced the overall rate of correct usage of inhalers.

Discussion

This study assessed the effectiveness of a multidisciplinary team-care model, including clinician and pharmacist participation, for patients with COPD. The results of this study showed that clinician and pharmacist participation significantly improved COPD patients' inhaler technique and medication adherence.

The intervention group showed a significant improvement in the overall rate of correct inhaler usage compared with the standard care group. However, the rate of correct usage for different inhaler devices in previous studies had great variability. One study in Australia found that the mean proportion of "correctly demonstrated steps" across different inhalers ranged between 55% and 97% [15]. This variability may be related to the small sample in the study (35 patients using 58 inhalers). Our data revealed that the correct usage rate for Evohaler® was relatively low in the standard care group (85.7%), but the correct usage rate for all devices in the intervention group was >90%. The better and similar rates of correct usage between different devices in the intervention group revealed that the multidisciplinary team-care model provided better efficacy, regardless of the inhaler devices used.

Previous studies indicated that the number of inhalers used may decrease medication adherence in COPD patients [16]. A previous retrospective study showed that users of multiple inhalers had a significantly higher discontinuation rate than single-inhaler users [17]. In our study, most patients used either 2 inhalers (57.3%) or 1 inhaler (40.5%). Patients who used more than 3 inhalers were rare (2.2%). Number of inhalers used was not shown to have a negative influence on medication adherence in our study.

In this study, independent variables includ-

ing age, BMI, CAT score, mMRC score, FEV_1, FVC, FEV_1/FVC, eosinophil count, and device number were shown to have no influence on COPD patients' rate of correct inhaler usage or medication adherence. Previous literature found that age was associated with COPD treatment adherence, especially among older patients (age ≥60 years) [5, 19]. In our study, the overall average patient age was 74.7±7.9 years. Although the average age was older in the intervention group (75.2±7.1 years) than in the standard care group (74.6±7.9 years), the intervention group (92.7±10.4%) still had a better rate of correct usage for inhaler devices than the standard care group (88.5±13.4%). The negative influence of old age on COPD medication adherence was not observed in our study. This result suggests that good education and guidance among elderly patients can provide a similar correct usage rate.

Medication adherence improved significantly in the intervention group, as did the MMAS score after intervention (p=0.045, <0.05). However, such benefits were not seen in the low adherence patient group (MMAS-8 score <6). How to increase the motivation of patients to improve inhaler adherence in this group is an important issue that requires further investigation.

Adherence to inhaled medication use in the real world varies, and there are currently no standardized instruments for its evaluation. Many studies use the Test of Adherence to Inhalers (TAI) questionnaire to assess adherence. A systematic review analyzed 25 articles representing 29 countries (27,660 COPD patients) and found that 46.3% of patients had a moderately good level of adherence to inhaled therapy [16]. However, a high level of adherence at baseline was noted in this study. In the intervention group, 93.2% of patients had an MMAS-8 score ≥6 before the intervention. This may also explain the "ceiling effect" phenomenon seen in the results of the rate of correct inhaler usage. The high baseline for the rate of correct inhaler usage (91.4% in the standard care group; 88.9% in the intervention group) may have limited the level of improvement that can be seen at the end of the study (93% in the standard care group; 89.7% in the intervention group).

In our study, no correlation was observed between the overall rate of correct inhaler usage and patients' demographic characteristics. Disease severity, the type of inhaler device and the number of inhalers, and non-pharmacological intervention attendance also did not influence the overall rate of correct inhaler usage. No matter the type of patient, health care providers always need to help patients understand the care setting and to influence the patients' behaviors, attitudes and skills needed to consistently improve their health.

The current study has several limitations. First, the 2 comparison groups were not randomized. Even if the baseline characteristics were similar, selection bias was possible. Due to the limitation of the geographical location, the patients' living area may have influenced their willingness to participate in the study. People who live a longer distance from the hospital may have reduced motivation to enroll in the intervention group due to the higher number of visits required. The main participants in this study were primarily from the region surrounding the E-Da Hospital, including north Kaohsiung City and North Pingtung County. Their population characteristics may be different from those of other communities. In addition, the duration of this study was only 12 months. Some indicators, such as the duration of smok-

ing cessation and keeping good medication adherence, may need longer before they can be fully observed. Our study focused on inhaled medications for COPD patients. However, some COPD patients still need oral medications for disease control. The role of, and association between oral and inhaled medications still needs exploration in future studies.

Pharmacist participation has been proven to be effective for inhaler adherence and technique in numerous studies, however, the management and definition of adherence and technique varies between different studies. Different countries and reimbursement systems also affect ongoing management by clinicians and pharmacists.

Conclusion

The use of a multidisciplinary team-care model, involving clinicians and pharmacists, may result in improved inhaler technique and medication adherence in patients with COPD. In the intervention group, there was similar correct inhaler usage across all different devices. However, there was non-significant improvement in the rate of correct inhaler usage after a 12-month interval in both the standard care and intervention group, which may be due to a ceiling effect. Further randomized controlled trials are needed to prove the applicability of the multidisciplinary team-care model in Taiwan.

References

1. 2021 GOLD REPORTS -- Global strategy for the diagnosis, management and prevention of chronic obstructive pulmonary disease. https://goldcopd.org/gold-reports.
2. Cause of Death Statistics - 2020. Ministry of Health and Welfare website, Taiwan (Republic of China). https://www.mohw.gov.tw/cp-5017-61533-1.html
3. Amin AN, Ganapathy V, Roughley A, *et al*. Confidence in correct inhaler technique and its association with treatment adherence and health status among US patients with chronic obstructive pulmonary disease. Patient Prefer Adherence 2017; 11: 1205-1212.
4. Chen W, FitzGerald JM, Sin DD, *et al*. Excess economic burden of comorbidities in COPD: a 15-year population-based study. Eur Respir J 2017; 50(1).
5. Kleinhenz ME, Lewis CY. Chronic ventilator dependence in elderly patients. Clin Geriatr Med 2000; 16(4): 735-56.
6. López-Campos JL, Gallego EQ, Hernández LC. Status of and strategies for improving adherence to COPD treatment. Int J Chron Obstruct Pulmon Dis 2019; 14: 1503-1515.
7. Bogart M, Stanford RH, Laliberte F, *et al*. Medication adherence and persistence in chronic obstructive pulmonary disease patients receiving triple therapy in a USA commercially insured population. Int J Chron Obstruct Pulmon Dis 2019; 14: 343-352.
8. Restrepo RD, Alvarez MT, Wittnebel LD, *et al*. Medication adherence issues in patients treated for COPD. Int J Chron Obstruct Pulmon Dis 2008; 3(3): 371-384.
9. Price D, Keininger DL, Viswanad B, *et al*., Factors associated with appropriate inhaler use in patients with COPD - lessons from the REAL survey. Int J Chron Obstruct Pulmon Dis 2018; 13: 695-702.
10. US Department of Health & Human Services. COPD national action plan. 2020.
11. Jia X, Zhou S, Luo D, *et al*. Effect of pharmacist-led interventions on medication adherence and inhalation technique in adult patients with asthma or COPD: A systematic review and meta-analysis. J Clin Pharm Ther 2020; 45(5): 904-917.
12. Morisky DE, Ang A, Krousel-Wood M, *et al*. Predictive validity of a medication adherence measure in an outpatient setting. J Clin Hypertens (Greenwich) 2008; 10(5): 348-54.
13. Wong LY, Chua SS, Husin AR. A pharmacy management service for adults with asthma: a cluster randomised controlled trial. Fam Pract 2017; 34(5): 564-573.
14. Normansell R, Kew KM, Mathioudakis AG. Interventions

to improve inhaler technique for people with asthma. Cochrane Database Syst Rev 2017; 3: CD012286.

15. Fathima M, Bawa Z, Mitchell B, *et al*. COPD management in community pharmacy results in improved inhaler use, immunization rate, COPD action plan ownership, COPD knowledge, and reductions in exacerbation rates. Int J Chron Obstruct Pulmon Dis 2021; 16: 519-533.
16. Świątoniowska N, Chabowski M, Polański J, *et al*. Adherence to therapy in chronic obstructive pulmonary disease: a systematic review. Adv Exp Med Biol 2020; 1271: 37-47.
17. Yu AP, Guerin A, Ponce de Leon D. Therapy persistence and adherence in patients with chronic obstructive pulmonary disease: multiple versus single long-acting maintenance inhalers. J Med Econ 2011; 14(4): 486-96.

Effect of ALK Fusion Variants on ALK Inhibitor Treatment in Patients with Non-small Cell Lung Cancer: A Systematic Review and Meta-analysis

Hsin-Pei Chung[1,2], Yu-Chu Ella Chung[3], Ying-Chih Cheng[4,5]

Background: Echinoderm microtubule-associated protein-like 4 (*EML*)-anaplastic lymphoma kinase (*ALK*) rearrangement variants have been shown to influence the treatment outcomes of tyrosine kinase inhibitors (*TKI*). However, due to small sample sizes and differences in methodology between previous studies, the results are still inconclusive. Therefore, the aim of this study was to investigate the association between *EML4-ALK* fusion variants and *ALK* inhibitor treatment outcomes using a meta-analysis approach.

Methods: We systematically searched 5 electronic databases, including PubMed, the Cochrane Library, Embase, Medline, and ClinicalTrials.gov, for clinical trial publications. *EML4-ALK* fusion variants were categorized into 2 subtypes: (1) *ALK* variant 1 carriers and non-variant 1 carriers; and (2) long form and short form. Clinical efficacy outcomes including objective response rate (ORR), disease control rate (DCR) and progression-free survival (PFS) were analyzed. A random-effects model was applied to aggregate risk ratios. Sensitivity and funnel plot analyses were also conducted to clarify possible bias in the meta-analysis process.

Results: No significant results were observed in the association between variants and ORR. There was no significant difference in DCR, except for a trend toward the long form group. However, there was a significant improvement in PFS in the *ALK* variant 1 carriers and in the long form group. Overall, no obvious bias was derived from a single study or publication process.

Conclusion: The current study suggests that *EML4-ALK* variants affect PFS with *ALK* inhibitor treatment. Future *TKI* therapeutic strategies with a focus on personalized medicine should be developed. ***(Thorac Med 2022; 37: 166-179)***

Key words: EML4-ALK variant 1, EML4-ALK non-variant 1, long form variant, short form variant, ALK TKI, ALK-positive NSCLC

[1]Division of Pulmonary and Critical Care Medicine, MacKay Memorial Hospital, Taipei, Taiwan, [2]Department of Medicine, MacKay Medical College, New Taipei City, Taiwan, [3]Center for Neuropsychiatric Research, National Health Research Institutes, Miaoli, Taiwan, [4]Department of Psychiatry, China Medical University Hsinchu Hospital, China Medical University, Hsinchu, Taiwan, [5]Department of Public Health and Institute of Epidemiology and Preventive Medicine, College of Public Health, National Taiwan University, Taipei, Taiwan.
Address reprint requests to: Dr. Ying-Chih Cheng, Department of Psychiatry, China Medical University Hsinchu Hospital, China Medical University, No.199, Sec. 1, Singlong Rd., Jhubei City, Hsinchu County 302056, Taiwan

Introduction

Lung cancer is the most prevalent and fatal cancer worldwide [1]. Approximately 1.8 million people were diagnosed with lung cancer and 3.4 million died of the disease globally in 2018 [2]. Non-small cell lung cancer (NSCLC) and small cell lung cancer (SCLC) are the 2 dominant types of lung cancer, of which NSCLC is more common (80-85% of cases). The overall 5-year survival rate of patients with stage IV NSCLC is around 5% [3]. Tyrosine kinase inhibitor (TKI) therapy has been developed in the recent decades, and has been shown to be a more efficient treatment for NSCLC.

ALK is one of the most important driver mutations, accounting for 3-5% of all NSCLC patients [4]. It was first reported in anaplastic large cell lymphomas [5]. Soda *et al*. later reported genetic rearrangements with the echinoderm microtubule-associated protein-like 4 (EML4) fusion gene as a driver mutation in NSCLC [6]. To date, over 20 *ALK* fusions have been identified, and *EML4-ALK* fusions continue to be the dominant type (80%). Most *EML4-ALK* variants contain the entire intracellular kinase domain of *ALK*, encoded by exons 20 through 29. The breakpoint lies in the amount of tandem atypical β-propeller (TAPE) domain in EML4. Variant 1 (E13:A20) and variant 2 (E20:A20) have various lengths of TAPE domain, while variant 3a/b (E6: A20) and variant 5a (E2:A20) express no TAPE domain. Therefore, *EML4–ALK* variants are further classified into 2 subtypes: short form (variant 3a/b and 5a/b), and long form (variant 1 and variant 2) [3].

Patients with stage IV *ALK*-positive NSCLC have prolonged overall survival (OS); previous studies have suggested a 5-year survival rate ranging from 36% [7] to 60% [8]. *EML-ALK* variants may influence the response to ALK inhibitors. However, the results of previous studies have been highly heterogeneous. Most studies have included patients treated with ALK inhibitors. For example, Yoshida *et al* [9] examined 35 *ALK*-positive patients treated with the first-generation ALK inhibitor, crizotinib, and suggested a significantly longer progression-free survival (PFS) in patients with variant 1 compared to those with non-variant 1. In addition, Woo *et al* [10] reported that in 54 patients who received crizotinib, ceritinib or alectinib (second-generation *ALK* inhibitors), variant 1/variant 2 carriers had a longer PFS, although there was no significant difference in OS. Several other studies have reported no significant difference in treatment response between patients with variant 1 and non-variant 1, and between those with long form and short form variants [11-15]. To date, the results of previous studies remain inconclusive.

The inconclusive results with regard to the effect of *EML-ALK* variants on the outcomes of TKI therapy are mainly due to differences between studies, including different categories of variant subtypes, the type of *ALK* inhibitor used, and the endpoint of treatment response. The technique used to detect the variants and the small sample sizes are also factors. However, no prior study has comprehensively aggregated the existing evidence. The aim of this study was to conduct a meta-analysis to summarize previous studies and clarify the relationship between *EML4-ALK* variants and TKI treatment response.

Methods

Data sources and literature searches

This systematic review and meta-analysis

was conducted according to the Preferred Reporting Items for Systematic Reviews and Meta-Analyses (PRISMA) statement guidelines [16]. We systematically conducted an electronic search of PubMed, the Cochrane Library, Embase, Medline, and ClinicalTrials.gov from the earliest available date to February 2019. The literature search was conducted by 2 researchers (Y, C. C. and H, P. C.), and employed the following sets of key terms: ("*non-small cell lung cancer*" OR "*lung cancer*" OR "*NSCLC*") AND ("*ALK variants*" OR "*ALK fusion variants*" OR "*anaplastic lymphoma kinase*") AND ("*ALK inhibitors*" OR "*crizotinib*" OR "*alectinib*" OR "*ceritinib*" OR "*brigatinib*" OR "*loratinib*" OR "*ensartinib*" OR "*entrectinib*" OR "*belizatinib (TSR-011)* OR "*ASP3026*"). These terms were used to search keywords, text, titles, and subject headings, as appropriate for each database. The full articles for titles meeting the inclusion criteria were retrieved and reviewed. Additional eligible studies were sought by searching the reference lists of the primary articles and relevant reviews.

Inclusion and exclusion criteria

Eligibility criteria for the current review were: 1) randomized controlled trials, case-control studies, or cohort studies focusing on the association between *EML4-ALK* variants and response to *ALK* inhibitor treatment; 2) articles written in English; 3) patients diagnosed with NSCLC; and 4) articles reporting the carrier status of *ALK* variants. Patients were classified as being ALK variant 1 carriers if they had 1 or more copies of the variant 1 allele, and as ALK non-variant 1 carriers if they had no copies of the variant 1 allele. They were further categorized into short and long form variant groups according to the classification mentioned above. The following types of studies were excluded: republished data, those with incomplete inclusion criteria data, other meta-analyses, reviews, letters and editorial articles.

Data extraction and quality assessment (PRISMA)

Two investigators (Y, C. C. and H, P. C.) independently extracted relevant information from the included studies and evaluated the methodological quality of the eligible trials using the Newcastle-Ottawa Quality Assessment Scale (NOS) [17]. The following information was collected from the selected articles: last name of the authors, date of publication, study design, region and population, study characteristics (e.g., age, sex), types of ALK inhibitors, number of participants, duration of follow-up and assessment of treatment effectiveness. The NOS is a freely available 8-item scale with a version for assessing the quality of non-randomized studies in meta-analyses. This scale evaluates the domains of selection, comparability and outcome or exposure. One star is allocated when a quality feature is present, up to a maximum of 9 stars (the comparability domain can be scored up to 2 stars); studies awarded 7 or more stars are considered to be high-quality studies. Disagreements between the 2 investigators were resolved through discussion.

Efficacy outcomes

The primary efficacy outcome was objective response rate (ORR), which was calculated as the total percentage of patients with a complete response or partial response. Other secondary efficacy outcomes included: (1) disease control rate (DCR), defined as the total percentage of patients with a complete response, partial response, or stable disease; and (2) PFS, defined as the length of time from medication

until RECIST 1.1 progressive disease. The best tumor response was evaluated with computed-tomography (CT) assessment using RECIST 1.1.

Data synthesis and statistical analysis

Data were pooled statistically using event rates calculated for the primary endpoint. Dichotomous analyses were conducted using risk ratios (RRs). Continuous data were analyzed using standardized mean difference (SMD), which accounted for the varied and non-standardized outcomes across studies. Possible sources of heterogeneity or inconsistencies in the magnitude or direction of effects in trials were investigated. Heterogeneity was assessed using the I^2 test [18]. A random-effects model was used to estimate methodological variation between studies. Leave-1-study-out sensitivity analysis was performed by excluding 1 trial at a time and examining whether the pooled effects remained robust. Due to the presence of heterogeneity, we conducted subgroup analyses to assess the source of heterogeneity based on suspected variables. Publication bias was examined using a funnel plot of effect size against the standard error for asymmetry. Egger's regression test was also used to assess publication bias [19]. All meta-analytic computations were performed using R software (with meta package version 3.5.1).

Results

Baseline characteristics of the included studies

Of the 1725 original studies screened, 14 met the inclusion criteria. A summary of the included studies and their results are presented in Table 1. Most of the studies (13 out of 14) focused on crizotinib treatment. All studies isolated variant 1 from other variants, and 8 of the 14 studies detected *ALK* fusions using a sequencing technique. Eleven of the 14 studies with detailed data were extracted for quantitative synthesis. The NOS scores of the included studies ranged from 6 to 8. The treatment duration ranged from 3 to 24 months. Figure 1

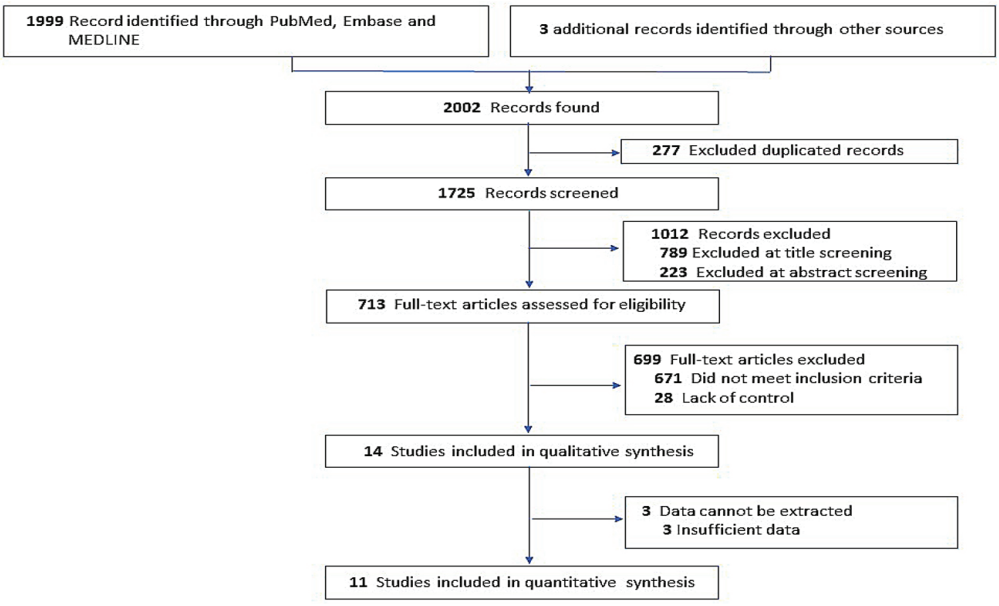

Fig. 1. PRISMA Flow Chart of the Current Meta-analysis

Table 1. Summary of the Included Studies

Study	Country	Study design	Detection of ALK fusion	ALK TKI or chemotherapy	Treatment line	Time range	Follow-up	Patient, n	Age (SD or range)	Reported outcomes	Adenocarcinoma %	Male, n (%)	Major finding	NOS
Yoshida *et al.* 2016	Japan	Retrospective cohort	RT-PCR	Crizotinib	Mixed	2007-2014	NR	Total n = 35 v1 = 19 Non-v1 = 16	57 (36-80) 57 (31-80) 52 (26-78)	ORR, DCR, PFS	100%	13 (37%) 6 (32%) 7 (44%)	Longer PFS and higher DCR in v1	7
Lei *et al.* 2016	China	Retrospective cohort	RACE-coupled PCR, sequencing	Crizotinib	Mixed	2008-2015	NR	Total n = 61 v1 = 22 v3 = 18 Other = 21	48 (23-76) 47 (23-73) 54 (32-76) 51 (36-74)	ORR, DCR, PFS	96.7%	29 (47.5%) 12 (54.5%) 7 (38.9%) 10 (47.6%)	No difference in ORR, DCR, PFS among v1, v3 and other	8
Cha *et al.* 2016	South Korea	Retrospective cohort	PNA mediated qPCR assay	Pemetrexed chemotherapy	Mixed	2000-2015	43.4 months	Total n = 35 v1 = 17 v2 = 1 v3 = 6 Non-EML4 = 11	52 (31–76)	ORR, DCR, PFS*	100%	23 (44.2%)	Longer PFS in variant 1, Longer PFS in EML4-ALK fusion variants than non-EML4	8
				Crizotinib	Mixed	2000-2015	43.4 months	Total n = 32 v1 = 17 v2 = 1 v3 = 6 Non-EML4 = 11	NR	ORR, DCR, PFS	NR	NR	No difference in ORR, DCR, PFS according to ALK fusion variant of pts with Crizotinib or Ceritinib	
				Ceritinib	Mixed	2000-2015	43.4 months	Total n = 14 v1 = 5 v2 = 1 v3a = 3 non-EM4 = 5	NR	ORR, DCR, PFS	NR	NR		
				Alectinib	100% ≥ 2nd line	2000-2015	43.4 months	Total n = 2 v1 = 0 v2 = 0 v3 = 1 non-EML4 = 1	NR	ORR, DCR	NR	NR		
Noh *et al.* 2017	South Korea	Retrospective cohort	RT-PCR	Crizotinib	Mixed	2001-2014	42.5 months	Total n = 42 v1 = 24 v3 = 18	NR 51 (32–68) 50 (38–74)	ORR, DCR, PFS	100%	NR 9 (37.5%) 9 (50%)	No difference in ORR, OS among long and short form with crizotinib; short form had trend of shorter PFS	7
				Crizotinib	Mixed	2001-2014	42.5 months	Total n = 46 Long form = 28 Short form = 18	51 (29–74) 52 (29–68) 50 (38–74)	ORR, DCR, PFS, OS*	100%	19 (41.3%) 10 (35.7%) 9 (50%)		
Woo *et al.* 2017	South Korea	Retrospective cohort	RT-PCR	Crizotinib	Mixed	2011-2015	NR 15 (1 - 53) 9.5 (1 - 49)	Total n = 54 v1/v 2/other = 24 v3 = 20	54 (27 - 78) NR NR	ORR, DCR, PFS*, OS*	52 (96.3%)	26 (48.1%)	Longer PFS in v1/2/others than in v3; a tendency for greater ORR and DCR; but no difference in OS	6
				Crizotinib, ceritinib, alectinib,	Mixed		NR 15 (1 - 53) 9.5 (1 - 49)	Total n = 51 v1/v2/other = 27 v3 = 24	NR 53 (27 - 68) 58 (37 - 77)	ORR, DCR, PFS*, OS*	NR 26 (96.3%) 23 (95.8%)	NR 13 (48.1%) 12 (50.0%)		

Study	Country	Study design	Detection of ALK fusion	ALK TKI or chemotherapy	Treatment line	Time range	Follow-up	Patient, n	Age (SD or range)	Reported outcomes	Adenocarcinoma %	Male, n (%)	Major finding	NOS
McLeer-Florin, *et al*. 2018	France	Retrospective cohort	RT-PCR, RNA-seq	Crizotinib	Mixed	2012-2015	NR	Total n = 14 v1/v2 = 6 v3 = 8	NR 49 (23-86) 59 (33-75)	ORR, DCR, PFS	NR	 2 (33.3%) 3 (37.5%)	Numerically longer PFS in v1/2 than v3	8
Lin *et al*. 2018	USA	Retrospective cohort	NGS, Sanger sequencing, RT-PCR	Crizotinib	Mixed	2008-2017	NR	Total n = 106 v1 = 51 v3 = 55	NR 55 (22-78) 51 (31-76)	OS	53 (96%) 50 (98%)	 30 (55%) 26 (51%)	No difference in OS & PFS with crizotinib or 2nd generation TKI among v1 and v3, but longer PFS in v3 than with lorlatinib	7
				Crizotinib	1st TKI			Total n = 99 v1 = 51 v3 = 48	NR	PFS	NR	NR		
				Crizotinib	1st line			Total n = 55 v1 = 27 v3 = 28	NR	PFS	NR	NR		
				Ceritinib, alectinib, brigatinib	2nd TKI ‡			Total n = 77 v1 = 37 v3 = 40	NR	PFS	NR	NR		
				Lorlatinib	3rd TKI §			Total n = 29 v1 = 12 v3 = 17	NR	PFS	NR	NR		
Li *et al*. 2018	China	Retrospective cohort	NGS	Crizotinib	Mixed	2011-2016	≥ 6 mons	Total n = 49 v1 = 14 v2 = 9 v3 = 20 Other = 6	48 (24–82) 45.5 (30-82) 44 (36-60) 52.5 (34-82) 53 (24-68)	ORR, DCR, PFS	48 (98%) 14 (100%) 9 (100%) 19 (95.5%) 6 (100%)	21 (42.9%) 7 (50%) 4 (44.5%) 6 (30.0%) 4 (66.7%)	No difference in PFS among v3 and non-v3, but a trend of a shorter duration of response in v3 with crizotinib	6
Lv *et al*. 2018	China	Retrospective cohort	NGS	Crizotinib	Mixed	2013-2016	NR	Total n = 31 v1/2 = 15 Other = 16	NR 45.0 (30.077.0) 54.0 (27.0–73.0)	ORR, DCR, PFS	20 (64.5%)	27 (87.1%)	No difference in PFS among v1, v3 and other uncommon variants	8
								Total n=31 v1 = 13 v2 = 2 v3 = 8 Other = 8	NR	PFS	NR	NR		

Study	Country	Study design	Detection of ALK fusion	ALK TKI or chemotherapy	Treatment line	Time range	Follow-up	Patient, n	Age (SD or range)	Reported outcomes	Adenocarcinoma %	Male, n (%)	Major finding	NOS
Mitiushkina *et al*. 2018	Russia	Retrospective cohort	RT-PCR	Crizotinib	1st line	2012-2017	NR	Total n = 22 Long form = 18 Short form = 4	NR 51 (25-76) 54 (34-78)	ORR, PFS*, OS*	NR 42 (97.7%) 16 (94.1%)	NR 17 (39.5%) 7 (41.2%)	No difference in ORR, PFS, OS among ALK fusion variants with crizotinib or ceritinib	8
				Ceritinib	1st line			Total n = 36 Long form = 24 Short form = 12		ORR, PFS*, OS*				
				Crizotinib	1st line			Total n = 23 v1 = 12 Non-v1 = 11	NR 51 (25-76) 53 (34-78)	ORR, PFS*, OS*	NR 32 (97%) 28 (90.3%)	NR 11 (33.3%) 14 (45.2%)		
				Ceritinib	1st line			Total n = 39 v1 = 20 Non-v1 = 19		ORR, PFS*, OS*				
Christopoulos *et al*. 2019	Germany	Retrospective cohort	RT-PCR	Crizotinib, ceritinib, alectinib, brigatinib	1st line	NR	29 mon (15-81)	Total n = 38 v1/2 = 19 v3 = 19	 59 (47-72) 59 (43-75)	PFS, OS	100%	NR 27 (54%) 18 (43.9%)	Longer PFS with 1st line TKI in v1/v2 than in v3	8
Su *et al*. 2019	China	Retrospective cohort	NGS	Crizotinib	Mixed	2014-2017	14.8 mon	Total n = 96 v1/v2/Other = 54 v3/v5 = 42	NR 50 (29-74) 51 (33-80)	PFS, OS	NR 47 (87%) 34 (81%)	NR 28 (51.9%) 16 (38.1%)	Longer PFS and OS in v1/2/other than in v3/v5	7
Horn *et al*. 2019	USA	Prospective cohort	NGS	Ensartinib	Mixed	2017	NR	Total n = 39 v1 = 17 v2 = 7 v3 = 7 v5 = 6 Other = 2	NR	ORR, DCR, PFS	NR	NR	Better ORR and PFS in v1 than in v3 with ensartinib	6
								Total n = 39 Long form = 26 Short form = 13		ORR, DCR				
Lin *et al*. 2019	Taiwan	Retrospective cohort	RT-PCR	Crizotinib	1st-13th line, median 3rd line	2010-2017	13.8 mon (IQR, 7.4–25.4)	Total n = 54 v1 = 23 v2 = 6 v3 = 18 Other = 7	NR 56 (47–62) 50 (45–57) 62 (55–65) 56 (46–61)	ORR, DCR, PFS, OS	NR	NR 13 (57%) 2 (33%) 12 (67%) 5 (71%)	No difference in ORR, PFS, OS among different variants	6
								Total n = 54 Long form = 33 Short form = 21	NR	PFS, OS	NR	NR		

RT-PCR, reverse transcription-polymerase chain reaction, RNA-seq, RNA sequencing; PNA, peptide nucleic acid; RACE, Rapid amplification of cDNA ends; NGS, Next Generation Sequencing; NOS, Newcastle-Ottawa Scale; ORR, objective response rate; DCR, disease control rate; PFS, progression-free survival; TKI, tyrosine kinase inhibitor; NR, not reported.

* Not disclosed in numbers, only Kaplan–Meier curves were available.

+ after crizotinib

╪ after crizotinib and at least 1 second-generation TKI

Table 2. Meta-analysis Results for All Studies

	Study No	Patients / Control	Effect size	Effect sizes (95%CI)	Effect size *p* value	Heterogeneity I^2 (%)
ORR						
Variant 1 vs Non-variant 1	10	166/174	RR	0.99 (0.88; 1.11)	0.80	27.5%
Subgroup by Crizotinib	7	124/160	RR	0.95 (0.84; 1.08)	0.46	0%
Long form vs Short form	10	191/124	RR	0.99 (0.89; 1.10)	0.82	0%
Subgroup by Crizotinib	6	117/78	RR	0.96 (0.83; 1.09)	0.53	0%
DCR						
Variant 1 vs Non-variant 1	7	120/153	RR	1.03 (0.95; 1.11)	0.52	0.0%
Subgroup by Crizotinib	6	116/149	RR	1.03 (0.94; 1.13)	0.53	0.0%
Long form vs Short form	7	131/100	RR	1.07 (0.99; 1.15)	0.08	0.0%
Subgroup by Crizotinib	5	99/74	RR	1.04 (0.96; 1.14)	0.30	0.0%
PFS						
Variant 1 vs Non-variant 1	6	158/158	SMD	0.24 (0.01; 0.46)	0.04	0.0%
Subgroup by Crizotinib	5	139/139	SMD	0.20 (-0.04; 0.44)	0.10	0.0%
Long vs Short	5	135/134	SMD	0.32 (0.07; 0.56)	0.01	0.0%
Subgroup by Crizotinib	4	116/115	SMD	0.29 (0.03; 0.55)	0.03	0.0%

DCR, disease control rate; ORR, objective response rate; PFS, progression-free survival, RR, risk ratios, SMD, standardized mean difference.

summarizes the review flowchart in accordance with the PRISMA statement [20].

ORR with ALK inhibitors

Binary data assessing the association between ALK variant 1 carrier status and ORR with ALK inhibitors were available in 10 studies. There was no significant difference in ORR between ALK variant 1 carriers and non-variant 1 carriers (RR = 0.99, 95% CI [0.88; 1.11], p = 0.80, I^2 = 28%) (Table 2) (Figure 2a), and also no significant difference in subgroup analysis of crizotinib (RR = 0.95, 95% CI [0.84; 1.08], p = 0.45, I^2 = 0%). Ten studies assessed the association between long/short form variants and treatment effect, but no significant difference was found (RR = 0.99, 95% CI [0.89; 1.10], p = 0.82, I^2 = 0%) (Figure 2b). There was also no significant difference in the subgroup analysis of crizotinib (RR = 0.96, 95% CI [0.84; 1.10], p = 0.53, I^2 = 0%).

DCR with ALK inhibitors

Seven studies assessed the association between ALK variant 1 carriers and DCR with ALK inhibitors. There was no significant difference in DCR between ALK variant 1 carriers and non-variant 1 carriers (RR = 1.03, 95% CI [0.95; 1.11], p = 0.52, I^2 = 0%) (Table 2) (Figure 3a). There was also no significant difference in the subgroup analysis of patients treated with crizotinib (RR = 1.03, 95% CI [0.94; 1.13], p = 0.53, I^2 = 0%).

Seven studies assessed the association between long/short form variants and DCR. A

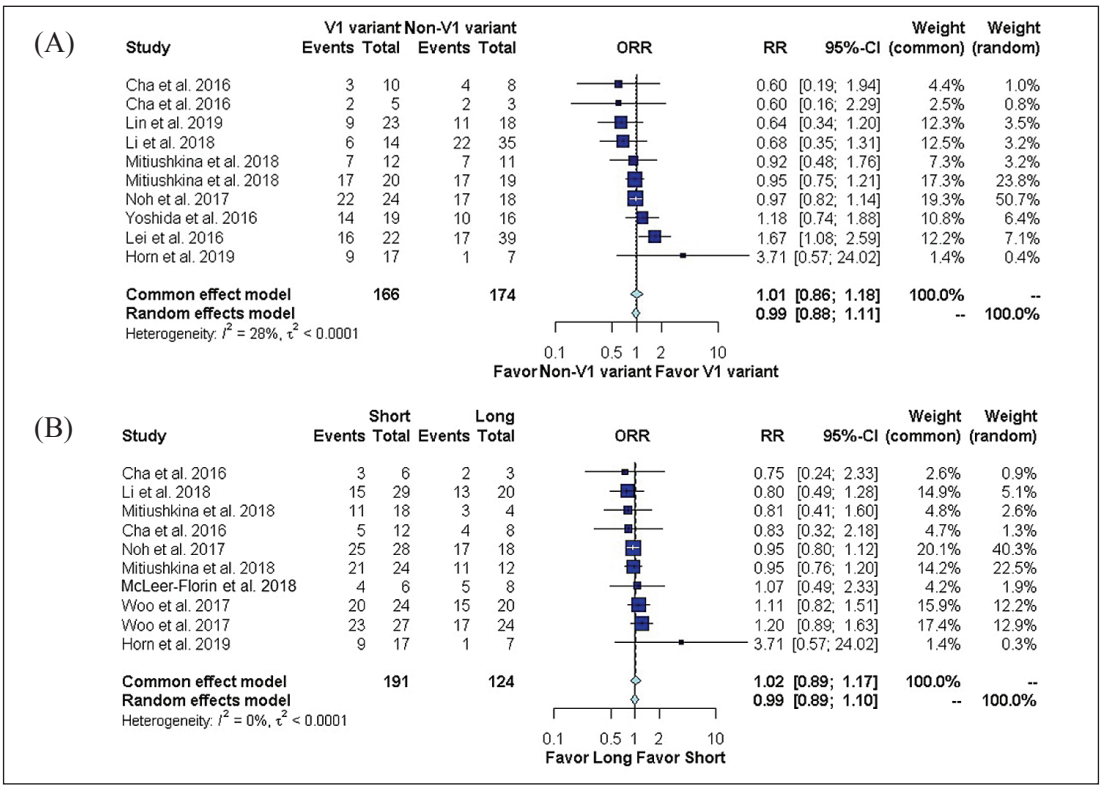

Fig. 2. Objective Response Rate, (a)Comparison between variant 1 and non-variant 1 carriers; (b)Comparison between long form and short form carriers.

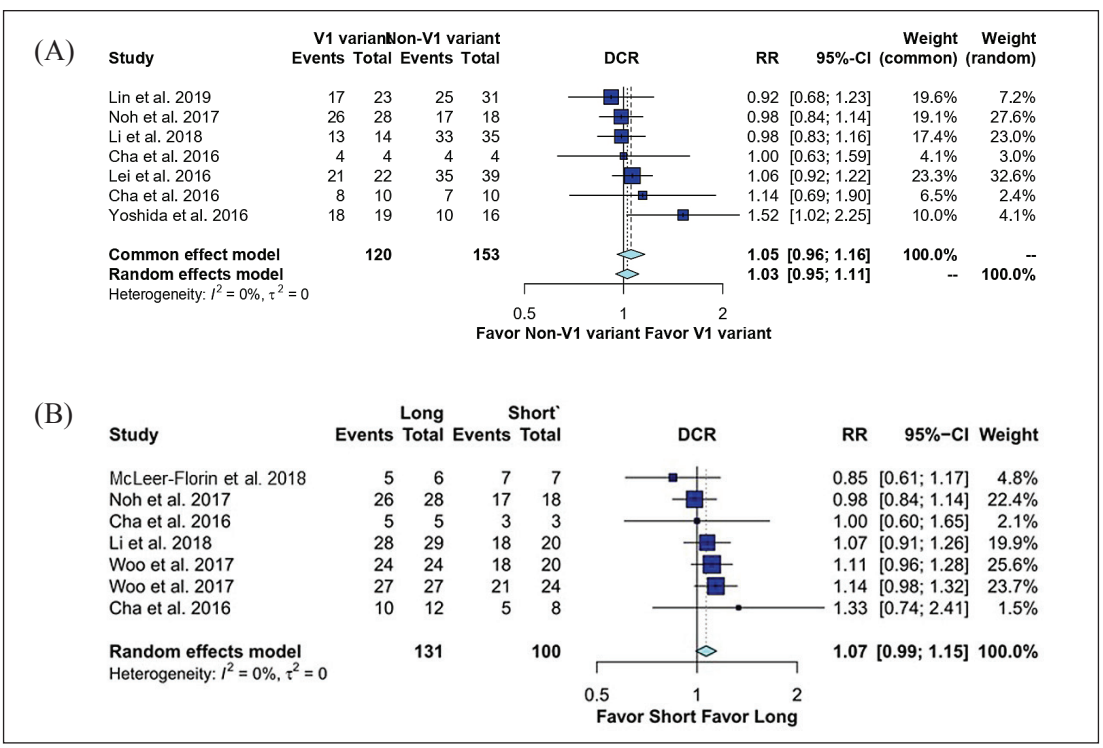

Fig. 3. Disease Control Rate, (a)Comparison between variant 1 and non-variant 1 carriers; (b)Comparison between long form and short form carriers.

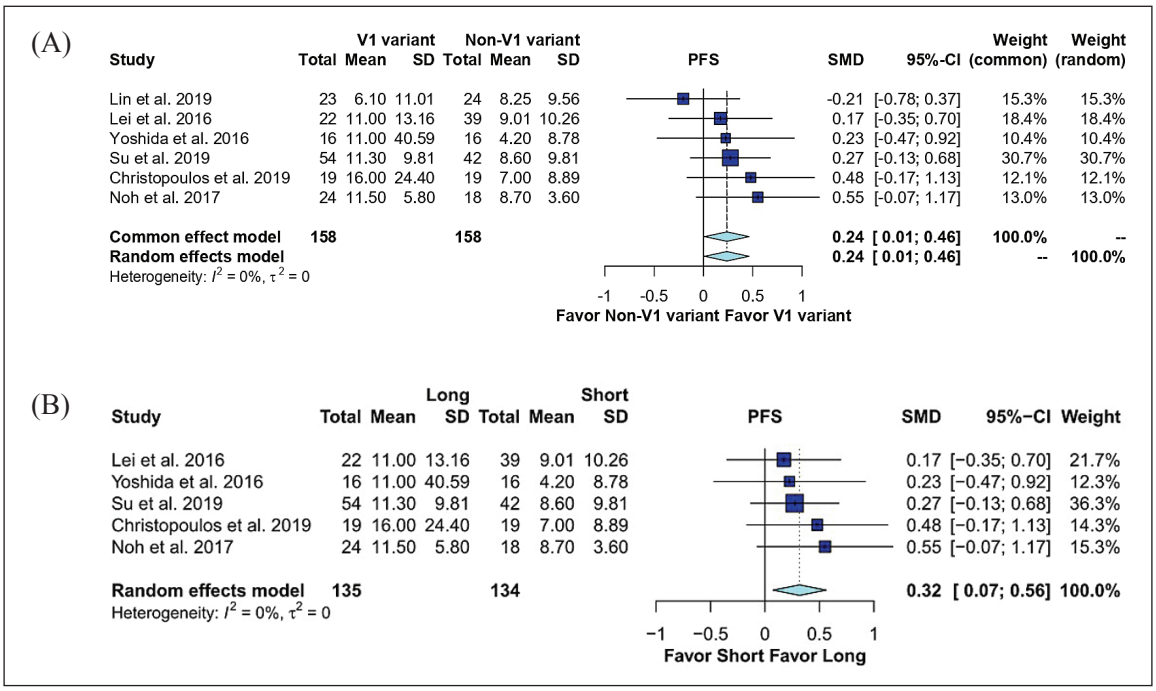

Fig. 4. Progression-free Survival, (a)Comparison between variant 1 and non-variant 1 carriers; (b)Comparison between long form and short form.

trend was found between long/short form variants and DCR (RR = 1.07, 95% CI [0.99; 1.15], $p = 0.08$, $I^2 = 0\%$) (Figure 3b); however, when focusing solely on crizotinib treatment, the results were not significant (RR = 1.04, 95% CI [(0.96; 1.14], $p = 0.30$, $I^2 = 0\%$).

PFS with ALK inhibitors

Six studies assessed the association between *ALK* variant 1 carrier status and PFS with ALK inhibitors. The results showed a significant improvement in PFS in the *ALK* variant 1 carriers (standardized mean difference = 0.24, 95% CI [0.01; 0.46], $p = 0.04$, $I^2 = 0\%$) (Table 2) (Figure 4a). However, in the subgroup analysis of crizotinib treatment, the results were not significant (SMD = 0.20, 95% CI [-0.04; 0.44], $p = 0.10$, $I^2 = 0\%$).

Five studies assessed the association between long/short form variants and PFS. The results showed an improvement in PFS in the long form carriers (SMD = 0.32, 95% CI [0.07; 0.56], $p = 0.01$, $I^2 = 0\%$) (Figure 4b). Moreover, in the crizotinib subgroup analysis, the results remained significant (SMD = 0.29, 95% CI [0.03; 0.55], $p = 0.03$, $I^2 = 0\%$).

Sensitivity analysis

We conducted leave-1-out sensitivity analysis for every random-effect model. The results are presented in Table 3. Overall, sensitivity analysis revealed no major influence of a single article on the overall effect in ORR. A trend observed in DCR reached significance if the studies by Noh KW, *et al* [13] and McLeer-Florin A, *et al* [21] were omitted. When focusing on PFS in variant 1 carriers and long/short form carriers, omitting the studies by Noh KW, *et al* [13] and Su Y, *et al* [22] resulted in non-significant results.

Table 3. Sensitivity Analyses for the Meta-analysis using a Leave-1-out Approach

Outcomes	Number of studies	Effect sizes (95% CI)	Effect size *p* value	Heterogeneity I^2 (%)
DCR Long form vs Short form	7	1.07 (0.99; 1.15)	0.08	0.0%
Leave one study out				
Noh *et al*. 2017	6	1.09 (1.01; 1.18)	0.04	0.0%
McLeer-Florina 2018	6	1.08 (1.00; 1.16)	0.05	0.0%
PFS Variant 1 vs Non-variant	6	0.24 (0.01; 0.46)	0.04	0.0%
Leave 1 study out				
Noh *et al*. 2017	5	0.19 (-0.05; 0.43)	0.12	0.0%
Su *et al*. 2019	5	0.22 (-0.05; 0.49)	0.11	0.0%
PFS Variant 1 vs Non-variant (subgroup by crizotinib)	5	0.20 (-0.04; 0.44)	0.08	0.0%
Leave one study out				
Lin *et al*. 2019	4	0.29 (0.03; 0.55)	0.04	0.0%
PFS Long form vs Short form (subgroup by crizotinib)	4	0.29 (0.03; 0.55)	0.03	0.0%
Leave 1 study out				
Noh *et al*. 2017	3	0.23 (-0.06; 0.52)	0.12	0.0%
Su *et al*. 2019	3	0.30 (-0.04; 0.65)	0.09	0.0%

DCR, disease control rate; PFS, progression-free survival, CI, confidence interval.

Funnel plot for publication bias assessment

The overall funnel plot (Figure 5a) suggested symmetry between publications with regard to significant and non-significant results. However, when comparing DCR among the variant 1 and non-variant 1 carriers, more non-significant reports were noted (Figure 5b). Other funnel plots within the analysis suggested that there was no publication bias.

Discussion

In this meta-analysis, we explored the effect of *EML4-ALK* variants on the treatment response to ALK inhibitors. The results showed no significant difference in primary endpoint ORR between the *EML4-ALK* variant 1/non-variant 1 groups or between the long/short form variant groups. A trend of greater DCR in the long form group was observed, and a better PFS was observed in the variant 1 carriers and long form group. These results suggest that patients with variant 1 or long form variants may have a better treatment effect with *ALK* inhibitors.

There are several important findings in this study. First, the heterogeneity was relatively small in this study. The meta-analysis within ORR exhibited $I^2 = 27.5\%$, while the I2 values of other analyses were mostly 0%. This suggests that the effect of using different *ALK* inhibitors and treatment lines, and the techniques used to detect the variants may have had a limited influence on the results. Second, in the sensitivity analysis, omitting the studies by Su Y, *et al* [22] and Noh KW, *et al* [13] affected the significance of PFS in the variant 1 and non-variant 1 carriers. The study by Su Y, *et al* [22] had the largest sample size, accounting for 1/3 of the whole sample. This revealed insufficient statistical power to detect the real difference due to the limited sample size. Additional studies with larger sample sizes are needed to vali-

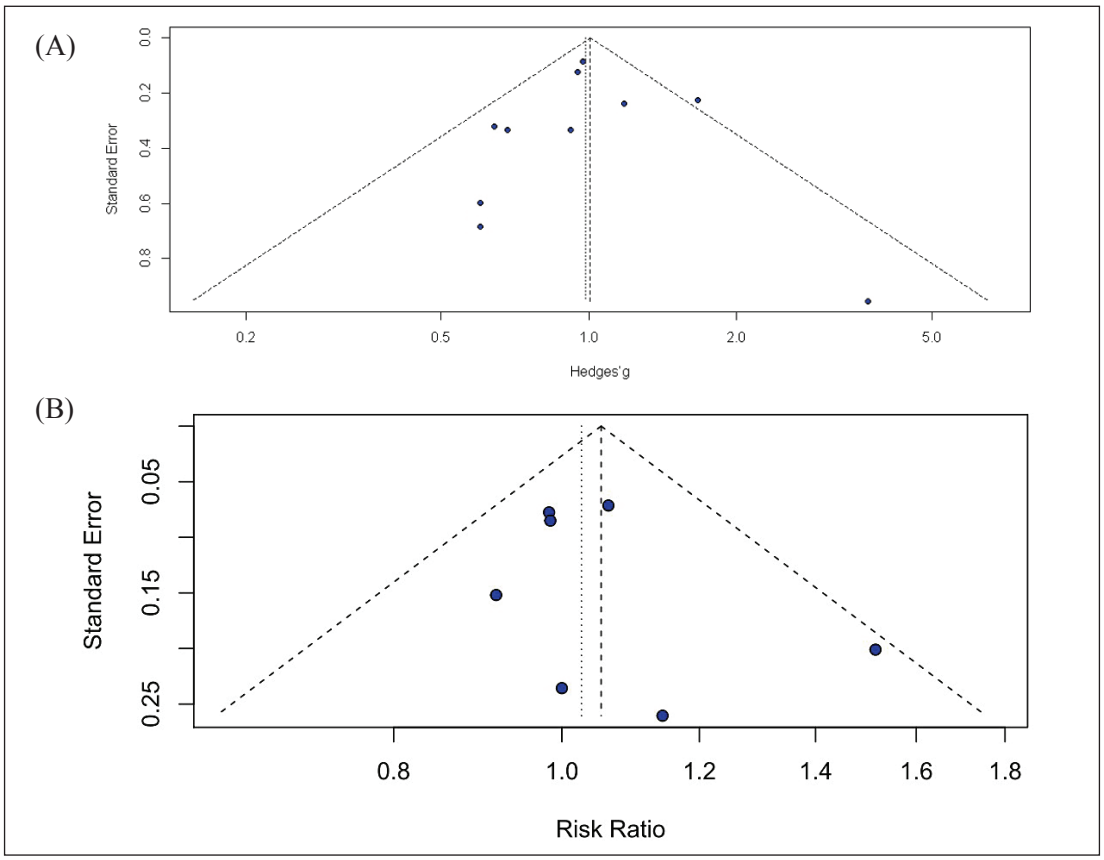

Fig. 5. Funnel Plot, (a)Overall funnel plot; (b)Funnel plot for DCR-related studies comparing variant 1 and non-variant 1 carriers.

date the PFS among *EML4-ALK* variants.

Another important finding of this study is the longer PFS in the variant 1 and long form groups. This could be supported by several factors. From the aspect of ALK inhibitor sensitivity, different degrees of protein instability caused by *EML4-ALK* variants have been reported to result in different sensitivities to ALK inhibitors [23-24]. Heuckmann JM, *et al* reported that variant 2 carriers had the greatest sensitivity to crizotinib, variant 1 and variant 3b carriers had intermediate sensitivity, and variant 3a carriers had the lowest sensitivity [23]. Another study reported that the half-maximal inhibition concentration (IC50) value required for crizotinib was at least 10-fold higher in short form carriers than in long form carriers, and that this further suggested that the lack of a HELP domain in EML4 resulted in less sensitivity to short form variants [10, 25]. Therefore, greater sensitivity to variant 1 and long form variants may have contributed to the longer PFS.

From the aspect of metastasis, previous studies have shown that patients with short form variants have more metastatic sites in the advanced stage [13] and a trend toward a higher clinical stage at diagnosis [26]. Another study reported that variant 3 was associated with cell migration and metastasis by promoting microtubule stabilization [27]. Hence, the lower disease volume at diagnosis in those with variant 1 and long form variants may also have led to the

longer PFS.

From the aspect of resistance mutations, emerging evidence has shown an association between *ALK* variants and kinase domain resistance mutations in patients receiving ALK inhibitor treatment. *ALK* G1202R is located in the solvent front of ALK kinase and plays an essential role in treatment failure with second-generation TKI therapy [28]. Lin JJ, *et al* reported that more refractory *ALK* G1202R mutations developed in variant 3 carriers than in variant 1 carriers. In addition, pre-clinical data have shown the diverse cellular IC50 potency of ALK inhibitors in variant 1 and variant 3 carriers in certain crizotinib-resistant mutations [29]. The lower probability of variant 1 carriers developing resistance mutations may also explain the longer PFS in variant 1 carriers. Taken together, this evidence supports the findings of the current study.

To our knowledge, this is the first meta-analysis to examine the association between the treatment effect of ALK TKIs and *EML4-ALK* variants. However, there are several limitations to this study. First, most studies in the meta-analysis were restricted to crizotinib treatment. Hence, the current results may not be generalizable to second- or third-generation therapies. Second, the limited number of studies and small sample sizes resulted in insufficient power to detect differences between *EML4-ALK* variants in subgroup analysis or sensitivity analysis. Third, most patients underwent multiple additive treatments concurrently. Hence, the main effect of the *EML4-ALK* variants may have been confounded by sequential treatments.

In conclusion, the current study shows the importance of *EML4-ALK* variants when considering the treatment effect of ALK inhibitors. Although more evidence is urgently needed, treatment plans based on an individual's E*EML4-ALK* variants will lead to personalized medicine in the future.

References

1. de Groot PM, Wu CC, Carter BW, *et al*. The epidemiology of lung cancer. Transl Lung Cancer Res 2018; 7(3): 220-33.
2. Ferlay J, Colombet M, Soerjomataram I, *et al*. Estimating the global cancer incidence and mortality in 2018: GLOBOCAN sources and methods. Int J Cancer 2019; 144(8): 1941-53.
3. Luo YH, Chiu CH, Kuo CHS, *et al*. Lung cancer in Republic of China. J Thorac Oncol 2021; 16(4): 519-27.
4. Solomon B, Varella-Garcia M, Camidge DR. ALK gene rearrangements: a new therapeutic target in a molecularly defined subset of non-small cell lung cancer. J Thorac Oncol 2009; 4(12): 1450-4.
5. Hernandez L, Beà S, Bellosillo B, *et al*. Diversity of genomic breakpoints in TFG-ALK translocations in anaplastic large cell lymphomas: identification of a new TFG-ALKXL chimeric gene with transforming activity. American J Pathol 2002; 160(4): 1487-94.
6. Soda M, Choi YL, Enomoto M, *et al*. Identification of the transforming EML4-ALK fusion gene in non-small-cell lung cancer. Nature 2007; 448(7153):561-6.
7. Rangachari D, Le X, Shea M, *et al*. Cases of ALK-rearranged lung cancer with 5-year progression-free survival with crizotinib as initial precision therapy. J Thorac Oncol 2017; 12(11): e175-e7.
8. Pacheco JM, Gao D, Smith D. Natural history and factors associated with overall survival in stage IV ALK-rearranged non–small cell lung cancer. J Thorac Oncol 2019; 14(4): 691-700.
9. Yoshida T, Oya Y, Tanaka K, *et al*. Differential crizotinib response duration among ALK fusion variants in ALK-positive non-small-cell lung cancer. J Clin Oncol 2016; 34(28): 3383-9.
10. Woo CG, Seo S, Kim SW, *et al*. Differential protein stability and clinical responses of EML4-ALK fusion variants to various ALK inhibitors in advanced ALK-

rearranged non-small cell lung cancer. Ann Oncol 2017; 28(4): 791-7.

11. Lei YY, Yang JJ, Zhang XC, *et al*. Anaplastic lymphoma kinase variants and the percentage of ALK-positive tumor cells and the efficacy of crizotinib in advanced NSCLC. Clin Lung Cancer 2016; 17(3): 223-31.
12. Lin YT, Liu YN, Shih JY. The impact of clinical factors, ALK fusion variants, and BIM polymorphism on crizotinib-treated advanced EML4-ALK rearranged non-small cell lung cancer. Front Oncol 2019; 9: 880.
13. Noh KW, Lee MS, Lee SE, *et al*. Molecular breakdown: a comprehensive view of anaplastic lymphoma kinase (ALK)-rearranged non-small cell lung cancer. J Pathol 2017; 243(3): 307-19.
14. Mitiushkina NV, Tiurin VI, Iyevleva AG, *et al*. Variability in lung cancer response to ALK inhibitors cannot be explained by the diversity of ALK fusion variants. Biochimie 2018; 154: 19-24.
15. Camidge DR, Dziadziuszko R, Peters S, *et al*. Updated efficacy and safety data and impact of the EML4-ALK fusion variant on the efficacy of alectinib in untreated ALK-positive advanced non-small cell lung cancer in the global phase III ALEX study. J Thorac Oncol 2019; 14(7): 1233-43.
16. Moher D, Liberati A, Tetzlaff J, *et al*. Preferred reporting items for systematic reviews and meta-analyses: the PRISMA statement. BMJ 2009; 339: b2535.
17. Wells G, Shea B, O'Connell D, *et al*. The Newcastle–Ottawa Scale (NOS) for assessing the quality of non-randomized studies in meta-analysis 2000.
18. Higgins JP, Thompson SG. Quantifying heterogeneity in a meta-analysis. Stat Med 2002; 21(11): 1539-58.
19. Egger M, Davey Smith G, Schneider M, *et al*. Bias in meta-analysis detected by a simple, graphical test. BMJ 1997; 315(7109): 629-34.
20. Moher D, Liberati A, Tetzlaff J, *et al*. Preferred reporting items for systematic reviews and meta-analyses: the PRISMA statement. BMJ 2009; 339.
21. McLeer-Florin A, Duruisseaux M, Pinsolle J, *et al*. ALK fusion variants detection by targeted RNA-next generation sequencing and clinical responses to crizotinib in ALK-positive non-small cell lung cancer. Lung Cancer 2018; 116:15-24.
22. Su Y, Long X, Song Y, *et al*. Distribution of ALK fusion variants and correlation with clinical outcomes in Chinese patients with non-small cell lung cancer treated with crizotinib. Target Oncol 2019; 14(2): 159-68.
23. Heuckmann JM, Balke-Want H, Malchers F, *et al*. Differential protein stability and ALK inhibitor sensitivity of EML4-ALK fusion variants. Clin Cancer Res 2012; 18:4682-90.
24. Richards MW, O'Regan L, Roth D, *et al*. Microtubule association of EML proteins and the EML4-ALK variant 3 oncoprotein require an N-terminal trimerization domain. Biochem J 2015; 467(3): 529-36.
25. Hrustanovic G, Olivas V, Pazarentzos E, *et al*. RAS-MAPK dependence underlies a rational polytherapy strategy in *EML4-ALK*–positive lung cancer. Nat Med 2015; 21(9): 1038-47.
26. Tao H, Shi L, Zhou A, *et al*. Distribution of *EML4-ALK* fusion variants and clinical outcomes in patients with resected non-small cell lung cancer. Lung Cancer 2020; 149: 154-61.
27. O'Regan L, Barone G, Adib R, *et al*. *EML4-ALK* V3 oncogenic fusion proteins promote microtubule stabilization and accelerated migration through NEK9 and NEK7. J Cell Sci 2020 May; 133(9): jcs2441505.
28. Lin JJ, Zhu VW, Yoda S, *et al*. Impact of *EML4-ALK* variant on resistance mechanisms and clinical outcomes in ALK-positive lung cancer. J Clin Oncol 2018; 36(12): 1199-206.
29. Horn L, Whisenant JG, Wakelee H, *et al*. Monitoring therapeutic response and resistance: analysis of circulating tumor DNA in patients with *ALK*+ lung cancer. J Thorac Oncol 2019; 14(11): 1901-11.

Inhaled Nitric Oxide in the Management of Severe COVID-19 Pneumonia-related Hypoxemic Respiratory Failure

Jenn-Yu Wu[1,2], Chien-Ting Pan[3], Sheng-Nan Chang[2,3], Chi-Ying Lin[4], Yen-Fu Chen[1,2], Chung-Yu Chen[1,2], Juey-Jen Hwang[2,3]

Previous experience with the 2003 Severe Acute Respiratory Syndrome Coronavirus (SARS-CoV) infection suggested the potential role of inhaled nitric oxide (NO) as a supportive measure for patients with respiratory failure. Treatment with inhaled NO reversed pulmonary hypertension, improved severe hypoxemia, and shortened the length of ventilator support in severe SARS patients. Inhaled NO can reduce inflammatory cell-mediated lung injury and lower pulmonary vascular resistance. Clinical use of inhaled NO may become an alternate treatment before extracorporeal membrane oxygenation for the management of acute respiratory distress syndrome in patients with COVID-19. Two patients with severe COVID-19 pneumonia-related hypoxemic respiratory failure were intubated with mechanical ventilator support and were treated with inhaled NO in our hospital. The patients showed improvement in oxygenation and were weaned successfully from the mechanical ventilator. ***(Thorac Med 2022; 37: 180-185)***

Key words: COVID-19; respiratory failure; inhaled nitric oxide; critical care

Introduction

2019-new Coronavirus (2019-nCoV) infection (COVID-19) is highly contagious and has caused hundreds of thousands of deaths worldwide. The clinical presentation of symptomatic patients ranges from mild upper airway syndromes to severe pneumonia resulting in multi-organ dysfunction, leading to death [1]. Around 25% of hospitalized patients with COVID-19 required intensive care. Of these, over 60% progressed to acute respiratory distress syndrome (ARDS) [2-3].

The previous Severe Acute Respiratory

[1]Division of Pulmonary and Critical Care Medicine, Department of Internal Medicine, National Taiwan University Hospital Yunlin Branch, Douliou, Yunlin, Taiwan, [2]Department of Internal Medicine, National Taiwan University Hospital and College of Medicine, National Taiwan University, Taipei, Taiwan, [3]Division of Cardiology, Department of Internal Medicine, National Taiwan University Hospital Yunlin Branch, Douliou, Yunlin, Taiwan, [4]Division of Infectious Disease, Department of Internal Medicine, National Taiwan University Hospital Yunlin Branch, Douliou, Yunlin, Taiwan.
Address reprint requests to: Dr. Chung-Yu Chen, Department of Internal Medicine, National Taiwan University Hospital Yunlin Branch, Yunlin County, Taiwan, No. 579, Sec. 2, Yunlin Road, Douliou City, Yunlin County, 640, Taiwan

Syndrome Coronavirus (SARS-CoV) epidemic broke out in 2003. Treatment with inhaled nitric oxide (NO) reversed pulmonary hypertension, improved severe hypoxemia and shortened the length of ventilator support, compared to matched control patients [4]. While no effective treatment for 2019-nCoV virus infection is available to date, inhaled NO may have the possible benefit of antiviral activity against coronavirus [5]. The coronavirus responsible for SARS-CoV shares most of the genome of COVID-19, which suggests the potential effectiveness of inhaled NO therapy in these patients.

Because of the potential harm from inhaled NO and the absence of a clear mortality benefit, the Society of Critical Care Medicine recommends against the routine use of inhaled NO in patients with COVID-19 ARDS [6]. Gattinoni L, *et al*. [7] found that the severe hypoxemia occurring in the compliant lungs of 16 patients with COVID-19 pneumonia-related ARDS resulted from the loss of lung perfusion regulation and hypoxemic vasoconstriction. There are no studies that describe the utility of pulmonary vasodilators in severe COVID-19 pneumonia patients, and no study has assessed the use of inhaled NO as a possible rescue therapy. Here, we report the use of inhaled NO as a rescue therapy in the treatment of severe COVID-19 pneumonia patients with hypoxemic respiratory failure.

Case Report

We report 2 patients who traveled abroad together, and came back to Taiwan on 15 March 2020. Patient 1 was a 51-year-old woman with a medical history of hypertension. She was found to have fever upon arriving in Taiwan, and was taken to our hospital for treatment. The COVID-19 polymerase chain reaction (PCR) test was positive. Chest radiography (CXR) revealed increased infiltration and consolidation in the right lung field. However, gradual deterioration of O_2 saturation was noticed on 17 March 2020. Follow-up CXR on 18 March 2020 showed progression of bilateral lung infiltration. On the same day, elective tracheal intubation was performed and the patient was transferred to our ICU.

Patient 2 was the mother of Patient 1. She was a 74-year-old woman with diabetes mellitus and hypertension. Patient 2 was also admitted to our hospital on 15 March 2020 for quarantine. Fever was noticed on 16 March 2020, and CXR showed increased reticular infiltration in bilateral lungs. The COVID-19 PCR test was positive. The patient experienced on-and-off fever during the first week of admission. However, rapid desaturation was noted on 22 March 2020. Intubation was performed due to hypoxemic respiratory failure, and she was transferred to our ICU for further management.

Both patients were considered to be at high risk of mortality from COVID 19 ARDS, because of age, obesity (body mass index, Patient 1: 34.89 and Patient 2: 29.96, respectively), and underlying comorbidities [8]. Lopinavir/ritonavir, hydroxychloroquine and azithromycin were administered to both patients after they were admitted to our hospital. Empirical anti-bacterial agents were also used, based on the attending physicians' clinical judgment.

We used the following strategies for both of our mechanically-ventilated patients with COVID-19 ARDS: low tidal volume (Vt) ventilation (Vt 4 to 8 mL/kg of predicted body weight), targeting plateau pressures (Pplat) of <30 cm H_2O, a higher positive end-expiratory pressure (PEEP) strategy, a conservative fluid strategy

over a liberal fluid strategy, and neuromuscular blocking and sedative agents, to facilitate protective lung ventilation. Pulmonary static compliance (Cst) was calculated based on the following formula: Cst=V/(Pplat–PEEP). Inhaled NO (iNO) was connected to the tubing by the adaptor, and was delivered at 10 parts per million (ppm) at initiation. The iNO treatment was started after we had discussed this with the family and they agreed to its use. The iNO dosage was adjusted every 8 hours. iNO was tapered when the oxygenation level of the patients improved to a PaO_2/FiO_2 (P/F) ratio >200 mmHg for more than 24 hours. To monitor the toxicity of iNO, CXR was performed every day to evaluate pulmonary edema, and blood methemoglobin levels were checked every 2 days. Physicians in our ICU followed the weaning protocols.

The PaO_2/FiO_2 (P/F) ratio of Patient 1 was below 100 on ICU day 3, which indicated severe ARDS. iNO 10 ppm was administered and the P/F ratio elevated (Figure 1). The hypoxemia improved after initiation of iNO, and the

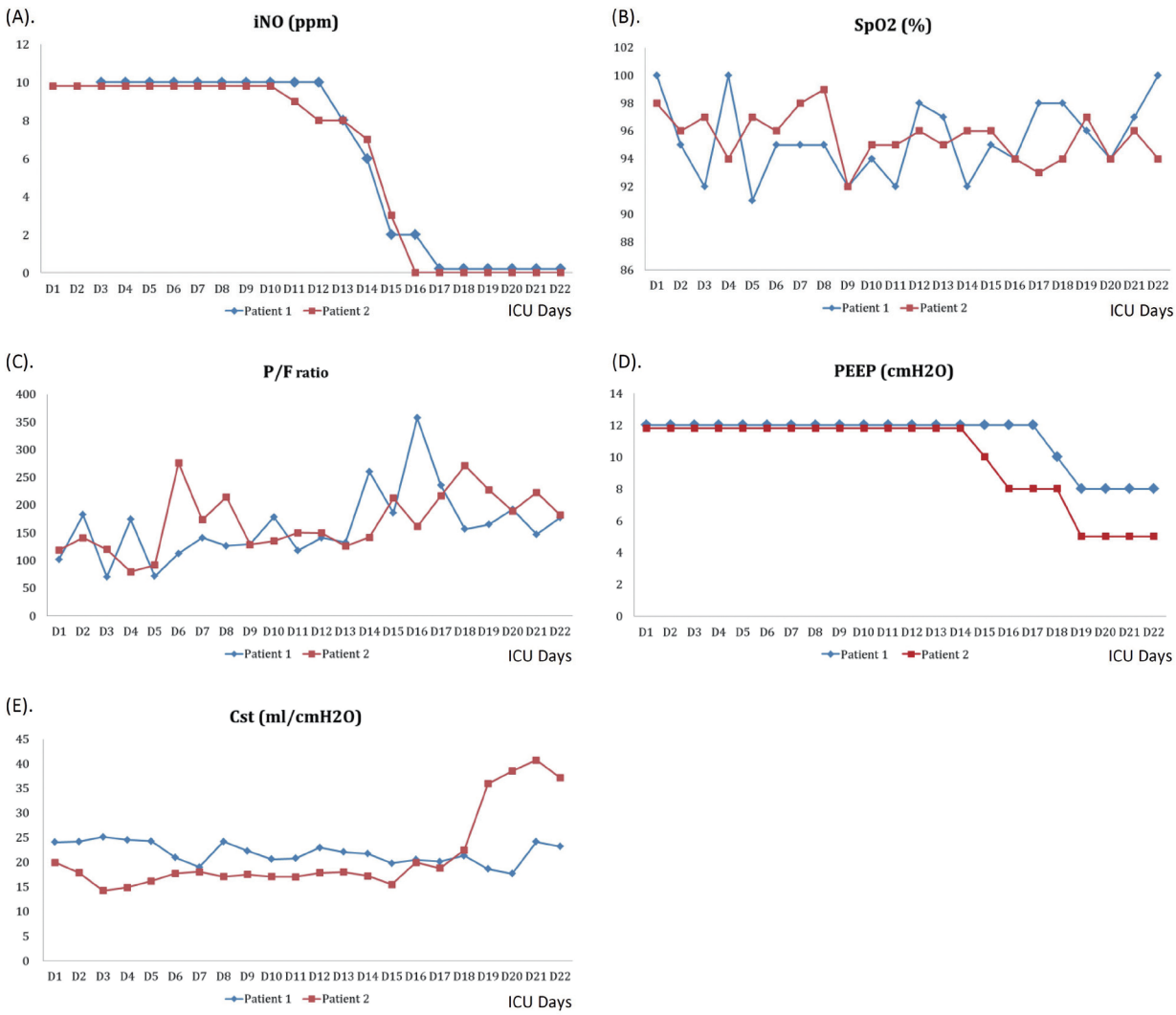

Fig. 1. Mechanical ventilator settings and change in pulmonary physiology parameters. (A). Parts per million (ppm) of inhaled nitric oxide (NO); (B). Oxyhemoglobin saturation by pulse oximetry (SpO2); (C). PaO2/FiO2 (P/F) ratio; (D). Positive end-expiratory pressure (PEEP); (E). Pulmonary static compliance (Cst). (ICU: intensive care unit).

P/F ratio could be kept above 100. On ICU day 14, the P/F ratio was over 200, and the iNO was tapered down. Patient 1 was extubated on ICU day 23. Patient 2 used iNO at the beginning of mechanical ventilator support because the initial P/F ratio was below 100. The P/F ratio could be maintained at 100 to 200 after iNO treatment was initiated. After 15 days, the iNO was withdrawn, and extubation of Patient 2 was performed on ICU day 23. Figure 1 illustrates the adjustment of the mechanical ventilator setting, and the change in the P/F ratio and static lung compliance (Cst).

CXR of Patient 1 revealed prominent right filtration initially, which then progressed to bilateral lungs 3 days later. CXR showed improved findings after 2 weeks of treatment (ICU day 14) (Figure 2A). In Patient 2, the initial CXR revealed no obvious patch. However, infiltration progressed 7 days after admission. CXR revealed progression of pneumonia on ICU day 4. After 10 days of medical treatment and mechanical ventilator support, the CXR finding was stationary (Figure 2B), but oxygenation had improved.

Discussion

Herein, we described an empirical therapeutic use of iNO in 2 patients with severe COVID-19 pneumonia-related hypoxemic respiratory failure. Severe hypoxemia occurring in COVID-19 ARDS may be due to a lung ventilation-perfusion (V/Q) mismatch. iNO will decrease the intrapulmonary shunt fraction and appear to improve oxygenation. On the basis of current data, it appears feasible to consider the use of 10 ppm iNO as an option for supportive treatment in severe COVID-19 pneumonia patients with hypoxemic respira-

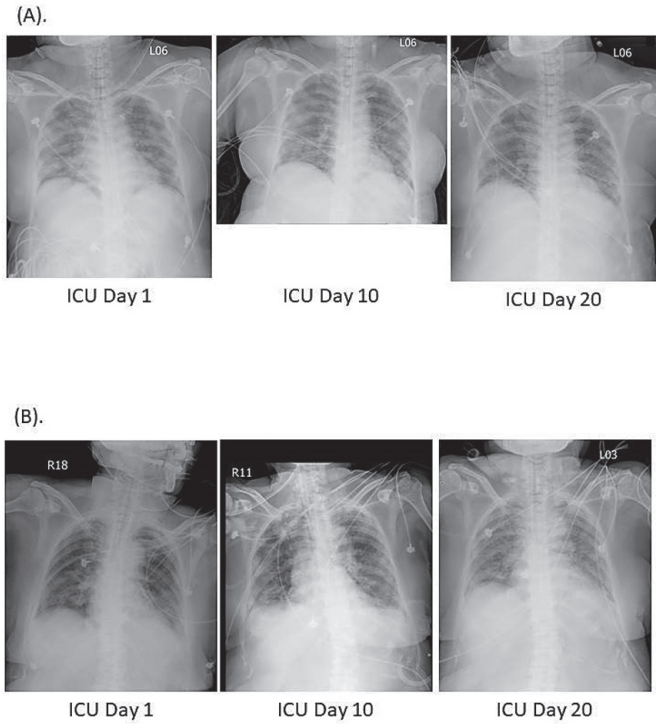

Fig. 2. Chest radiography of (A). Patient 1, and (B). Patient 2 during intensive care unit (ICU) stay.

tory failure. No solid evidence is available to support the use of iNO to improve the survival of patients with ARDS. Despite the initial oxygenation improvement, iNO does not appear to shorten the duration of mechanical ventilation. Both of our patients with severe COVID-19 pneumonia used iNO, and had improvement in oxygenation. Though the durations of mechanical ventilation were long (23 days, respectively, for each patient), both patients were weaned from the mechanical ventilator successfully and survived.

Besides a lung-protective strategy that incorporates low tidal volume ventilation and low airway plateau pressure (Pplat), higher PEEP has been used to improve oxygenation in patients with ARDS. Several studies reported that early prone positioning reduced mortality in patients with severe ARDS. A study of 12 patients with COVID-19-related ARDS suggested that prone positioning may improve lung recruitability [9]. Prone ventilation for 12 to 16 hours and recruitment maneuvers are not strongly recommended for mechanically ventilated adults with COVID-19 and moderate-to-severe ARDS [6]. However, neither prone ventilation nor recruitment maneuvers were performed for our patients. Prone positioning of patients with relatively high compliance may result in less benefit. Besides, a high demand for stressed human resources may also increase exposure and the risk of virus infection in health care workers.

iNO may improve oxygenation and provide a rescue treatment for ARDS patients with severe hypoxemia [4]. Compared with prone positioning and ECMO, iNO therapy requires less loading of medical staff and is less invasive to patients. Besides, NO has potential anti-viral and immunomodulatory effects [5, 10]. The coronavirus responsible for SARS-CoV shares most of the genome of COVID-19, indicating the potential effectiveness of iNO therapy in these patients. Since there is no solid and effective treatment for 2019-nCoV virus to date, iNO may be considered as a possible useful treatment option for COVID-19-related ARDS [10].

The treatment course of our 2 patients provided interesting findings. They had traveled abroad in the same tour group. They received similar drug treatment, they used the same ventilator setting and weaning protocols, and both were provided iNO support. Both of them survived severe COVID-19 ARDS and benefited from iNO use, and the ventilation duration was the same (23 days). Patient 1, the daughter, had an earlier pneumonia and ARDS onset, about 4 days earlier than Patient 2. This difference in the disease course may be due to different viral transmission orders.

In conclusion, treatment with 10 ppm iNO in patients with severe COVID-19 pneumonia may improve oxygenation without adverse effects such as organ function impairment, and helps to liberate the patients from mechanical ventilation. As a supportive maneuver, iNO could decrease the work load of ICU personnel and lessen the possibility of contamination with viral infection, compared to prone ventilation or recruitment. We look forward to seeing the final results from the NOSARSCOVID trial to evaluate the efficacy of NO gas inhalation for SARS in COVID-19 (NCT04290871) patients.

References

1. Xu Z, Shi L, Wang Y, *et al*. Pathological findings of COVID-19 associated with acute respiratory distress syndrome [published correction appears in Lancet Respir Med. 2020 Feb 25;:]. Lancet Respir Med 2020; 8(4): 420-422.

2. Wang D, Hu B, Hu C, *et al*. Clinical characteristics of 138 hospitalized patients with 2019 novel coronavirus-infected pneumonia in Wuhan, China. JAMA 2020; 323(11):1061-1069.
3. Yang X, Yu Y, Xu J, *et al*. Clinical course and outcomes of critically ill patients with SARS-CoV-2 pneumonia in Wuhan, China: a single-centered, retrospective, observational study. [published correction appears in Lancet Respir Med. 2020 Feb 28;:] Lancet Respir Med 2020; 8(5): 475-481.
4. Chen L, Liu P, Gao H, *et al*. Inhalation of nitric oxide in the treatment of severe acute respiratory syndrome: a rescue trial in Beijing. Clin Infect Dis 2004; 39(10): 1531-1535.
5. Keyaerts E, Vijgen L, Chen L, *et al*. Inhibition of SARS-coronavirus infection in vitro by S-nitroso-N-acetylpenicillamine, a nitric oxide donor compound. Int J Infect Dis 2004; 8(4): 223-226.
6. Alhazzani W, Møller MH, Arabi YM, *et al*. Surviving sepsis campaign: guidelines on the management of critically ill adults with coronavirus disease 2019 (COVID-19). Crit Care Med 2020; 48(6): e440-e469.
7. Gattinoni L, Coppola S, Cressoni M, *et al*. Covid-19 does not lead to a "typical" acute respiratory distress syndrome. Am J Respir Crit Care Med 2020; 201(10): 1299-1300.
8. Onder G, Rezza G, Brusaferro S. Case-fatality rate and characteristics of patients dying in relation to COVID-19 in Italy [published online ahead of print, 2020 Mar 23]. JAMA 2020; 10.1001.
9. Pan C, Chen L, Lu C, *et al*. Lung recruitability in SARS-CoV-2-associated acute respiratory distress syndrome: a single-center, observational study. Am J Respir Crit Care Med 2020; 201(10): 1294-1297.
10. Alvarez RA, Berra L, Gladwin MT. Home nitric oxide therapy for COVID-19. Am J Respir Crit Care Med 2020; 202 (1): 16-20.

Positive Correlation between Pendelluft and Breathing Effort in a Case of Severe Acute Respiratory Distress Syndrome

Chien-Ming Chiang[1], Chien-Yu Lin[2], Chang-Wen Chen[2]

Sedation and paralysis are often required for patients with moderate to severe acute respiratory distress syndrome. Daily interruption of sedation and paralysis is a standard of care in the current concept. However, physicians may be concerned that the excessive breathing effort generated by the patients themselves following discontinuation of a muscle relaxant could be harmful. The phenomenon of pendelluft is hypothesized to be associated with such hazards, but the association of pendelluft and breathing effort has not been well established. Here, we report a patient with severe acute respiratory distress syndrome who underwent an electrical impedance tomography recording with simultaneous esophageal manometry monitoring during daily interruption of sedation and paralysis. A positive correlation between the volume of pendelluft, the global inhomogeneity index and breathing effort was noted. ***(Thorac Med 2022; 37: 186-191)***

Key words: pendelluft, acute respiratory distress syndrome (ARDS), electrical impedance tomography (EIT)

Background

Patients with moderate to severe acute respiratory distress syndrome (ARDS) may benefit from early use of neuromuscular blocking agents during mechanical ventilation [1]. Daily interruption of sedative and paralyzing agents is a widely accepted practice, and may result in a shorter duration of mechanical ventilation and shorter length of stay in the intensive care unit (ICU) [2]. One undesirable consequence of such a practice is an excessive breathing effort, which may be disadvantageous to the injured lung as excessive pendelluft may occur [3-4]. Pendelluft is a phenomenon described as regional gas movement from the mostly ventral (non-dependent) part to the dorsal (dependent) part of the lung, without changing the tidal volume. Therefore, regional over-distension may result, despite the application of a low tidal vol-

[1]Department of Internal Medicine, National Cheng Kung University Hospital, [2]Division of Pulmonary Medicine, Department of Internal Medicine, National Cheng Kung University Hospital.
Address reprint requests to: Dr. Chang-Wen Chen, Division of Pulmonary Medicine, Department of Internal Medicine, National Cheng Kung University Hospital, No.138, Sheng Li Road, Tainan, Taiwan

ume strategy.

Electrical impedance tomography (EIT) is a real-time, non-invasive, bedside monitoring technique that allows quantitative changes in regional lung volume to be measured without radiation exposure [5]. Pendelluft can be observed via EIT as the time course of regional ventilation is continuously monitored.

There is limited human data on the relationship between the extent of pendelluft and breathing effort in ARDS patients. Here, we report a patient with severe ARDS in whom pendelluft was detected with both EIT and esophageal manometry monitoring during transient discontinuation of paralysis.

Case Presentation

Clinical Course:

The patient was a 68-years-old gentleman with esophageal squamous cell carcinoma who had undergone radiotherapy for around 4 months.

On the day of admission to National Cheng Kung University Hospital (March 10, 2020), the patient had symptoms with spiking fever up to 40.5°C and progressive dyspnea for 2 days. Severe hypoxemia was noticed via arterial blood gas analysis, with PaO_2 81 mmHg under oxygen supplementation with a non-rebreathing mask, so the patient subsequently underwent endotracheal intubation with mechanical ventilation. Arterial blood gas under positive end-expiratory pressure (PEEP) of 10 cmH_2O revealed a PaO_2/FiO_2 ratio of 131.

Chest radiograph with an anterior-posterior view (Figure 1.) and computed tomography of the chest disclosed diffuse, ill-defined mixed alveolar and interstitial pattern opacities in bilateral lungs, with reticulonodular pattern densities centrally distributed in the upper lung field. Bronchoalveolar lavage was positive for Pneumocystic jirovecii, using polymerase chain reaction.

Under the tentative diagnosis of pneumonia with moderate -to severe ARDS superimposed with radiation pneumonitis, the patient was admitted to our medical ICU and treated with sulfamethoxazole/trimethoprim and intravenous methylprednisolone.

On March 12, 2020 (admission day 3), the patient showed improvement following sedation and paralysis and low tidal volume ventilation, with PEEP 10 cmH_2O and FiO_2 to 35%. Arterial blood gas analysis revealed a PaO_2/FiO_2 ratio of 165.7. The patient was placed under low tidal volume ventilation of approximately 6 ml/kg of ideal body weight and a constant flow of 40L/min. Infusion of the neuromuscular blocking agent with cisatracurium was discontinued, and we started the EIT and esophageal pressure recording for 60 minutes. Cisatracurium was resumed as clinically significant breathing effort developed with elevated airway occlusion

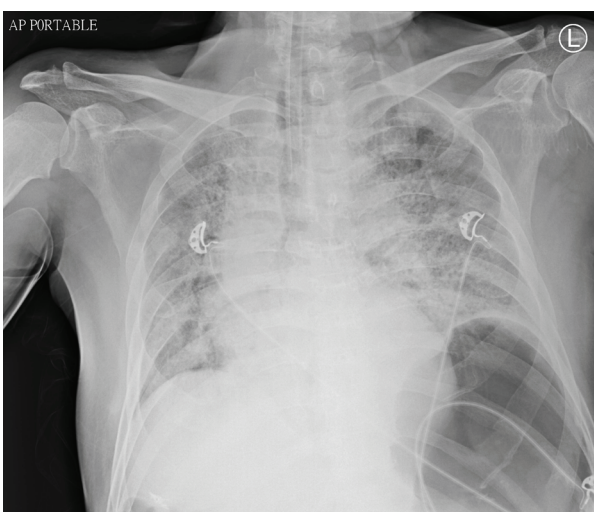

Fig. 1. Chest radiograph anterior-posterior view taken on March 10th, 2020, the day the patient was intubated.

pressure at 100ms (P0.1) as -9.6 cmH_2O prior to completion of the 60 minutes. A total of 873 breaths were recorded.

Air flow was measured with a pneumotachograph (Hamilton AG, or Hans Rudolf) connected to a differential pressure transducer (MP 45, Validyne Corp., Northridge, CA). Airway pressure and esophageal pressure were measured using differential pressure transducers (P300D, Validyne Corp., Northridge, CA.). An appropriate esophageal pressure signal was confirmed according to the standard guideline [6]. A commercial EIT monitor (PulmoVista 500, Dräger Medical GmbH, Lübeck, Germany) was used for recording and monitoring regional lung ventilation. EIT data were registered at 20 Hz, and then low-pass filtered (35 per minute) and stored for offline analysis. The National Cheng Kung University Hospital Ethics Committee approved this study. The patient's next of kin gave informed consent.

The presence of pendelluft was defined as the presence of an opposite impedance change (ΔZ) between dependent and independent zones during a breathing effort. The breathing could occur in an inspiration phase, expiratory phase or in transition. Estimation of the volume of the pendelluft was determined by the integrated volume and corresponding impedance change [7]. For calculation of the global inhomogeneity (GI) index, the cut-off value for the region of interest (ROI, lung area) boundary was set as 20% of the global linear regression coefficient change within the area throughout the recording course (5). The GI index was calculated as the sum of the difference between median impedance values of the tidal images (in absolute values) divided by the sum of the impedance values of the lung area, which was introduced by Zhao et al with the following equation:

$$GI = \frac{\sum_{x,y\in lung}|DI_{xy} - Median(DI_{lung})|}{\sum_{x,y\in lung} DI_{xy}}$$

with DI representing values of differential impedance in differential images; DIxy as the DI of the pixel in a certain lung region over coordinates (x,y); DIlung representing pixels we observe in the lung regions [8]. The peak and plateau airway pressure, total PEEP, flow, and esophageal pressure were recorded in the meantime.

Findings:

During the recording, the occurrence of pendelluft gradually became obvious along with the increase in breathing effort, as illustrated in Figure 2. At baseline, when spontaneous breathing had just started (Figure 2A), the peak and trough impedance changes over the 4 layers (L1 to L4, nondependent to dependent parts of the lung) occurred at nearly the same time, indicating minimal occurrence of pendelluft. Pendelluft became evident as ΔPes became greater than 15 cmH_2O. Further analysis of the pendelluft volume and the breathing effort revealed a positive correlation that fit in an exponential growth equation (Figure 3) with an acceptable goodness of fit ($R^2 = 0.8419$). The GI index was highly positively correlated with the breathing effort in linear regression (Figure 4, $R^2 = 0.9700$, $p<0.0001$). Serial EELI values revealed the decrease in EELI as breathing effort developed: mean 7030 AU at baseline; 2969 AU when mean ΔPes was 11.3 cmH_2O (ranging from 9.1 to 14.7 cmH_2O); mean 1073 AU when mean ΔPes was 23.4 cmH_2O (ranging from 21.3 to 24.8 cmH_2O); mean 732 AU when mean ΔPes was 26 cmH_2O (ranging from 22.3 to 31 cmH_2O).

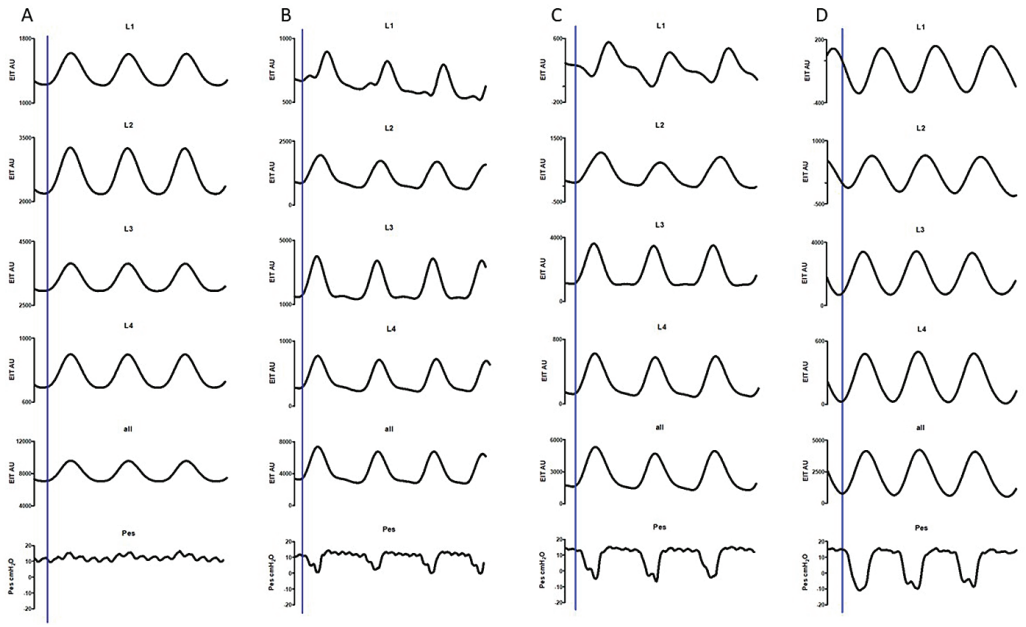

Fig. 2. Electrical impedance tomography recording while gradually tapering down sedation. Impedance curves were scaled in arbitrary units (AU). Pendelluft could be noticed as breathing effort developed; breathing effort was presented as Pes swing (ΔPes). Layer 1(L1) represented the non-dependent parts of the lung, with layer 4 (L4) the most dependent ones. Electrical impedance tomography was recorded (A) as baseline (B) when mean ΔPes was 11.3 cmH_2O (ranging from 9.1 to 14.7 cmH_2O) (C) mean ΔPes 23.4 cmH_2O (ranging from 21.3 to 24.8 cmH_2O) (D) mean ΔPes 26 cmH_2O (ranging from 22.3 to 31 cmH_2O).

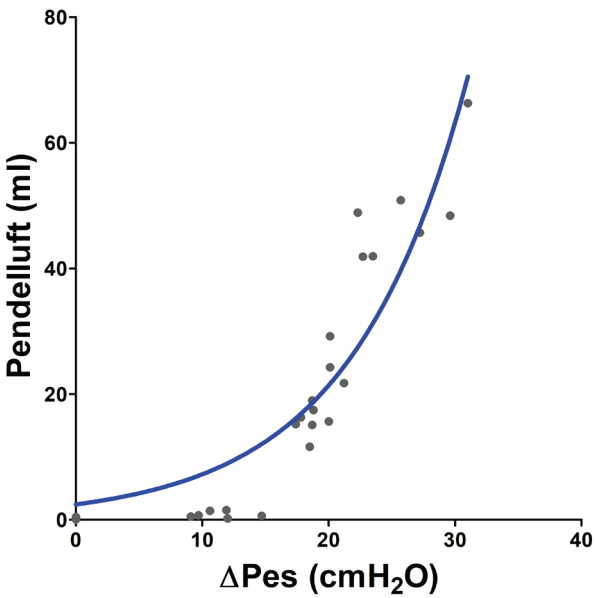

Fig. 3. The relationship of breathing effort (presented as Pes swing) over pendelluft volume. The positive correlation is presented as an exponential growth equation with $R^2 = 0.8673$.

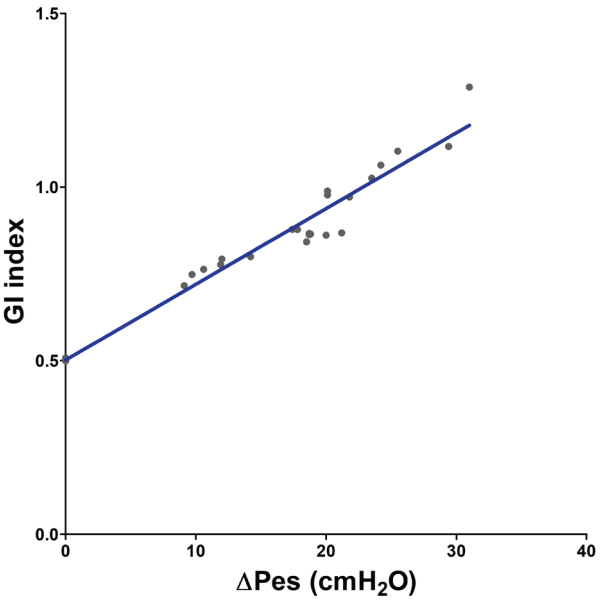

Fig. 4. The relationship of breathing effort (presented as Pes swing) over GI indices presented in linear regression, $R^2 = 0.9700$, $p < 0.0001$. The baseline GI index was around 0.5 when there was little breathing effort.

Discussion

In this case we observed a significant correlation between breathing effort and volume of pendelluft in an ARDS patient during discontinuation of neuromuscular blocking agent infusion. To the best of our knowledge, this is the first case report revealing the relationship between spontaneous effort and pendelluft in an ARDS patient with esophageal pressure monitoring.

Pendelluft was first observed by Yoshida *et al* in a postoperative ARDS patient following EIT monitoring. The mechanism was postulated to be non-uniform transmission of pleural pressure generated by diaphragmatic contraction; this theory was supported in an animal model study [4]. Greenblatt *et al* suggested that the degree of pendelluft may be higher in diseases that cause more heterogeneous changes in lung compliance [9]. Quantitation of pendelluft was recently reported in a study by Coppadoro *et al* on weaning patients during pressure support ventilation [7]. In this study, patients were divided into a high-pendelluft group and a low-pendelluft group, with a cut-off pendelluft volume of 6 ml. The high-pendelluft group comprised 40% of the cases. However, esophageal pressure monitoring was not used in that study. In our patient, we noticed that once the esophageal pressure swing exceeded 15 cmH_2O, a very significant volume of pendelluft would be generated, which suggested that an excessive breathing effort might be hazardous for our patient.

The GI index, uniquely derived from EIT monitoring, has been used to quantitate appropriateness of ventilation. The GI index has been shown to be a reliable index for ventilation distribution [8]. A lower GI index implies better distribution of ventilation. The GI index was used to determine the "best PEEP" when at its lowest value for post-cardiac surgery patients [10]. There is little description of the association between GI indices and breathing effort. Based on our observation, it can be speculated that vigorous spontaneous breathing is closely linked with the heterogeneity of ventilation distribution of the ARDS lung, which is considered unfavorable for maintenance of effective ventilation.

As breathing effort increased, the absolute values of global impedance decreased. Resuming sedation and paralysis resulted in elevation of the global impedance curve. Kassis *et al* demonstrated with a Campbell diagram that excessive expiratory effort could reduce the end-expiratory lung volume even more than the estimated lung volume at relaxation, which could promote derecruitment of the lungs [11]. In our patient, the findings of both a decreased global impedance level and an increasing GI index could support the hypothesis that excessive breathing effort can potentially lead to atelectrauma.

Conclusion

We found a positive correlation between pendelluft and breathing effort in a patient with severe ARDS during the daily discontinuation of the neuromuscular blocking agent. This observation might be helpful in raising physician awareness of excessive spontaneous effort in an ARDS patient.

References

1. Papazian L, Forel JM, Gacouin A, *et al*. Neuromuscular blockers in early acute respiratory distress syndrome. N

Engl J Med, 2010; 363(12): 1107-16.
2. Kress JP, Pohlman AS, O'Connor MF, *et al*. Daily interruption of sedative infusions in critically ill patients undergoing mechanical ventilation. N Engl J Med, 2000; 342(20): 1471-7.
3. Brochard L, Slutsky A, Pesenti A. Mechanical Ventilation to Minimize Progression of Lung Injury in Acute Respiratory Failure. Am J Respir Crit Care Med, 2017; 195(4): 438-442.
4. Yoshida T, Torsani V, Gomes S, *et al*. Spontaneous effort causes occult pendelluft during mechanical ventilation. Am J Respir Crit Care Med, 2013; 188(12): 1420-7.
5. Frerichs I, Amato MB, van Kaam AH, *et al*. Chest electrical impedance tomography examination, data analysis, terminology, clinical use and recommendations: consensus statement of the TRanslational EIT developmeNt stuDy group. Thorax, 2017; 72(1): 83-93.
6. Akoumianaki E, Maggiore SM, Valenza F, *et al*. The application of esophageal pressure measurement in patients with respiratory failure. Am J Respir Crit Care Med, 2014; 189(5): 520-31.
7. Coppadoro A, Grassi A, Giovannoni C, *et al*. Occurrence of pendelluft under pressure support ventilation in patients who failed a spontaneous breathing trial: an observational study. Ann Intensive Care, 2020; 10(1): 39.
8. Zhao Z, Moller K, Steinmann D, *et al*. Evaluation of an electrical impedance tomography-based Global Inhomogeneity Index for pulmonary ventilation distribution. Intensive Care Med, 2009; 35(11): 1900-6.
9. Greenblatt EE, Butler JP, Venegas JG, *et al*. Pendelluft in the bronchial tree. J Appl Physiol (1985), 2014; 117(9): 979-88.
10. Blankman P, Hasan D, Erik G, *et al*. Detection of 'best' positive end-expiratory pressure derived from electrical impedance tomography parameters during a decremental positive end-expiratory pressure trial. Crit Care, 2014; 18(3): R95.
11. Baedorf Kassis E, Loring SH, Talmor D. Lung volumes and transpulmonary pressure are decreased with expiratory effort and restored with passive breathing in ARDS: a reapplication of the traditional Campbell diagram. Intensive Care Med, 2018; 44(4): 534-536.

Pulmonary Cryptococcosis Presenting with Multiple Cavitary Nodules in an Immunocompetent Patient: a Case Report

Sheng-Wei Gao[1], Erh-Lun Chen[1]

Pulmonary cryptococcosis can occur in immunocompetent individuals, and most are asymptomatic. We report a 48-year-old male without significant underlying risk factors who presented with multiple nodules scattered in the lung parenchyma and several eccentric cavities with an irregular wall in the bilateral upper lobes and right lower lobe. Bronchoalveolar lavage culture yielded Cryptococcus grubii. High-risk patients, including patients with diabetes, immunosuppressed patients, and patients with T lymphocyte deficiency, leukemia, AIDS or other immunodeficiencies, are the most common groups to develop pulmonary cryptococcosis infection. Similar to our patient, immunocompetent hosts with pulmonary cryptococcosis may present a wide variety of radiographic abnormalities, including nodules and cavitation. ***(Thorac Med 2022; 37: 192-197)***

Key words: immunocompetent patient, pulmonary cryptococcosis

Introduction

Cryptococcosis is a fungal infection that can lead to pulmonary involvement after the inhalation of Cryptococcus spores. In the natural environment, cryptococci can be isolated from avian species, especially pigeons, and decayed wood and soil contaminated with avian excreta [1,8]. Pulmonary infection is often asymptomatic. Exposure to this fungus often results in subacute disease. Pulmonary cryptococcosis is known to occur in people with acquired immunodeficiency syndrome (AIDS) and in those in immunocompromised states, such as patients with diabetes mellitus, liver cirrhosis, leukemia, and T-cell immunodeficiency diseases, including severe combined immunodeficiencies, and in patients undergoing organ transplantation or those on immunosuppressive regimens. Pulmonary cryptococcosis presents a broad spectrum

[1]Division of Chest Medicine, Department of Internal Medicine, Tungs' Taichung Metroharbor Hospital, Taichung, Taiwan.
Address reprint requests to: Dr. Erh-Lun Chen, Division of Chest Medicine, Department of Internal Medicine, Tungs' Taichung Metroharbor Hospital, No. 699, Sec. 8, Taiwan Blvd., Wuqi Dist., Taichung City 435, Taiwan (R.O.C)

of abnormal chest image appearances, including both single or multiple nodules, segmental consolidation, cavitation, bilateral bronchopneumonia, a diffuse miliary pattern, mass-like appearances, or mixed patterns [2]. CT appearances of cavitation and halo signs are more typically seen in immunocompromised patients than in non-compromised patients. Immunocompetent patients more often appear with solitary and well-defined nodules [3].

Case Presentation

In January 2020, a 48-year-old Taiwanese male who had a past medical history of hypertension with medication for 20 years presented at our department. He was a non-smoker, with a height of 168 cm, a weight of 120 kg and a body mass index of 42.5 kg/m^2. He consumed alcohol socially only. He had had a chronic cough with whitish sputum for 4 to 5 months. During this period, he did not have symptoms such as fever, dyspnea, hemoptysis or body weight loss. Therefore, he underwent a self-paid, complete health examination. Laboratory data revealed a white blood cell count of 10.8 k/μL, with 58.8% neutrophils, 31.2% lymphocytes, 7.9% monocytes, 1.5% eosinophils, and 0.6% basophils. HIV, HBsAg, anti-HCV, VDRL, TPHA, rheumatic factor, ANA and tumor marker were all negative. He also underwent an esophagogastroduodenoscopy, colonoscopy, sonography (abdomen, thyroid and prostate), brain MRI and angiography of the coronary artery, but all without significant findings. However, chest high resolution computed tomography showed multiple nodules scattered in the lung parenchyma, as well as several eccentric cavities with irregular walls in the bilateral upper lobes and right lower lobe (Figure 1). The largest cavity was 1.7 cm and was located in the right upper lobe.

The patient had been referred by his physician to our thoracic outpatient department. Physical examination was unremarkable. His HbA1C was 5.6%, and in the normal range. Serum aspergillus antigen was negative, but serum cryptococcal antigen showed 1:32(+). Lumbar puncture and blood culture were negative. Bronchoscopy was arranged under a suspicion of subacute infection such as tuberculosis, cryptococcosis or aspergillosis. The cytologic examination of the broncho-alveolar lavage revealed no findings, but the fungus culture of the

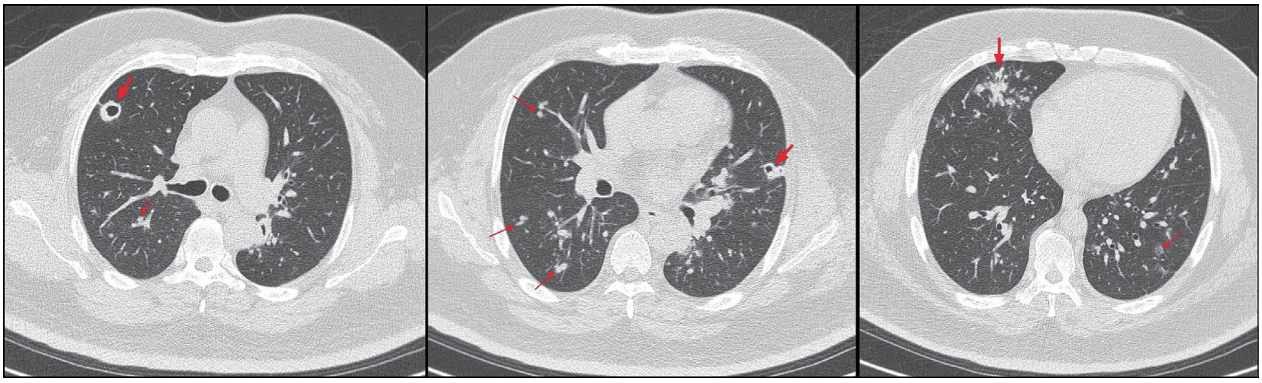

Fig. 1. The regions with cavities (diameter: a 17 mm cavity at the right upper lobe and a 12 mm cavity at the left upper lobe) and nodules were seen in the chest computed tomography series in the axial view before treatment.

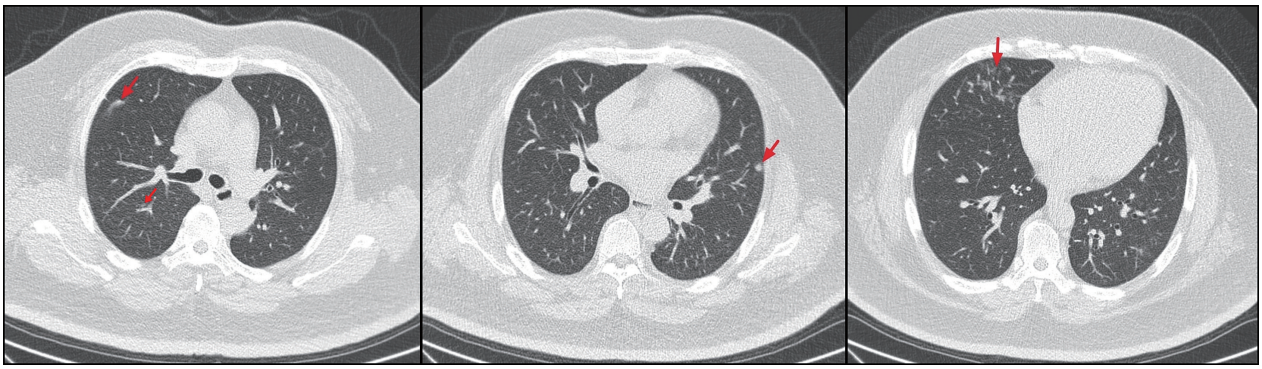

Fig. 2. Resolution of cavities and nodules after 6 months of antifungal therapy.

broncho-alveolar lavage yielded Cryptococcus grubii. The patient was treated with fluconazole 600 mg/day, based on his body weight, for 6 months. Repeated imaging 6 months later revealed resolution of most of the cavitary lesions and nodules (Figure 2).

Discussion

Cryptococcosis occurs in various parts of the world. Cryptococcus neoformans var. grubii (serotype A) and Cryptococcus neoformans var. neoformans (serotype D) were previously classified as neoformans species. However, it has been recommended that the serotype A Cryptococci be considered as a single variety based upon genotypic differences [4-5]. Meanwhile, these 2 serotypes differ in geographic prevalence and dermatotropism. Cryptococcus neoformans var. grubii (serotype A) is a widespread saprobic yeast throughout the world and accounts for over 70% of the world's cryptococcosis. It is found in the feces of pigeons or other birds such as sparrows and parrots. The overwhelming majority of isolates recovered from AIDS patients throughout the world are serotype A. It is an opportunistic pathogen of immunocompromised patients, with HIV infection, corticosteroid therapy, hematological malignancies, and solid organ transplantation identified as major risk factors [6]. Infections caused by Cryptococcus var. neoformans (serotype D) in such individuals are more prevalent in isolated geographic areas, especially northern Europe, Denmark, France and Italy. Serotype D is more strongly correlated with older patients, skin infections, and use of corticosteroids. Serotype D is more acute in its clinical course and patients are more likely to develop fever, and cutaneous and systemic infection [7]. In the natural environment, Cryptococcus neoformans species can be isolated from avian species, especially from pigeons, decayed wood and soil contaminated with avian excreta [1,8]. Mammalian infection with Cryptococcus neoformans species is usually acquired by the inhalation of airborne spores or yeasts. The yeast cells may disseminate to any part of the body, but Cryptococcus neoformans species is more neurotropic; the typical, life-threatening clinical manifestation of cryptococcosis is meningoencephalitis [9]. Cryptococcal disease occurs primarily in people with impaired immunity, but individuals with normal host defenses may also develop grave infections [10].

In immunocompetent hosts, single or mul-

tiple pulmonary nodules are the most common findings [11-12]. This patient was a 48-year-old male with no apparent underlying conditions that could lead to an immunocompromised state, such as diabetes mellitus, liver cirrhosis, AIDS, or being under immunosuppressive medication. An inquiry into his medical history revealed that the patient had fed pigeons in his garden every morning and evening during the past 5 years. Though the causal relationship between pulmonary cryptococcus and exposure to birds in this case was not well-established, this exposure, and the effect of the patient's obesity on his immunity, could be considered as risk factors. A previous study revealed that cavitation within nodules was significantly less common in immunocompetent patients than in immunocompromised patients [13]; however, this immunocompetent individual presented with both multiple nodules and cavitations.

Pulmonary cryptococcosis is known to occur in patients with AIDS and in those with an immunocompromised status, such as patients on immunosuppressive regimens or those undergoing organ transplantation. However, it can also occur in immunocompetent subjects [14]. Radiographic image studies reveal that single or multiple pulmonary nodules are the most common findings in immunocompetent hosts, though immunocompromised hosts have a wide variety of radiographic abnormalities, including single or multiple nodules that progress to cavitation, segmental consolidation or a bronchopneumonia pattern [1]. A previous study found that cavitation within nodules and parenchymal consolidations were significantly less common in immunocompetent patients than in immunocompromised patients [15]. In another retrospective evaluation of 136 patients with pulmonary cryptococcosis, including 94 immunocompromised and 42 immunocompetent patients, cavitation was significantly more common among the immunocompromised patients (31 patients) than among the immunocompetent patients (4 patients) [16].

The medication of choice for cryptococcosis without central nervous system involvement is fluconazole. In both symptomatic and asymptomatic immunocompetent patients, fluconazole 400 mg/day orally for 6 to 12 months is suggested [12,16]. Antifungal therapy can prevent or diminish the risk of disease progression. Oral itraconazole or voriconazole 200 mg twice daily may be the alternative choice if fluconazole is not available or is contraindicated. In cryptococcal meningitis or severe pulmonary cryptococcosis, flucytosine is used in combination therapy with amphotericin B deoxycholate as first-line therapy at a dosage of 100 mg/kg/day [17]. Mortality was associated with underlying diseases including malignancy, chronic hepatitis and diabetes. These observations suggest that, as in many other invasive fungal infections, host immunity plays a major role in determining the outcome and prognosis [3]. A recent study of pulmonary cryptococcosis in both immunocompromised and non-compromised patients showed that 70.3% (n = 71) were successfully treated [18]. However, another study showed the mortality rate of pulmonary cryptococcosis in HIV patients was 74% after the first year post-diagnosis [19]. Fungemia is an important manifestation of cryptococcosis, and it can predict a poorer prognosis; therefore, every patient with cryptococcosis should have blood cultures performed for fungal isolation [20].

Most of the previous case reports related to C. neoformans var. grubii involved HIV patients and patients in immumocompromised states [16]. Our patient was not an immunocompro-

mised patient, but still developed a progressive pattern of pulmonary cryptococcosis, including cavitation lesions within nodules. According to previous reports, pulmonary cryptococcosis in non-immunocompromised and immunocompetent subjects might be related to fungus-contaminated environmental exposure, hormonal influences, or a genetic predisposition, all of which have been suggested as contributing factors [16-17].

Although the long-term exposure of this patient to wild pigeons could not be confirmed as the cause of the disease, it drew our attention to the importance of environmental exposure. It reminded us that pulmonary cryptococcosis is not just confined to immunocompromised patients, and that a substantial proportion of patients who are apparently immunocompetent could develop a more aggressive presentation like cavitary lesions within multiple nodules [21]. Clinical presentations and outcomes of cryptococcal infections are related to host immune status; nevertheless, long-term treatment is required to achieve patient improvement.

Conclusion

Pulmonary cryptococcosis continues to cause significant morbidity and mortality in immunocompromised as well as immunocompetent patients. Cryptococcus neoformans var. grubii is the usual cause of disease among immunocompetent patients worldwide. Clinical presentations and outcomes of cryptococcal infections are affected by host immune status, and the major choices of treatment are antifungal drugs. Above all, clinicians should keep in mind that pulmonary cryptococcosis can not only present as regions of nodules, but also progress to cavitary lesions in immunocompetent patients. Early diagnosis based on symptoms and special imaging findings may help improve the prognosis.

References

1. Kwon-Chung KJ, Fraser JA, Doering TL, *et al*. Bahn Cryptococcus neoformans and Cryptococcus gattii, the etiologic agents of cryptococcosis. Cold Spring Harb Perspect Med 2014; 4: a019760.
2. Skolnik K, Huston S, Mody CH. Cryptococcal lung infections. Clin Chest Med 2017 Sep; 38(3): 451-464.
3. Setianingrum F, Rautemaa-Richardson R, Denning DW. Pulmonary cryptococcosis: a review of pathobiology and clinical aspects. Med Mycol 2019 Feb 1; 57(2): 133-150.
4. Hiremath SS, Chowdhary A, Kowshik T, *et al*. Long-distance dispersal and recombination in environmental populations of Cryptococcus neoformans var. grubii from India. Microbiology 2008; 154: 1513-1524.
5. Franzot SP, Salkin IF, Casadevall A. Cryptococcus neoformans var. grubii: separate varietal status for Cryptococcus neoformans serotype A isolates. J Clin Microbiol 1999; 37: 838.
6. Bastón Paz N, Hernández Betancor A, Esparza Morera R, *et al*. Pulmonary nodules: an unusual onset of HIV infection belatedly diagnosed. Rev Iberoam Micol 2019 Jul-Sep; 36(3): 151-154.
7. Dromer F, Mathoulin S, Dupont B, *et al*. Individual and environmental factors associated with infection due to Cryptococcus neoformans serotype D. French Cryptococcosis Study Group. Clin Infect Dis 1996 Jul; 23(1): 91-6.
8. Gugnani, HC, Mitchell TG, Litvintseva AP, *et al*. Isolation of Cryptococcus gattii and Cryptococcus neoformans var. grubii from the flowers and bark of eucalyptus trees in India. Med Mycol 2005; 43: 565-569.
- ●. Vu K, Garcia JA, Gelli A. Cryptococcal meningitis and anti-virulence therapeutic strategies. Front Microbiol 2019 Feb 26; 10: 353.
9. Srikanta D, Santiago-Tirado FH, Doering TL. Cryptococcus neoformans: historical curiosity to modern pathogen. Yeast 2014 Feb; 31(2): 47-60.
10. Morita S, Shirai T, Asada K, *et al*. Pulmonary cryptococcosis presenting with a large cavity. Respirol

Case Rep 2014 Jun; 2(2): 61-3.

11. Fisher JF, Valencia-Rey PA, Davis WB. Pulmonary cryptococcosis in the immunocompetent patient — many questions, some answers. Open Forum Infect Dis 2016; 3(3): 1-6.
12. Chang WC, Tzao C, Hsu HH, *et al*. Pulmonary cryptococcosis: comparison of clinical and radiographic characteristics in immunocompetent and immunocompromised patients. Chest 2006; 129: 333-340.
13. Xie LX, Chen YS, Liu SY, *et al*. Pulmonary cryptococcosis: comparison of CT findings in immunocompetent and immunocompromised patients. Acta Radiol 2015 Apr; 56(4): 447-53.
14. Qu J, Zhang X, Lu Y, *et al*. Clinical analysis in immunocompetent and immunocompromised patients with pulmonary cryptococcosis in western China. Sci Rep 2020 Jun 10; 10(1): 9387.
15. Xie X, Xu B, Yu C, *et al*. Clinical analysis of pulmonary cryptococcosis in non-HIV patients in south China. Int J Clin Exp Med 2015 Mar 15; 8(3): 3114-9.
16. Maziarz EK, Perfect JR. Cryptococcosis. Infect Dis Clin North Am 2016 Mar; 30(1):179-206.
17. Huang J, Lan C, Li H, *et al*. Retrospective analysis of 117 Chinese patients with pulmonary cryptococcosis. Chest 2016; 149: A124.
18. Meyohas MC, Roux P, Bollens D, *et al*. Pulmonary cryptococcosis: localized and disseminated infections in 27 patients with AIDS. Clin Infect Dis 1995 Sep; 21(3): 628-33.
19. Pasqualotto AC, Bittencourt Severo C, de Mattos Oliveira F, *et al*. An analysis of 28 cases with emphasis on the clinical outcome and its etiologic agent. Rev Iberoam Micol 2004 Sep; 21(3): 143-6.
20. Lui G, Lee N, Ip M, *et al*. Cryptococcosis in apparently immunocompetent patients. QJM 2006 Mar; 99(3): 143-51.

Acute Eosinophilic Pneumonia after Use of E-cigarettes: A Case Report

Po-Wei Hu[1], Fang-Chi Lin[1]

Use of electronic cigarettes (e-cigarettes) can have serious adverse effects on the respiratory tract. This is termed e-cigarette or vaping product use associated lung injury (EVALI). EVALI involves more than 1 mechanism, and reflects a spectrum of disease processes. Acute eosinophilic pneumonitis (AEP) is a relatively uncommon pattern of EVALI. Here, we reported a previously healthy young man who developed AEP following vaping for 4 months. ***(Thorac Med 2022; 37: 198-204)***

Key words: e-cigarette, vape, e-cigarette or vaping product use associated lung injury (EVALI), acute eosinophilic pneumonia (AEP)

Introduction

Electronic cigarettes (e-cigarettes) are battery-operated devices that heat to aerosolize liquids, mixtures of nicotine, and flavorings for inhalation [1-2]. Since their invention in China in 2003 and introduction to Europe and the United States (US) in 2006 and 2007, respectively [1], the numbers of e-cigarette users have continued to skyrocket, with the most dramatic rise in adolescents in the US [1-3]. In addition to aiding in smoking cessation [2, 4], e-cigarettes have been regarded as a safer substitute for the conventional cigarette because of the absence of combustion, which generates various harmful substances [2-4]. However, reports from animal models suggested that exposure to e-cigarettes might be directly toxic to lung tissues and impair the host defense against pathogens [2]. In 2019, the US Centers for Disease Control and Prevention (CDC) reported an epidemic of a newly identified lung disease caused by vaping, termed e-cigarette or vaping product use associated lung injury (EVALI). EVALI has received a lot of attention because the CDC reported more than 2,800 cases of lung injuries requiring hospitalization and 68 deaths across all 50 states by mid-February 2020 [5-6].

EVALI is a heterogeneous collection of pneumonitis patterns, including lipoid pneumonitis, hypersensitivity pneumonia, organizing pneumonia, eosinophilic pneumonia (EP), and others. [7]. An association was found between inhalational exposures and acute eosinophilic

[1]Department of Chest Medicine, Taipei Veterans General Hospital, Taipei, Taiwan, R.O.C.
Address reprint requests to: Dr. Fang-Chi Lin, Department of Chest Medicine, Taipei Veterans General Hospital, Taipei, Taiwan

pneumonia (AEP) [8-9], which is not a common pattern in EVALI [10]. Here, we present the case of a graduate student who developed AEP following the use of e-cigarettes.

Case Report

A previously healthy 23-year-old male graduate student presented to the emergency department (ED) of our hospital with a 3-day history of intermittent fever and chills. One week prior to this presentation, he experienced intractable cough with increased sputum, for which he visited a general practitioner. His condition did not improve despite antitussive and antibiotic treatment.

He denied any respiratory disease such as asthma, sinusitis, or chronic pulmonary disease. There were no preceding common cold-like symptoms. He denied any travel history to areas with confirmed cases of coronavirus disease 2019 (COVID-19) or any contact with ill individuals. He denied illicit drug use, alcohol consumption, or traditional cigarette smoking; however, he had been vaping 30 minutes per day (disclosure of the brand was refused) for 4 months, and did not quit until 1 to 2 weeks before this presentation, when there was a foreign body sensation in the throat.

In the ED, he was afebrile with body temperature of 37.2 degrees Celsius, blood pressure of 152/118 mmHg, respiratory rate of 20 breaths per minute, and heart rate of 90 beats per minute. His oxygen saturation was 98% while breathing ambient air. On physical examination, he revealed no respiratory distress and his breathing sound was unremarkable.

Laboratory examination disclosed leukocytosis (18,200 per mm^3) with a high percentage of eosinophils (37.7%), and an elevated C-reactive protein level (2.08 mg/dL, reference range: <0.5 mg/dL). The tests for renal and hepatic function were within normal limits. The BIOFIRE® FILMARRAY® Respiratory◦*2 plus*◦Panel (bioMérieux, Inc., Marcy-l'Étoile, France) qualitative multiplexed nucleic acid-based diagnostic method was used for the rapid test, which revealed negative results for influenza virus, human metapneumovirus, parainfluenza virus, respiratory syncytial virus, *Bordetella pertussis, Chlamydophila pneumoniae*, and *Mycoplasma pneumoniae* on nasopharyngeal swab. Compared with the results of the previous chest radiography, which showed no active lung lesion (Figure 1A), there were newly-developed alveolar processes in bilateral apical lung areas (Figure 1B). Blood and sputum were obtained for bacterial, fungal, and mycobacterial cultures. He was discharged from the ED and amoxicillin/clavulanate was prescribed as empirical treatment under the tentative diagnosis of community-acquired pneumonia.

He then sought medical attention at the pulmonology outpatient department because there was no symptomatic improvement after a 5-day course of empirical antibiotics. Follow-up chest radiography revealed no regression. The bacterial and fungal cultures of the blood and sputum, the sputum acid-fast stain, and serologic tests for *Chlamydophila pneumoniae, Mycoplasma pneumoniae, Cryptococcal* antigen, and *Aspergillus* galactomannan antigen were all negative. Computed tomography (CT) of the chest disclosed patchy consolidation and ground-glass opacities (GGO) in the bilateral upper lung fields, with a peripheral predominance, and enlarged lymph nodes in paratracheal and paraaortic areas (Figure 2). Non-infectious diseases such as autoimmune disease-related interstitial lung disease or allergic lung

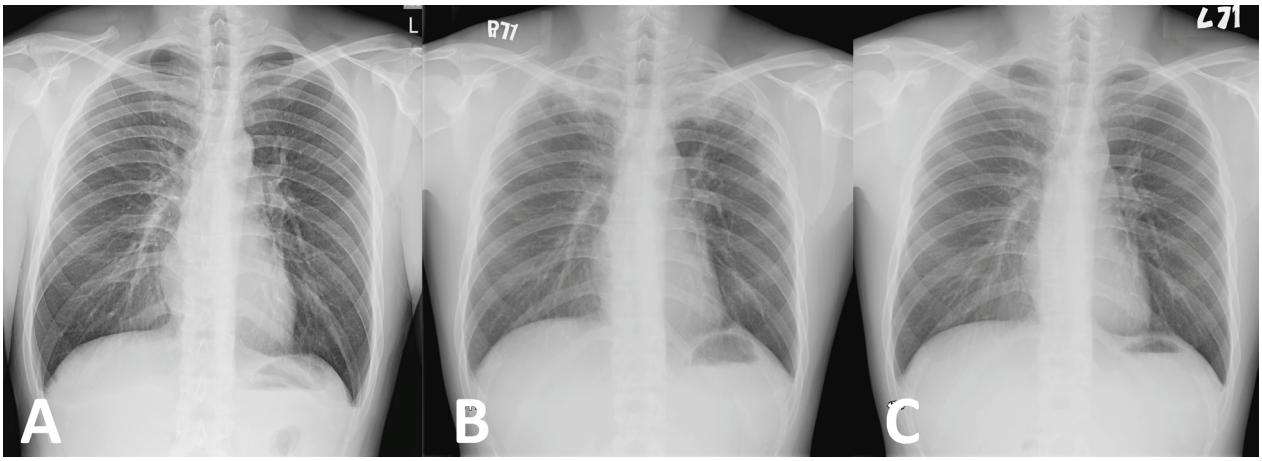

Fig. 1. Serial Changes in Chest Radiography.(1A). Chest radiography taken 3 months before presentation showed no active lung lesion.(1B). Chest radiography taken on the day of presentation showed airspace lesions in bilateral apical areas; (1C). Chest radiography taken 10 days after steroid treatment showed marked regression of the apical lesions.

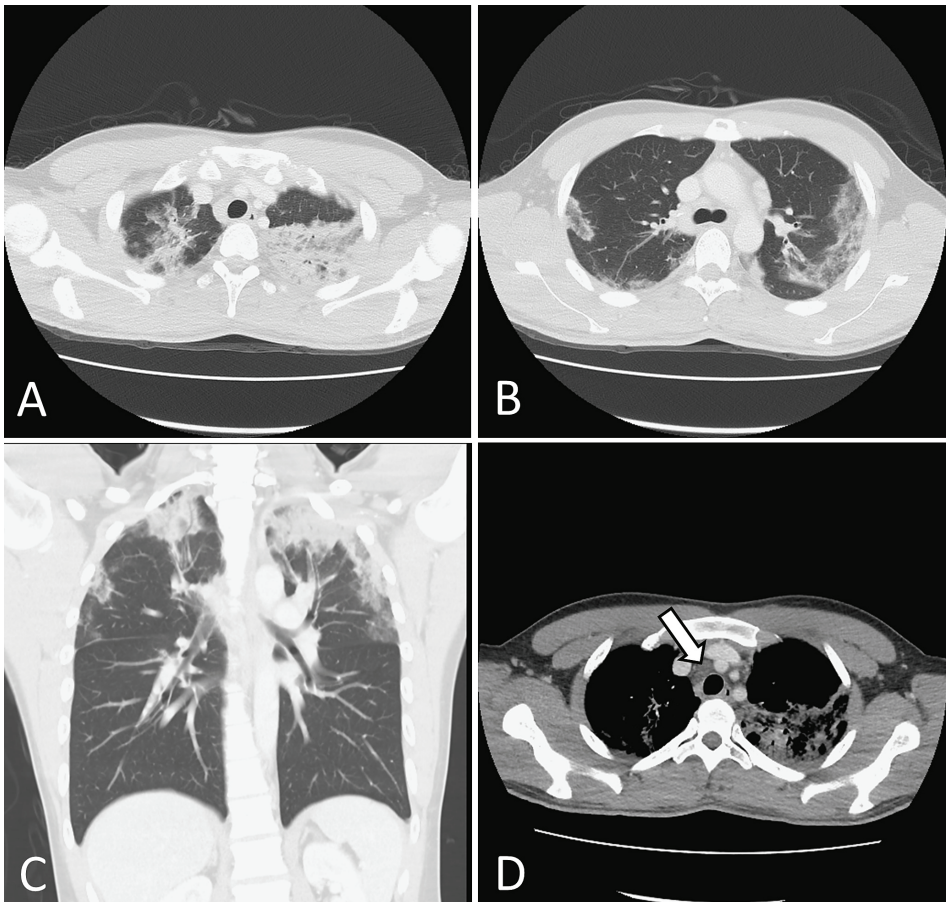

Fig. 2. Computed Tomography of the Chest before Treatment.
2A. Consolidation in bilateral apical regions.
2B. Ground-glass opacity in bilateral upper lobes with a peripheral predominance.
2C. Airspace lesions showing an upper zone predominance.
2D. Enlarged mediastinal lymph nodes in the right paratracheal region (arrow).

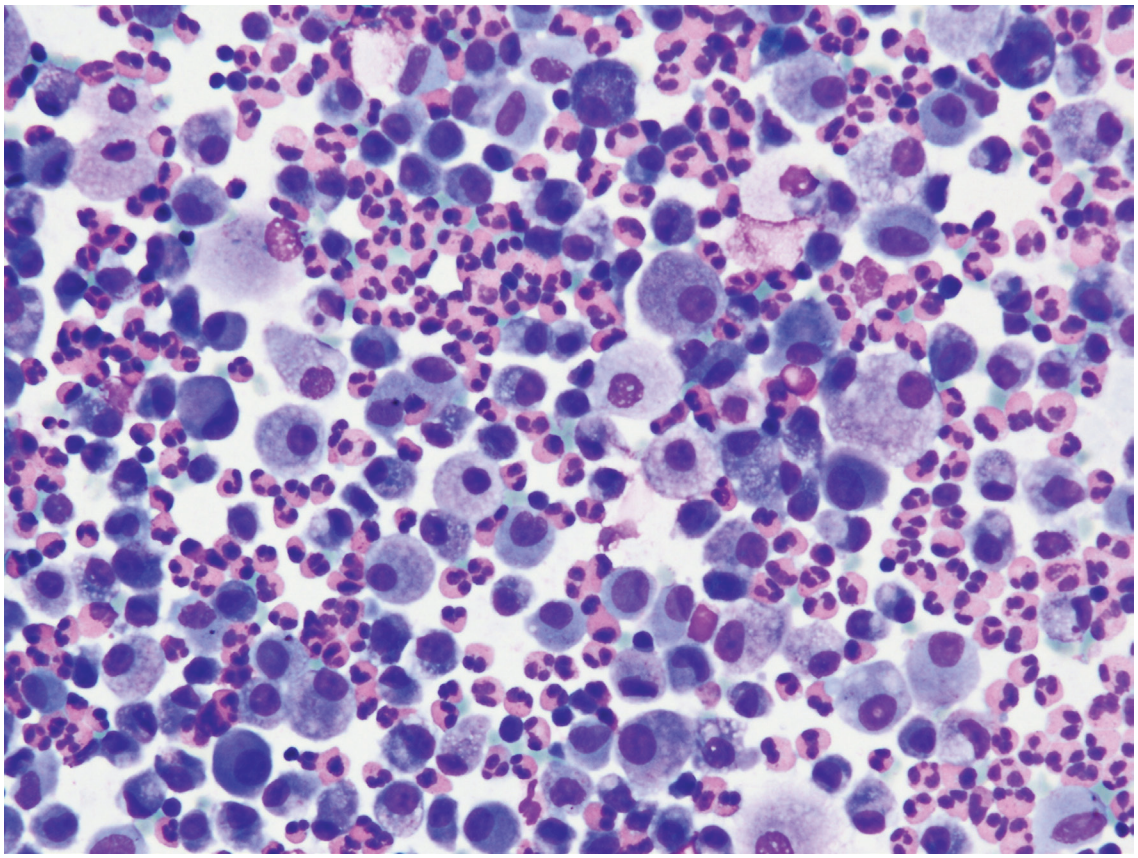

Fig. 3. Significant Increases in Eosinophils in Bronchoalveolar Lavage Fluid (Liu's Stain 400X).

disease were considered, but no autoantibodies or associated signs were detected. However, there was a marked increase in the serum total IgE level (1198 kU/l, reference range: <200 kU/l).

Diagnostic bronchoalveolar lavage (BAL) was recommended because of persistent symptoms and unresolved pulmonary lesions. However, no remarkable abnormality was observed within visible range during the bronchoscopic examination. Significant increases in the percentage of eosinophils (40%) were observed in the BAL fluid (Figure 3). There were no malignant cells or parasites in the BAL cytological examinations and cultures of BAL fluid were negative for bacteria, viruses, and fungi. No other infectious etiologies, including *Tuberculosis, Legionella, Strongyloides*, and *Pneumocystis jirovecii*, were identified.

Owing to remarkable eosinophilia in the BAL fluid and that no infectious etiologies were found, he was started on prednisolone 40 mg/day orally under the diagnosis of AEP. He became afebrile within 24 hours, and his cough abated during the following 3 days. Another chest radiography performed 10 days after prednisolone treatment showed marked regression of the air-space lesions in the bilateral apical region (Figure 1C); the serum total IgE levels (159 kU/l) and eosinophil percentage (0.8%) had decreased to normal limits, as well. As of this writing, he is on a tapering dose of prednisolone

and doing well 4 months after the diagnosis. Oral prednisolone will be discontinued soon.

Discussion

Eosinophilic pneumonia (EP) comprises a broad range of infectious and

noninfectious pulmonary conditions that involve accumulations of eosinophils in the alveolar space and the interstitium [8-9]. AEP was first described in 1989 as an acute febrile illness, with diffuse bilateral lung opacities and eosinophilia in BAL, and potentially rapid progression to acute respiratory failure [8-10]. AEP is also characterized by prompt clinical improvement after treatment, with no relapses, and improvement of radiographic abnormalities without fibrosis [8-11].

The first 4 reported cases of AEP had unknown etiologies; however, further investigations suggested that AEP can be idiopathic or have identifiable causes, including tobacco smoke, environmental or occupational dust exposures, toxin inhalations, infection, and medications [8-10]. Moreover, several studies highlighted the association between AEP and smoking. A newly initiated smoking habit, alterations in an existing smoking habit (including restarting smoking and increasing the number of cigarettes smoked), and short-term exposure to passive smoking can probably result in AEP [8-9, 11].

To the best of our knowledge, the English-language literature linking e-cigarettes with AEP is scarce. Only 3 cases of e-cigarette-associated AEP were reported in PubMed [12-14]. They were 1 female and 2 male vapers aged from 18 to 23 years old. The symptoms included cough, shortness of breath, chest pain, facial flushing, nausea, vomiting, and fever, with a duration of 1 day to 2 weeks. At the initial presentation, none of them had an elevated eosinophil count in the peripheral blood, but there was significant eosinophilia in the BAL fluid. Serum IgE level with a mild elevation (279 kU/l) was available in 1 case. The intervals between vaping initiation and onset of symptoms were 1 hour in the first case and 2 months in the latter 2 cases. Intensive care unit care was needed in the latter 2 cases, and 1 of the patients was intubated. Nevertheless, the effect of corticosteroid treatment was dramatic, in that the symptoms showed improvement within 12 hours to 5 days. All of the 3 patients survived. Compared to the previously reported patients, our patient had a longer duration of vaping (4 months), but there was no significant desaturation at the initial presentation. In addition, he had significant peripheral blood eosinophilia and serum IgE elevation, which are more common in chronic EP (CEP). CEP and AEP share some pathophysiological features, such as significant eosinophil infiltrations in the pulmonary parenchyma and a favorable response to corticosteroid treatment [9]. Unlike AEP, CEP is not linked to smoking, but closely associated with allergic diseases, such as bronchial asthma, atopic dermatitis, and allergic rhinitis [9]. Since this patient denied asthma or sinusitis, CEP and Churg-Strauss syndrome were less likely [15].

Diagnosing AEP is a challenge, because it may be indistinguishable from community-acquired pneumonia at first, potentially leading to a misdiagnosis or delayed diagnosis [9]. The current diagnostic criteria for AEP were modified from those proposed by Philit et al. in 2002, and include the following: (1) acute respiratory illness of ≤1-month duration before presentation; (2) pulmonary infiltrates on chest radiography or CT scan; (3) pulmonary eosino-

philia as demonstrated by >25% eosinophils in the BAL differential cell count or EP on lung biopsy findings (transbronchial or surgical); and (4) absence of other specific pulmonary eosinophilic diseases, including eosinophilic granulomatosis with polyangiitis (Churg-Strauss syndrome), hypereosinophilic syndrome, and allergic bronchopulmonary aspergillosis. Patients with peripheral eosinophilia (total eosinophil count ≥500 cells/mL) and who satisfied diagnostic criteria 1, 2, and 4 were also included when patients did not undergo BAL or lung biopsy and the illness could not be explained by other potential diagnoses [9]. The current diagnostic criteria for CEP are quite similar to those for AEP, except the symptoms have to last more than 2 weeks [16].

Characteristic chest radiography findings of AEP were described as bilateral airspace opacity, interlobular septal thickening, and pleural effusions with no cardiomegaly [11]. The image presentation we reported here did not show characteristic findings of AEP; however, most of these referenced studies were based on only a small number of AEP patients [11]. The chest CT of our patient revealed mixed consolidation/GGO with peripheral and upper lung zone predominance, without significant interlobular septal thickening or pleural effusion. Actually, the CT patterns of AEP are diverse. A study on the CT findings of 29 AEP cases [11] showed that all the patients had bilateral GGO. One-third of the patients had centrilobular nodules. Interlobular septal thickening could be seen in 90% of the patients, and bilateral pleural effusion was common. The distribution of the infiltrates was mainly random (>50%); otherwise, peripheral was more common than central, and lower was more common than upper. Intrathoracic lymphadenopathy in EP is very rare, and is probably due to a hypersensitivity reaction [17-18]. Repeated chest CT was recommended for this patient for confirmation of the regression of mediastinal lymphadenopathy.

Determining the treatment strategy for AEP is dependent on whether the underlying cause is identifiable. Cessation of exposure to the offending agent is mandatory when AEP is caused by exogenous exposure [10]. Systemic corticosteroid is the mainstay therapy for AEP [8]. Spontaneous regression without corticosteroid treatment has been reported in patients with mild AEP [10]. There is no consensus on the optimal dose and duration of corticosteroid treatment. In clinical practice, the initial dose is determined by disease severity. In patients with severe hypoxemic respiratory failure requiring mechanical ventilation, intravenous methylprednisolone with doses ranging from 60 to 125 mg every 6 hours or equivalent is recommended. For those without respiratory failure at presentation, oral prednisone 40 to 60 mg daily or equivalent is started and then progressively tapered over 2 to 6 weeks, depending on the pace of improvement in symptoms and radiologic findings [8, 10, 19]. An earlier study showed no significant differences in symptomatic or radiographic resolution between a 2-week and a 4-week course of steroid therapy [19]. Relapse of AEP is rare and most patients had complete recovery [20].

Conclusion

Recent studies have shown that the mechanism of inflammation and that of cytokine stimulation were similar in both those who used e-cigarettes and those who smoked cigarettes [12-13]. AEP, an uncommon acute respiratory illness of varying severity, may be life-threaten-

ing if not promptly diagnosed and appropriately treated [8-10]. The patient's e-cigarette use history should be obtained and the physician should take AEP into consideration when approaching a patient with respiratory symptoms and pulmonary infiltrates with a recent history of e-cigarette use.

References

1. Kligerman S, Raptis C, Larsen B,*et al*. Radiologic, pathologic, clinical, and physiologic findings of electronic cigarette or vaping product use-associated lung injury (EVALI): evolving knowledge and remaining questions. Radiology 2020; 294: 491-505.
2. Chun LF, Moazed F, Calfee CS, *et al*. Pulmonary toxicity of e-cigarettes. Am J Physiol Lung Cell Mol Physiol 2017; 313: L193-L206.
3. Winnicka L, Shenoy MA. EVALI and the pulmonary toxicity of electronic cigarettes: a review. J Gen Intern Med 2020.
4. Borrelli B, O'Connor GT. E-cigarettes to assist with smoking cessation. N Engl J Med 2019; 380: 678-9.
5. Evans ME, Twentyman E, Click ES, *et a*. Lung Injury Response Clinical Task Force; Lung Injury Response Clinical Working Group. Update: interim guidance for health care professionals evaluating and caring for patients with suspected e-cigarette, or vaping, product use-associated lung injury and for reducing the risk for rehospitalization and death following hospital discharge - United States, December 2019. MMWR Morb Mortal Wkly Rep 2020; 68: 1189-94.
6. Layden JE, Ghinai I, Pray I, *et al*. Pulmonary illness related to e-cigarette use in Illinois and Wisconsin - Final report. N Engl J Med 2020; 382: 903-16.
7. Mukhopadhyay S, Mehrad M, Dammert P, *et al*. Lung biopsy findings in severe pulmonary illness associated with e-cigarette use (vaping). Am J Clin Pathol 2020; 153: 30-39.
8. Suzuki Y, Suda T. Eosinophilic pneumonia: A review of the previous literature, causes, diagnosis, and management. Allergol Int 2019; 68: 413-9.
9. De Giacomi F, Decker PA, Vassallo R, *et al*. Acute eosinophilic pneumonia: correlation of clinical characteristics with underlying cause. Chest 2017; 152: 379-85.
10. De Giacomi F, Vassallo R, Yi ES, *et al*. Acute eosinophilic pneumonia: causes, diagnosis, and management. Am J Respir Crit Care Med 2018; 197: 728-36.
11. Daimon T, Johkoh T, Sumikawa H, *et al*. Acute eosinophilic pneumonia: Thin-section CT findings in 29 patients. Eur J Radiol 2008; 65: 462-7.
12. Thota D, Latham E. Case report of electronic cigarettes possibly associated with eosinophilic pneumonitis in a previously healthy active-duty sailor. J Emerg Med 2014; 47: 15-7.
13. Arter ZL, Wiggins A, Hudspath C, *et al*. Acute eosinophilic pneumonia following electronic cigarette use. Respir Med Case Rep 2019; 27: 100825.
14. Puebla Neira D, Tambra S, Bhasin V, *et al*. Discordant bilateral bronchoalveolar lavage findings in a patient with acute eosinophilic pneumonia associated with counterfeit tetrahydrocannabinol oil vaping. Respir Med Case Rep 2020; 29: 101015.
15. Akuthota P, Weller PF. Eosinophilic pneumonias. Clin Microbiol Rev 2012; 25: 649-60.
16. Crowe M, Robinson D, Sagar M, *et al*. Chronic eosinophilic pneumonia: clinical perspectives. Ther Clin Risk Manag 2019; 15: 397-403.
17. Esme H, Sahin O, Sezer M, *et al*. Acute eosinophilic pneumonia accompanied by mediastinal lymphadenopathy and thrombocytopenia. J Natl Med Assoc 2006; 98: 1848-50.
18. Sugawara T, Ako H, Tsukaguchi K, *et al*. A case of eosinophilic pneumonia with histologically proven mediastinal lymph node involvement. Nihon Kyobu Shikkan Gakkai Zasshi 1993; 31: 608-13. [In Japanese English abstract]
19. Rhee CK, Min KH, Yim NY, *et al*. Clinical characteristics and corticosteroid treatment of acute eosinophilic pneumonia. Eur Respir J 2013; 41: 402-9.
20. Philit F, Etienne-Mastroïanni B, Parrot A, *et al*. Idiopathic acute eosinophilic pneumonia: a study of 22 patients. Am J Respir Crit Care Med 2002; 166: 1235-9.

Endobronchial Actinomycosis — a Case Report

Ko-Ling Chien[1], Chi-Li Chung[1,2], Chi-Long Chen[3]

Endobronchial actinomycosis is a rare manifestation of thoracic actinomycotic infection that can mimic malignancy, tuberculosis, fungal infection or lung abscess, and thus usually leads to a misdiagnosis. Here, we reported an unusual case of actinomycosis with endobronchial involvement that was initially misdiagnosed as a lung abscess with organizing pneumonia. Endobronchial actinomycosis was confirmed by bronchial pathology, and the patient was treated successfully with a 6-month course of antibiotics, showing both marked symptomatic and image improvement. The follow-up bronchoscopic image revealed nearly total resolution of the endobronchial nodule and no evidence of obscure abnormalities. This case highlights the critical role of bronchoscopy, rather than conventional chest computed tomography only, in the definite diagnosis of endobronchial actinomycosis. Repeated bronchoscopy following treatment is mandatory, given the close association of endobronchial actinomycosis with a broncholith, inhaled foreign body and lung cancer. ***(Thorac Med 2022; 37: 205-210)***

Key words: pulmonary actinomycosis, endobronchial actinomycosis, bronchoscopy

Introduction

Pulmonary actinomycosis, an unusual thoracic infection caused by Actinomyces, accounts for only 15% of human actinomycosis cases [1-2]. As both clinical presentations and radiological findings are not specific and vary widely among individuals, pulmonary actinomycosis is frequently misdiagnosed as malignancy, tuberculosis, fungal infection or lung abscess [3]. Moreover, endobronchial involvement is a rare manifestation of actinomycosis, and is often associated with a broncholith [4-5], inhaled foreign body [6], or lung cancer [7-8]. We herein reported a patient with endobronchial actinomycosis who presented with intermittent hemoptysis for the past 3 years and a right hilar mass lesion. He was initially misdiagnosed as having a lung abscess with organizing pneumonia.

Case Report

This 62-year-old male patient had a history

[1]Division of Pulmonary Medicine, Department of Internal Medicine, Taipei Medical University Hospital, Taipei, Taiwan, [2]School of Respiratory Therapy, College of Medicine, Taipei Medical University, Taipei, Taiwan, [3] Department of Pathology, Taipei Medical University Hospital, Taipei, Taiwan.
Address reprint requests to: Dr. Chi-Li Chung, Division of Pulmonary Medicine, Department of Internal Medicine, Taipei Medical University Hospital, No.252, Wusing St., Sinyi Dist., Taipei City 110301, Taiwan (R.O.C.)

of type 2 diabetes mellitus (DM) under treatment with metformin for many years, and L4/L5 spondylolisthesis status post-transforaminal lumbar interbody fusion surgery 7 years prior to this admission. He suffered from intermittent hemoptysis with a small amount of bright red blood in the sputum for the past 3 years. He reported no fever or other respiratory symptoms. He had no history of a dental hygiene problem or foreign body aspiration. He denied smoking, alcohol abuse or a betel nut chewing habit. His temperature was 36.9°C, pulse, 81 beats per minute, blood pressure, 131/90 mm Hg, and respiratory rate, 18 breaths per minute; oxygen saturation was 99% under room air, and did not decrease with exertion. There was no palpable cervical lymphadenopathy and chest auscultation revealed neither crackles nor a wheezing sound. Laboratory test results showed a white blood cell count of 9860/uL, with neutrophils at 61.9%, lymphocytes 18.9% and monocytes 8.0%. Hemoglobin was 12.7g/dl, platelet count 272000/uL, C-reactive protein 0.97mg/dl, and HbA1C: 9.6%. Chest radiograph showed a right hilar mass (Figure 1A), and chest computed tomography (CT) revealed a lobulated heterogeneously enhancing mass, about 5.24 x 3.07 cm in diameter and 3.37 cm in length, at the anterior segment of the right upper lung (Figure 1B). According to the image study report, lung cancer or an infectious process was highly suspected. However, the serial axial CT images did not reveal visible endobronchial lesions.

The patient refused bronchoscopy intervention to identify the potential endobronchial obstructive lesion, but he agreed to undergo CT-guided lung biopsy of the mass. The pathology report showed diffuse inflammatory cell infiltration with granulation tissue formations in the bronchial and alveolar spaces (Masson-bodies), compatible with the features of organizing pneumonia. Neither malignancy nor granulomatous infection was found. Moreover, the sputum bacterial culture grew Klebsiella pneumoniae, while sputum acid-fast stain and culture for Mycobacterium tuberculosis were negative. Accordingly, with the presumptive diagnosis of bacterial lung abscess with organizing pneumonia, based on the microbiology results and the antibiogram, moxifloxacin 400 mg was administered.

After the antibiotics therapy, the patient still

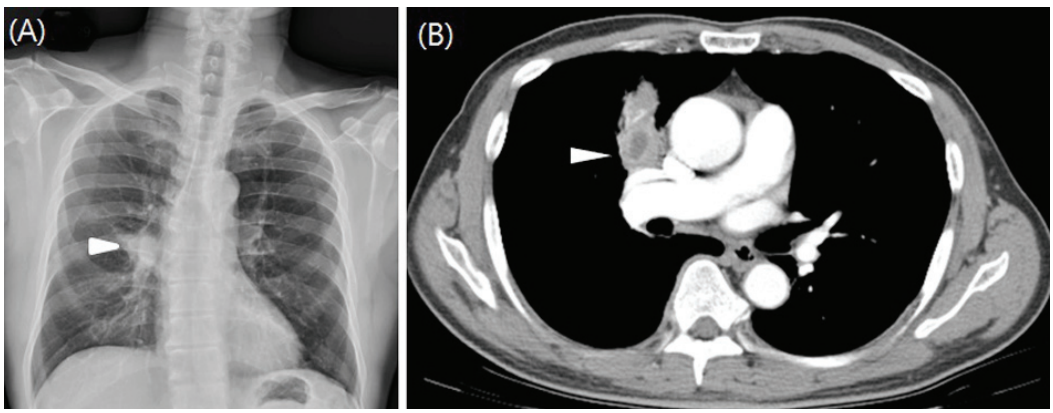

Fig. 1. The initial chest radiograph showed a right hilar mass (arrowhead) (A), and chest computed tomography (CT) revealed a lobulated heterogeneously enhancing mass (arrowhead) at the anterior segment of the right upper lung (B).

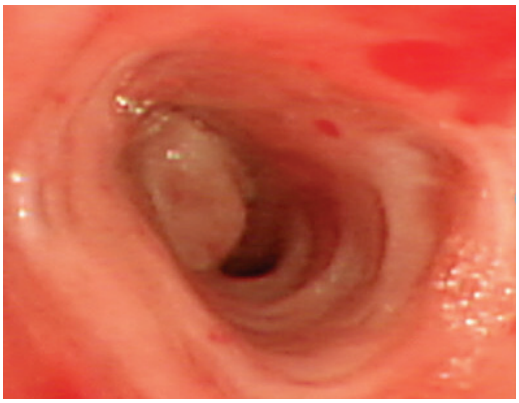

Fig. 2. Bronchoscopic examination showed a yellowish friable glossy nodule at the orifice of sub-segmental b of the anterior bronchus of the right upper lobe (RB3b).

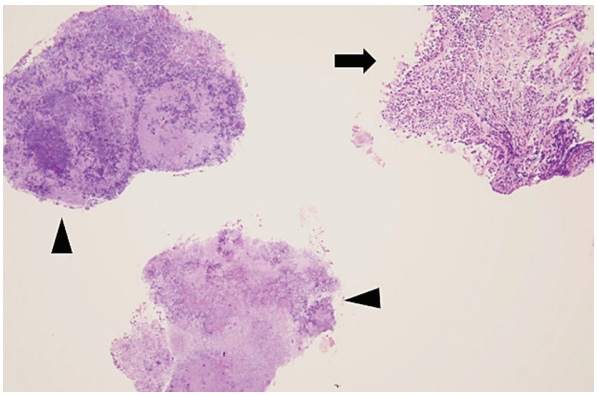

Fig. 3. Histopathologic examination of the endobronchial glossy nodule showed chronically inflamed bronchial tissue with granulation (arrow), and some Actinomyces bacterial clumps (sulfur granules) with basophilic radiating filaments (arrowhead). (Hematoxylin & Eosin stained, 100X magnification).

experienced intermittent hemoptysis, and the follow-up chest x-ray 1 month later revealed no resolution of the mass lesion. Repeated sputum cultures showed negative results. Therefore, in order to seek out the obscure etiology and possible endobronchial lesions, he underwent fiberoptic bronchoscopy, which disclosed a yellowish friable glossy nodule at the orifice of the sub-segmental branch of the anterior bronchus of the right upper lobe (RB3b), with partial obstruction of the lumen (Figure 2). Neither a foreign body nor a broncholith was identified. Bronchial biopsy was performed and the histological examination revealed some abscess formations with actinomyces-like "sulfur granules", and Gram staining disclosed Gram-positive bacterial clumps with basophilic radiating filaments (Figure 3). The diagnosis of endobronchial actinomycosis finally was confirmed.

The antibiotic regimen was shifted to oral amoxicillin-clavulanate, after which, the patient reported no further hemoptysis. The antibiotic treatment was continued for a total duration of 6 months, and the follow-up chest x-ray and chest CT revealed marked regression of the right upper lung mass lesion (Figures 4A and

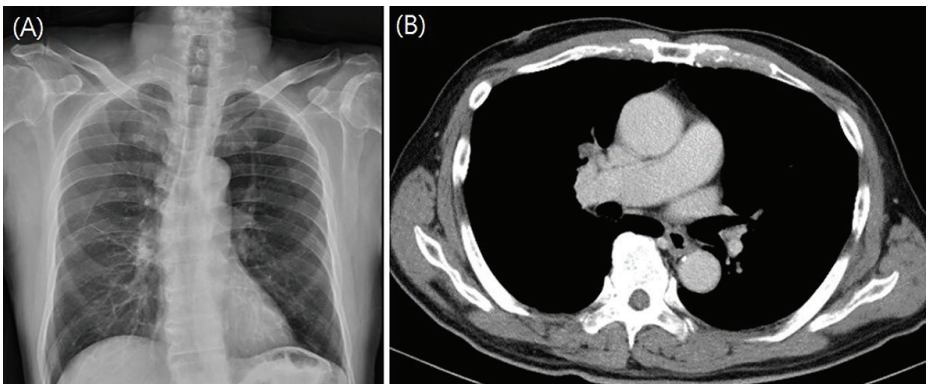

Fig. 4. Follow-up chest radiograph (A), and chest CT (B), following a 6-month amoxicillin-clavulanate treatment course revealed resolution of the right hilar mass.

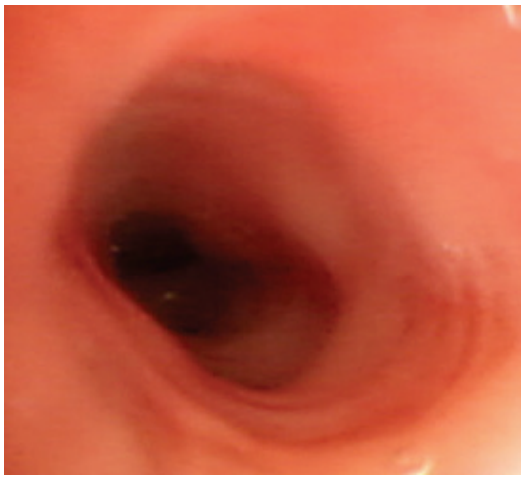

Fig. 5. Follow-up bronchoscopic examination showed complete resolution of the previous endobronchial nodule at the orifice of subsegmental b of the anterior bronchus of the right upper lobe (RB3b).

4B). Moreover, follow-up bronchoscopy was performed and showed complete resolution of the previous endobronchial nodule at the RB3 orifice and no residual abnormality (Figure 5).

Discussion

Actinomyces are a group of filamentous, anaerobic, Gram-positive bacteria. They are commensal flora of the pharynx and gastrointestinal and urogenital tract in humans, and rarely cause a chronic suppurative infection [1]. The infection site frequency is as follows: cervicofacial (55%), abdominopelvic (20%), and thoracopulmonic (15%). Endobronchial actinomycosis is an infrequent thoracopulmonic infection [2]. Pulmonary actinomycosis is acquired mainly through microaspiration of oropharyngeal materials; poor oral hygiene, preexisting dental disease and facial trauma are also important risk factors [9]. Moreover, underlying pulmonary disorders and chronic debilitating diseases prone to aspiration, including emphysema, chronic bronchitis, bronchiectasis, DM, alcoholism and neurologic diseases, may also increase the infection hazard [3]. The main symptoms include cough, productive sputum, chest pain, dyspnea, and hemoptysis [3]. The chest radiological findings are very diverse and have large-scale variations, ranging from peripheral lung infiltrates, multiple nodules, pleural effusions, and hilar and/or mediastinal lymphadenopathies to a cavitating mass involving the pleura, chest wall or even the spinal vertebrae [3,10].

In general, pulmonary actinomycosis exhibits a peripheral and lower lobe predominance, reflecting the role of aspiration in its pathogenesis [11]. As both clinical manifestations and radiological findings are non-specific and vary widely with time and among individuals [3], pulmonary actinomycosis is likely to be misdiagnosed as malignancy, tuberculosis, fungal infection or lung abscess, and there is often a delay in diagnosis [12]. A positive culture from an adequate specimen and the histopathological demonstration of sulfur granules in infected tissue are required for a definite diagnosis [3]. As it is difficult to isolate Actinomyces with bronchial brushing or washing for a distal airway lesion, fiberoptic bronchoscopy is usually not diagnostic unless there is an endobronchial lesion on which biopsy can be performed [13]. Therefore, a more invasive diagnostic procedure such as ultrasound- or CT-guided biopsy, or even surgical excision is usually needed for peripheral lesions [3].

Endobronchial actinomycosis is a rare manifestation of actinomycosis with infections located in the proximal airways [14]. It has been reported to be associated with an Actinomyces-contaminated broncholith or inhaled foreign body, often presenting as a proximal obstructive endobronchial nodule with distal post-ob-

structive pneumonia or atelectasis [4-6], which usually simulates lung cancer clinically [15]. Accordingly, bronchoscopy may not very useful for confirming parenchymal actinomycosis [16], but bronchial biopsy is mandatory for the diagnosis of endobronchial actinomycosis. The bronchial lesion often presents as a friable, exophytic necrotic nodule with purulent exudate [3, 16], and should be differentiated from bronchogenic carcinoma. Previous studies found that endobronchial actinomycosis had a favorable prognosis if recognized early and treated with antibiotics for a period of 3 to 12 months [3, 6, 14]. In addition, bronchoscopic removal of the broncholith or foreign body may facilitate a shorter duration of antibiotic treatment for endobronchial actinomycosis [17]. Further studies on using cryobiopsy or electrocautery as an adjunctive treatment are needed, given the risk of critical airway obstruction by endobronchial actinomycosis [6].

The initial CT-guided lung biopsy of our patient revealed a pattern of organizing pneumonia, and the preliminary sputum culture grew Klebsiella pneumoniae, which led to the misdiagnosis of lung abscess with a common pathogen. Organizing pneumonia has been depicted to be associated with various bacterial infections and, to the best of our knowledge, rarely with actinomycosis [18-19]. Moreover, previous studies found that co-infection with other bacteria, especially Gram-negative bacteria such as Eikenella corrodens and Actinobacillus actinomycetemcomitans, is not uncommon in thoracic actinomycosis [3, 20, 21], which might suggest the potential contribution of accompanying microorganisms to actinomycotic infection [22]. Although bacteria growth in the sputum culture may merely indicate colonization, co-infection with Klebsiella pneumoniae has seldom been reported. The current case indicates that actinomycosis is usually a mixed infection and that the histological finding of organizing pneumonia or the culturing of common pathogens does not suffice to exclude actinomycosis, and may lead to a misdiagnosis of organizing pneumonia or lung abscess.

In contrast to previous reports [4-6], the bronchoscopy for this patient did not reveal a broncholith or foreign body, but an endobronchial tumor with partial occlusion of the bronchi. The pathogenic process of endobronchial actinomycotic infection remains unknown. Nevertheless, a foreign body might not be identified at the initial bronchoscopy [6], and actinomycosis has been reported, not infrequently, to co-exist with lung cancer [7-8]. It thus seems essential to perform follow-up bronchoscopy after antibiotic treatment to exclude the presence of an associated foreign body or concealed bronchogenic carcinoma. Fortunately, after a 6-month antibiotic treatment course, our patient had obvious improvement in both respiratory symptoms and chest imaging, and the subsequent bronchoscopy showed nearly total resolution of the endobronchial nodule and no evidence of obscure abnormalities.

In conclusion, we have reported a rare case of endobronchial actinomycosis not linked with foreign body aspiration, that mimicked lung cancer, and that was misdiagnosed as a lung abscess with organizing pneumonia. Bronchoscopy is the key procedure for diagnosis of endobronchial actinomycosis, and repeated bronchoscopy following treatment response is mandatory, given the close relationship between endobronchial actinomycosis and other bacterial co-infections, a broncholith, inhaled foreign body and lung cancer.

References

1. Buchanan RE. Actinomycosis. In: Gibbons NE ed. Bergey's Manual of Determinative Bacteriology, 8th ed. Baltimore; Williams & Wilkins, 1974: 660-7.
2. ennhoff DF. Actinomycosis: diagnostic and therapeutic considerations and a review of 32 cases. Laryngoscope 1984; 94: 1198-1217.
3. Mabeza GF, Macfarlane J. Pulmonary actinomycosis. Eur Respir J 2003: 21: 545-551.
4. Kim TS, Han JH, Koh WJ, *et al*. Endobronchial actinomycosis associated with broncholithiasis: CT findings for nine patients. Am J Roentgenol 2005; 185(2): 347-353.
5. Tsubochi H, Endo S, Suhara K, *et al*. Endobronchial aspergillosis and actinomycosis associated with broncholithiasis. Eur J Cardiothorac Surg 2007; 31(6): 1144-1146.
6. Chouabe S, Perdu D, Deslée G, *et al*. Endobronchial actinomycosis associated with foreign body: four cases and a review of the literature. Chest 2002; 121(6): 2069-2072.
7. lade PR, Slesser BV, Southgate J. Thoracic actinomycosis. Thorax 1973; 28(1): 73-85.
8. Subramanian A, Lipatov K, Ghamande SA. Mimicking the mimicker: a case of concurrent actinomycosis and small cell lung cancer. Am J Respir Crit Care Med 2018; 197: A5456.
9. Sarkonen N, Könönen E, Summanen P, *et al*. Oral colonization with Actinomyces species in infants by two years of age. J Dent Res 2000; 79: 864-867.
10. Kim SR, Jung LY, Oh IJ, et al. Pulmonary actinomycosis during the first decade of 21st century: cases of 94 patients. BMC Infect Dis 2013; 13: 216.
11. Kwong JS, Muller NL, Godwin JD, *et al*. Thoracic actinomycosis: CT findings in eight patients. Radiology 1992; 183(1): 189-192.
12. Weese WC, Smith IM. A study of 57 cases of actinomycosis over a 36-year period. A diagnostic 'failure' with good prognosis after treatment. Arch Intern Med 1975; 135(12): 1562-1568.
13. Hsieh MJ, Liu HP, Chang JP, *et al*. Thoracic actinomycosis. Chest 1993; 104(2): 366-370.
14. Skehan N, Naeem M, Reddy RV. Endobronchial actinomycosis: successful treatment with oral antibiotics. BMJ Case Rep 2015; 2015(pii): bcr2015212754.
15. Ariel I, Breuer R, Kamal NS, *et al*. Endobronchial actinomycosis simulating bronchogenic carcinoma. Diagnosis by bronchial biopsy. Chest 1991; 99(2): 493-495.
16. Han JY, Lee KN, Lee JK, *et al*. An overview of thoracic actinomycosis: CT features. Insights Imaging 2013; 4(2): 245-252.
17. Ahn S, Chang JS, Kim YI, *et al*. A case of primary endobronchial actinomycosis presenting with a broncholith that was cured by bronchoscopic removal and short-term antibiotic treatment. Austin J Pulm Respir Med 2017; 4(2): 1057.
18. Alfaro TM, Bernardo J, Garcia H, *et al*. Organizing pneumonia due to actinomycosis: an undescribed association. Respiration 2011; 81(5): 433-436.
19. Fujita Y, Iikura M, Horio Y, *et al*. Pulmonary Actinomyces graevenitzii infection presenting as organizing pneumonia diagnosed by PCR analysis. J Med Microbiol 2012; 61(8): 1156-1158.
20. Morris JF, Sewell DL. Necrotizing pneumonia caused by mixed infection with Actinobacillus actinomycetemcomitans and Actinomyces israelii: case report and review. Clin Infect Dis 1994; 18(3): 450-452.
21. Jordan HV, Kelly DM. Persistence of associated Gram-negative bacteria in experimental actinomycotic lesions in mice. Infect Immun 1983; 40(2): 847-849.
22. Jordan HV, Kelly DM, Heeley JD. Enhancement of experimental actinomycosis in mice by Eikenella corrodens. Infect Immun 1984; 46: 367-371.

Successful Management of Tracheobronchial Injury with Endobronchial Stenting in an Adult with Thoracic Trauma

Tse-Bin Yang[1], Hsiu-Ling Cheng[2], Yun-Hsiang Chan[1], Shuenn-Wen Kuo[3]

Tracheobronchial injury (TBI) is a serious condition caused by blunt or penetrating trauma. Prompt diagnosis after the initial insult can sometimes be difficult due to subtle air-leakage. The management of TBI includes conservative treatment, endobronchial stenting and surgical repair. Here, we describe the case of a 27-year-old man who suffered from thoracic trauma with TBI and who was successfully managed with endobronchial stenting. ***(Thorac Med 2022; 37: 211-216)***

Key words: tracheobronchial injury, pneumothorax, pneumomediastinum, endobronchial stenting

Introduction

Tracheobronchial injury (TBI) is a rare but potentially life-threatening clinical scenario consequent to cervical and thoracic trauma. Clinical manifestations of TBI can be obscure initially, or present with delayed or refractory signs of air-leakage. Early detection of any airway defect is important. The treatment plan should be made individually for TBI patients based on underlying conditions and injury severity. Here, we present the case of an adult male who had suffered from TBI in a severe car accident.

Case Report

The patient was a 27-year-old male. He was a college student with no underlying disease. He was involved in a serious car accident and suffered contusion injury of the neck, right-side chest wall, and hip, and was sent to Taipei City Hospital Renai Branch. The patient's body temperature was 36°C, heart rate: 88 beats per minute, and respiratory rate: 20 breaths per minute. His blood pressure was 86/54mmHg and saturation by pulse oximetry was 97% under a nasal cannula at 3L/min. Physical examination showed right-side decreased breathing sounds.

[1]Division of Chest Medicine, Department of Internal Medicine, Taipei City Hospital Renai Branch, [2]Department of Thoracic Surgery, Taipei City Hospital Renai Branch, [3]Department of Thoracic Surgery, National Taiwan University Hospital.
Address reprint requests to: Dr. Tse-Bin Yang, Division of Chest Medicine, Department of Internal Medicine, Taipei City Hospital Renai Branch, 2F., No. 70, Sec. 3, Xinsheng N. Rd., Zhongshan Dist., Taipei City 104, Taiwan (R.O.C.)

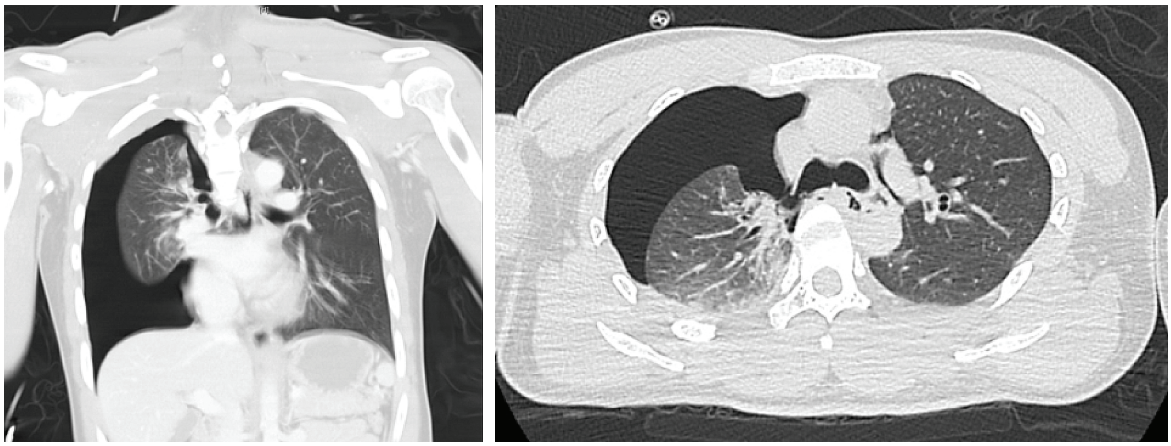

Fig. 1. Chest CT showed right pneumothorax with a collapsed right lung.

Chest radiograph and computed tomography (CT) at the emergency department revealed right 2nd and 3rd rib fractures, right C5 and C6 transverse process fractures, and right-side pneumothorax with a collapsed lung (Figure 1, Figure 2). Due to the right-side pneumothorax, a 28 French chest tube was inserted via the right 4th intercostal space.

However, persistent air-leakage from the chest tube and poor expansion of the lung were detected. Follow-up CT scan the next day showed that right-side pneumothorax and the collapsed right lung still remained. Pneumomediastinum with extension to the neck, and pneumopericardium were also noticed (Figure 3). Bronchoscopy showed laceration at the right vestibular fold and a large laceration at the right main bronchus (Figure 4). The right main bronchus laceration was about 0.7cm in length, and was located between the carina and the right secondary carina, near the right upper lobe orifice. It was covered by some blood and tissue debris. Due to tracheobronchial injury with continued air-leakage, the patient was transferred to National Taiwan University Hospital and another bronchoscopy was arranged for wound assessment.

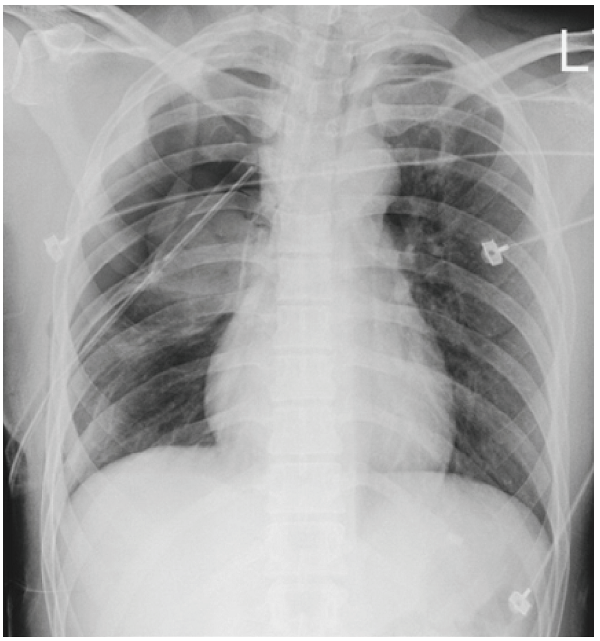

Fig. 2. Chest radiograph showed multiple rib fractures, right pneumothorax and a chest tube inserted via the right 4th intercostal space.

Under intravenous general anesthesia, flexible bronchoscopy was performed and a 12mm x 2cm endobronchial stent was deployed (Figure 5). The stent's location was modified using grasping forceps to ensure the laceration wound was fully covered without overlapping the carina or occluding the left main bronchus. After endobronchial stenting, the pneumothorax

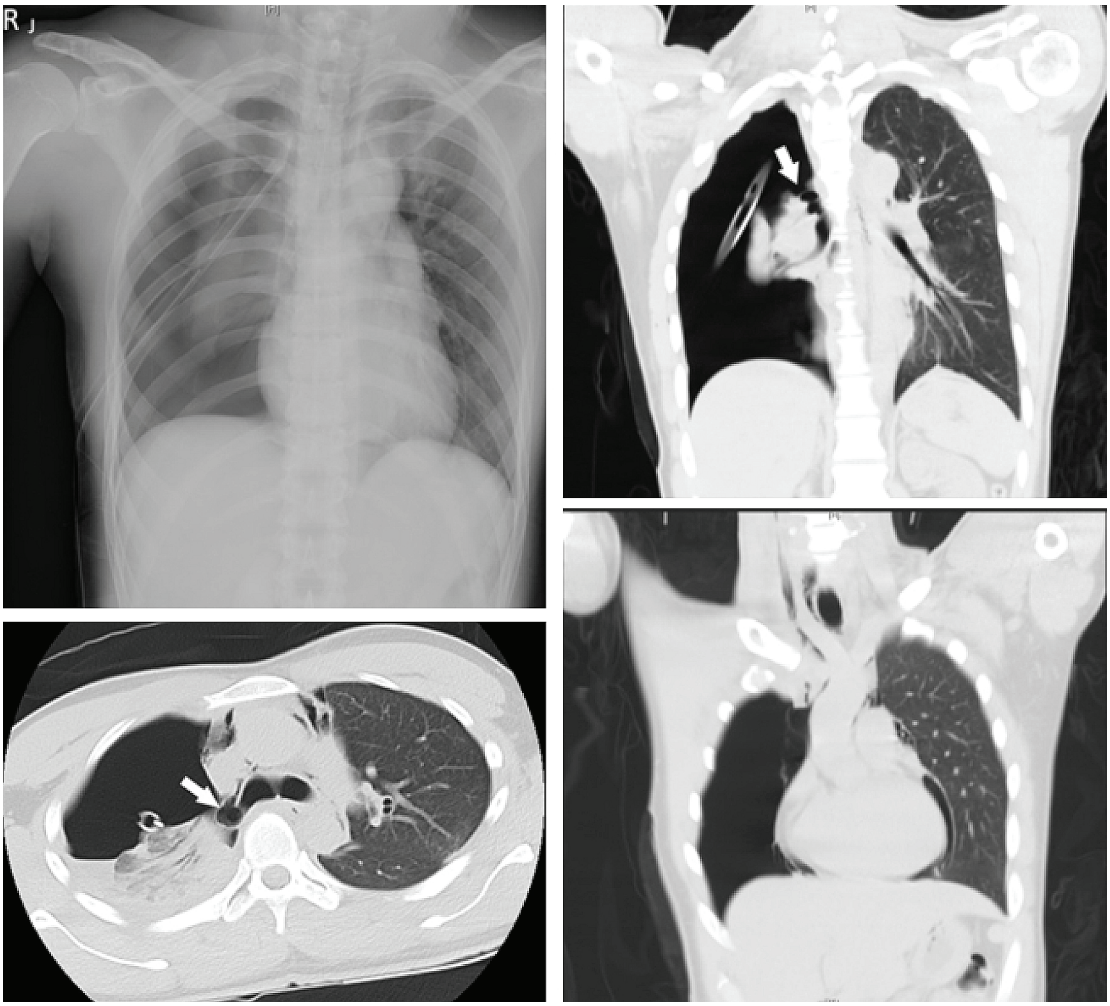

Fig. 3. Chest radiograph showed right pneumothorax. CT showed right pneumothorax, pneumomediastinum, pneumopericardium and a bronchial wall defect.

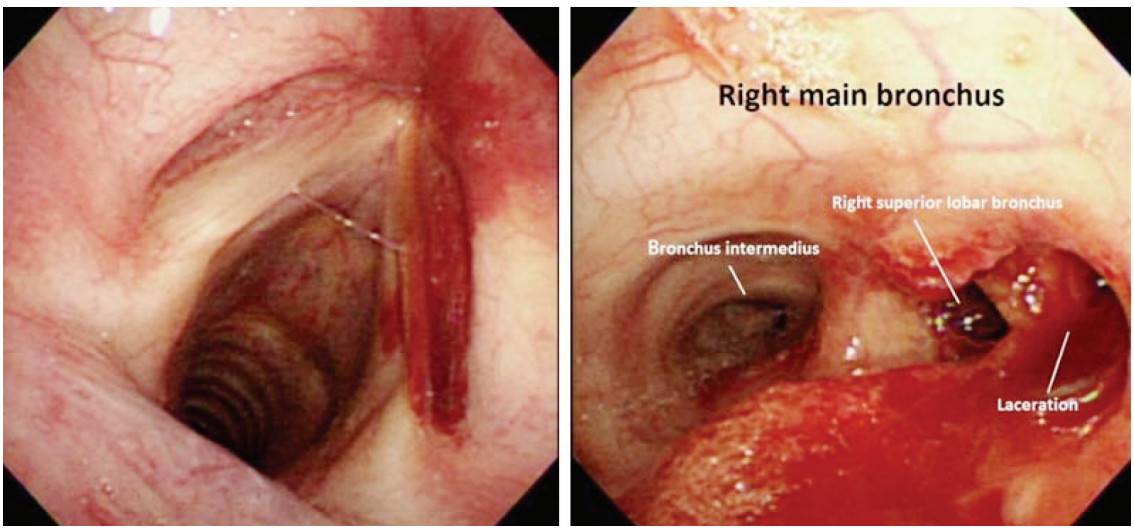

Fig. 4. Bronchoscopy showed laceration at the right vestibular fold and a large laceration at the right main bronchus.

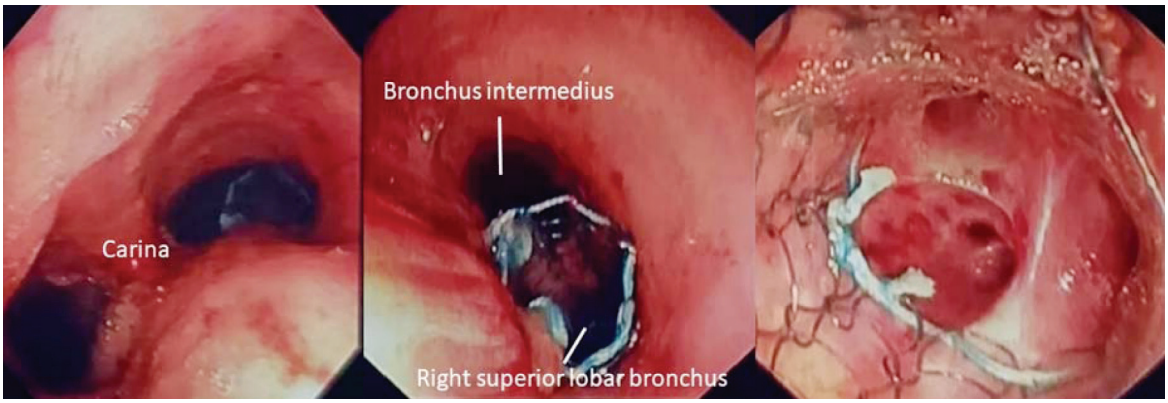

Fig. 5. Deployment of an endobronchial stent in the right main bronchus.

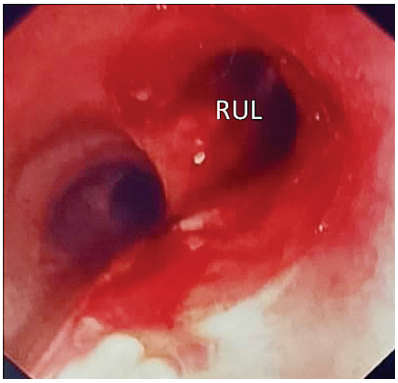

Fig. 6. The laceration healed and the endobronchial stent was removed 2 weeks later.

and pneumomediastinum gradually resolved, as seen on chest x-ray. After removal of the chest tube, no further sign of air-leakage was detected. The patient was discharged under a stable condition. Follow-up bronchoscopy 2 weeks later showed that the right main bronchus laceration had healed successfully (Figure 6), without development of stenosis, so the endobronchial stent was also removed.

Discussion

We presented a case with chest blunt trauma and right main bronchial injury, which was detected due to unresolved pneumothorax and persistent air leakage from the chest tube. TBI can be caused by neck or thoracic trauma, as well as iatrogenic injury. The incidence of traumatic TBIs is reported to be about 2~3%, although this was thought to be underestimated due to the fact that many victims had died before reaching the hospital [1,2]. Iatrogenic TBI can result from surgery or endotracheal intubation. The incidence of routine endotracheal intubation-induced TBI is very low -- about 0.005% for a single-lumen tube and 0.05% for a double-lumen tube [3]. However, the incidence of TBI in emergency intubation can reach up to 15% [4]. Surgical intervention involving the middle and lower esophagus has the highest incidence – approximately 0.4~1.8% among surgery-related TBIs [5,6]. With endobronchial ultrasound (EBUS)-guided transbronchial biopsy, the incidence of TBI is extremely low [7]

More than 75% of TBIs occur within 2.5 cm from the carina, and most of them are located in the main stem bronchus [8]. The mechanisms of TBI include penetrating and high-energy blunting injuries. Penetrating injuries resulting from stab wounds are usually located in the cervical trachea, whereas gunshot wounds can involve either the cervical or intrathoracic airways [9]. High-energy TBIs can be caused by rapid deceleration and shearing forces of the

cervical trachea, a surge in airway pressure, and compression between the sternum and vertebral bodies. These mechanisms frequently produce bone fractures, spinal cord injuries and laceration of the esophagus, blood vessels and lung parenchyma.

The typical manifestations of TBIs are subcutaneous emphysema, pneumothorax and pneumomediastinum [10]. Clinically, the patient may have dyspnea, hoarseness, stridor, hemoptysis, respiratory failure or even shock. Physical examinations can reveal subcutaneous crepitation on palpation, diminished breathing sound or a precordial crunching sound that occurs in synchrony with heartbeats (Hamman's sign). CT scans may reveal gas dispersion around the leakage site, bronchial lumen displacement and discontinuity of the tracheal wall. However, CT imaging has limitations in detecting a minor tear. It is important to know that symptoms and signs of TBIs are sometimes subtle at first, and that the correct diagnosis can be difficult to make. A delayed presentation may be encountered when the tracheal tear is tiny, or when the air leakage site was previously covered by the endotracheal tube cuff in intubated patients. It is crucial to include TBI in the differential diagnosis when dealing with pneumothorax or pneumomediastinum refractory to chest drainage.

The definite diagnosis of TBI is made by direct visualization of the injury in bronchoscopy or surgery. Both interventions have diagnostic and therapeutic value. The management of TBIs starts with establishing a secure airway. When intubation is needed, flexible bronchoscopy can guide and place the cuff of the endotracheal tube beyond the injury site or into the unharmed bronchus. In cases of severe trauma, direct intubation through an open wound into the transected airway and emergency tracheostomy may be required. After securing the airway, patients who can breathe spontaneously, those who require minimal ventilator support, have a superficial or small tracheal tear (≤2cm), or have no evidence of a persistent air leak can be treated non-operatively [11,12]. Non-operative treatment includes the use of broad-spectrum prophylactic antibiotics for 1 week, setting the ventilator with a minimal acceptable airway pressure, and avoiding oral intake or insertion of a nasogastric tube if there is concomitant esophageal injury [13].

The introduction of endobronchial stent placement, particularly self-expanding metallic stent (SEMS), brings more therapeutic options to TBI patients [14]. This is a minimally invasive technique, and better suits patients at high surgical risk. Deploying the stent can provide mechanical obstruction of the tracheal defect. As the granulation tissue over the covered stent grows, it can structurally strengthen the closure of the tracheobronchial defect. Usually the stent can be removed after 4~6 weeks of adequate healing. Prolonged stent placement may cause complications like tracheal stenosis, stent migration, mucus plugging and infection [15].

Surgical interventions for TBIs generally include exposure of the injury site, conservative debridement, creating a tension-free anastomosis and autologous tissue repair or reconstruction. Sometimes sleeve resection, lobectomy or even pneumonectomy may be needed [16]. A transthoracic or trans-sternal approach to repair depends on the location of the injury. Once the surgery is finished, bronchoscopy should be performed to ensure proper repair of the injury. Follow-up bronchoscopies for assessment of granulation tissue or stenosis formation during the healing process may also be needed. The

prognosis of TBI is affected by the severity of trauma and the patient's underlying status. Early detection of air-leakage, accurate location of the defect site and prompt establishment of a patent airway can lead to a better outcome, although this is quite challenging in clinical settings.

In conclusion, TBI should be considered in cervical or thoracic trauma patients, especially those presenting with a delayed or refractory sign of air leakage. Non-operative treatment in TBI includes securing airway patency, the use of broad-spectrum prophylactic antibiotic therapy, and avoiding excessive airway pressure. Apart from traditional open surgery, endobronchial stenting provides an effective and minimally invasive approach to managing TBIs. Our case demonstrates the classic clinical signs of TBI, and once more emphasizes the importance of a correct diagnosis and appropriate treatment for these patients.

References

1. Johnson SB. Tracheobronchial injury. Semin Thorac Cardiovasc Surg 2008; 20:52.
2. Bertelsen S, Howitz P. Injuries of the trachea and bronchi. Thorax 1972;27: 188.
3. Schneider T, Storz K, Dienemann H, *et al*. Management of iatrogenic tracheobronchial injuries: a retrospective analysis of 29 cases. Ann Thorac Surg 2007; 83: 1960.
4. Prokakis C, Koletsis EN, Dedeilias P, *et al*. Airway trauma: a review on epidemiology, mechanisms of injury, diagnosis and treatment. J Cardiothorac Surg 2014; 9: 117.
5. Koshenkov VP, Yakoub D, Livingstone AS, *et al*. Tracheobronchial injury in the setting of an esophagectomy for cancer: postoperative discovery a bad omen. J Surg Oncol 2014;109: 804.
6. Parekh K, Iannettoni MD. Complications of esophageal resection and reconstruction. Semin Thorac Cardiovasc Surg. 2007;19(1): 79-88.
7. Liberman M, Duranceau A, Martin J, *et al*. Major airway laceration secondary to endobronchial ultrasound transbronchial lymph node biopsy. J Bronchol Interv Pulmonol. 2010;17(3): 264-265.
8. Kiser AC, O'Brien SM, Detterbeck FC. Blunt tracheobronchial injuries: treatment and outcomes. AnnThorac Surg 2001;71: 2059.
9. Lee RB. Traumatic injury of the cervicothoracic trachea and major bronchi. Chest Surg Clin N Am1997;7: 285.
10. Karmy-Jones R, Wood DE. Traumatic injury to the trachea and bronchus. Thorac Surg Clin 2007;17: 35.
11. Gómez-Caro Andrés A, Moradiellos Díez FJ, Ausín Herrero P, *et al*. Successful conservative management in iatrogenic tracheobronchial injury. Ann Thorac Surg. 2005;79(6): 1872-1878.
12. Mussi A, Ambrogi MC, Ribechini A, *et al*. Acute major airway injuries: clinical features and management. Eur J Cardiothorac Surg. 2001;20(1): 46-51.
13. Jougon J, Ballester M, Choukroun E, *et al*. Conservative treatment for postintubation tracheobronchial rupture. Ann Thorac Surg. 2000;69(1): 216-220.
14. Hussein E, Pathak V, Shepherd RW, *et al*. Bronchoscopic management of iatrogenic tracheal laceration using polyurethane covered nitinol tracheal stents. J Trauma Acute Care Surg. 2016;81(5): 979-983.
15. Zakaluzny SA, Lane JD, Mair EA. Complications of tracheobronchial airway stents. Otolaryngol- Head Neck Surg. 2003;128(4): 478-488.
16. Mussi A, Ambrogi MC, Menconi G, Ribechini A, Angeletti CA. Surgical approaches to membranous tracheal wall lacerations. J Thorac Cardiovasc Surg. 2000;120(1): 115-118.

Pulmonary Amyloidosis Mimicking Multiple Lung Metastasis – A Case Report

Cheng-Hsiang Chu[1], Lu-Jen Chen[2], Yen-Hsiang Huang[1], Tsung-Ying Yang[1]

Pulmonary amyloidosis was previously recognized as a benign disorder. However, both its clinical and its radiologic presentations could mimic malignancies. We reported the case of a 76-year-old woman with the initial presentation of a tongue tumor 8 years ago, and who developed progressive dyspnea on exertion 2 years previous to this evaluation. The chest X-ray and computed tomography (CT) scan of the chest showed multiple lung nodules. The patient was told she likely had stage IV tongue cancer with lung metastasis, but she declined any biopsy. However, massive hemoptysis occurred, complicated with respiratory failure, so she was referred for further surveillance and treatment. The follow-up CT of the chest revealed increasing numbers and sizes of calcifications, consolidations, cystic lesions and slow-growing nodules. Pulmonary amyloidosis was highly suspected, so tissue proof was strongly suggested. The patient finally agreed to undergo tissue biopsy, and the pathologic report confirmed the diagnosis of amyloidosis. ***(Thorac Med 2022; 37: 217-222)***

Key words: Pulmonary amyloidosis; hemoptysis

Introduction

Amyloidosis is a group of disorders with an extracellular deposition of insoluble misfolding amyloid fibrils in tissues and organs, leading to organ dysfunction and ultimately death [1]. Amyloidosis with respiratory tract involvement was once recognized as a benign disorder. Although pulmonary amyloidosis is rarely symptomatic, its clinical and radiologic presentations could mimic malignancies [2-3, 6-7]. Some elderly persons in Taiwan tend to decline undergoing an invasive procedure, such as a biopsy. However, a delayed diagnosis would alter their management and prognoses. We present a case of pulmonary amyloidosis mimicking multiple lung metastases, and review the available literature.

[1]Division of Chest Medicine, Department of Internal Medicine, Taichung Veterans General Hospital, Taichung, Taiwan, [2]Department of Pathology and Laboratory Medicine, Taichung Veterans General Hospital, Taichung, Taiwan. Address reprint requests to: Dr. Yen-Hsiang Huang, Division of Chest Medicine, Department of Internal Medicine, Taichung Veterans General Hospital, 1650 Taiwan Boulevard Sect. 4, Taichung, Taiwan 40705

Case Report

A 76-year-old woman was transferred to our hospital due to massive hemoptysis, complicated with respiratory failure. Her medical history revealed hypertension, which was kept under control with an angiotensin receptor blocker. The woman was a retired hair stylist, with no history of tobacco smoking, alcohol drinking, or betel nut consumption. There were no remarkable findings in her family history.

Eight years ago, she reported a painless tongue mass and visited our ear, nose and throat outpatient clinic, where a firm nodular lesion approximately 1.5 centimeters (cm) in size was noted at the right side of the posterior lateral tongue border. She was told that she most likely had tongue cancer, but declined to receive either surgical intervention or punch biopsy, and was lost before any follow-up.

Two years prior to this admission, the patient was referred to our chest medicine outpatient clinic for reasons of a progressive shortness of breath on exertion, as well as having an intermittent dry cough for nearly 1 year. The tumor at the right tongue border had enlarged to 2 cm in size; furthermore, another newly formed 1-cm nodular lesion was noted at the left side of the tongue base. Radiographs of the chest showed multiple lung nodules at the bilateral lung zones (Figure 1A). Computed tomography (CT) of the chest revealed multiple cystic lesions in both lungs, bilateral basal consolidations, and diffuse lung nodules, some of which had partial calcification (Figures 2A,

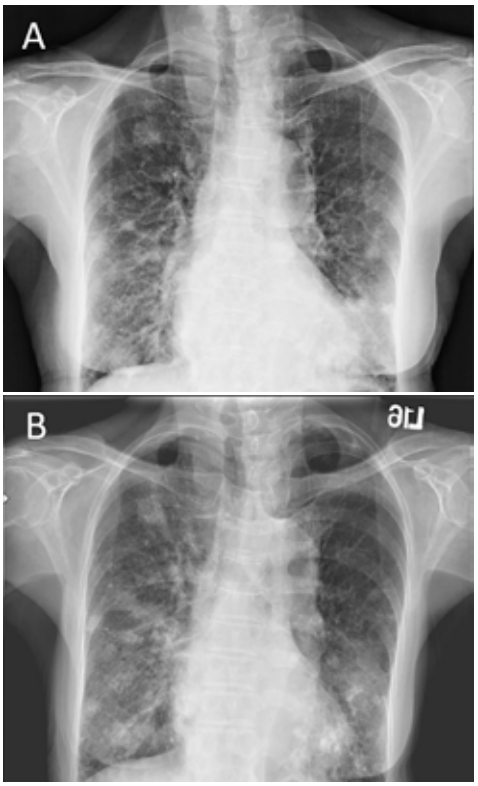

Fig. 1. (A) Chest radiography revealed bilateral lung nodules 2 years before this visit; (B) Follow-up chest radiography while in admission revealed bilateral lung nodules with calcification. The size of the lung nodules enlarged slowly.

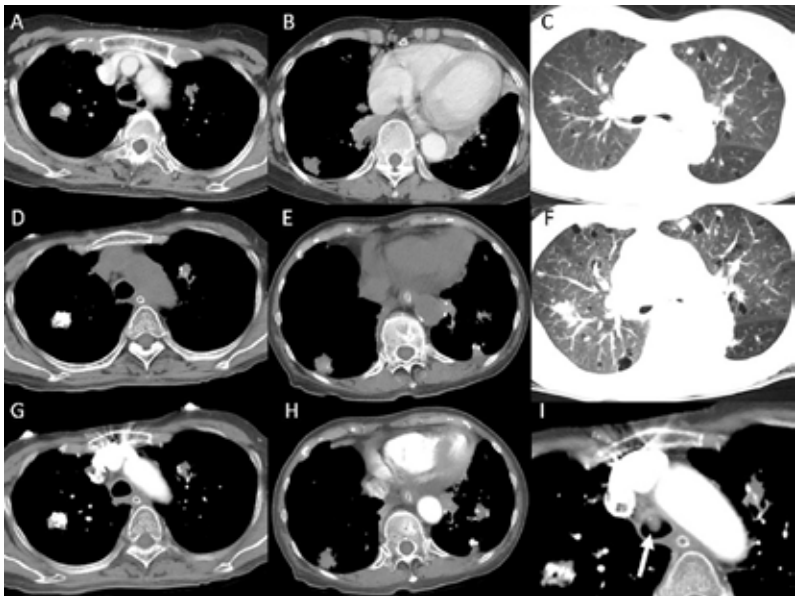

Fig. 2. (A) (B) and (C) Two years before this admission, a computed tomography scan of the chest revealed bilateral basal consolidations, cystic lesions, and diffuse lung nodules, some of which were partially calcified. (D) (E) (F) (G) and (H) Unenhanced and enhanced chest CT scans at this admission revealed enlarged nodules, calcifications, consolidations and cystic lung lesions. (I) An endotracheal lesion (arrow).

2B, 2C). Both a tongue biopsy and a bronchoscopic biopsy were suggested, but once again the patient refused.

Two months before this evaluation, the patient's exertional dyspnea had become worse, and she had to take a short break after climbing 2 flights of stairs. She began having a frequent cough with blood-tinged sputum, a poor appetite, dry mouth, easy drooling and a husky voice.

On the day prior to being transferred to our hospital, a sudden onset of massive hemoptysis was noted without any prodrome or other specific symptom. Oral endotracheal intubation was performed due to hypoxic respiratory failure.

During the initial presentation at our hospital, dark red sputum could still be sucked out from the endotracheal tube. The patient's body temperature was 36.5 degrees Celsius; pulse was 80 beats per minute; blood pressure was 142/71 millimeters of mercury (mmHg), and oxygen saturation was 98% under mechanical ventilation with a 40% fraction of inspiration oxygen at 5 cm of water (cmH_2O) of positive end expiratory pressure (PEEP). Physical examination showed pale conjunctivae and bilateral rales, with a further examination showing otherwise normal findings. The patient's hemoglobulin was 10.8 grams per deciliter (g/dL). Additional blood routine studies, blood chemistry values, and coagulopathy profiles were within normal range, except for the reverse albumin-globulin ratio, where the albumin and total protein were 2.8 and 6.3 milligrams per deciliter (mg/dL), respectively. A CT-pulmonary angiography demonstrated no extravasation, but did reveal an endotracheal lesion (Figure 2I), with increasing numbers and sizes of calcifications, consolidations, cystic lesions and slow-growing nodules (Figures 2D-2H), compared with the prior chest CT.

Fig. 3. At this admission, 2 tumors (arrows) were seen at the bilateral tongue base.

On hospital Day 2, the patient's hemoptysis stopped after epinephrine inhalation and tranexamic acid administration. Extubation was performed after the patient passed a spontaneous breathing trial on Day 4. Macroglossia with tongue tumors was noted (Figure 3). The following chest radiogram showed bilateral lung nodules, as in the previous plain film (Figure 1B).

Based on the clinical manifestations and chest CT findings, pulmonary amyloidosis and lymphocytic interstitial pneumonia, which is most commonly seen in Sjögren's syndrome, were highly suspected. Serum rheumatologic profiles revealed positive findings of antinuclear antibodies (ANA, titer 1:2560) in a fine speckled pattern, anti-Sjögren's-syndrome-related antigen A (anti-SSA, > 240 EliA U/ml, positive: > 10 EliA U/ml), and anti-Sjögren's-syndrome-related antigen B (anti-SSB, > 240 EliA U/ml, positive: > 10 EliA U/ml). Upon discussion with the patient and her family after extubation,

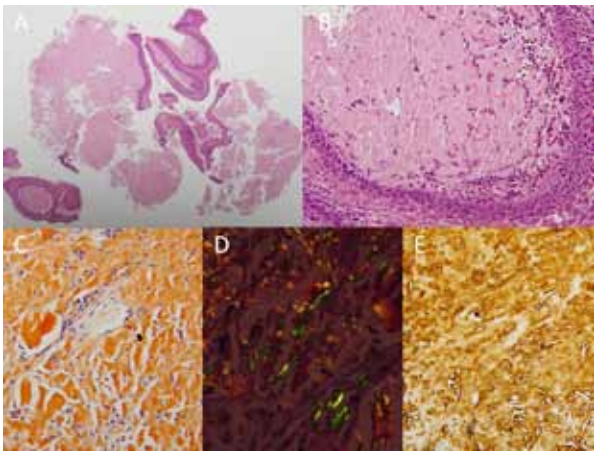

Fig. 4. (A) and (B) Homogeneously eosinophilic and acellular substances deposited in the stroma, with inflammatory cell infiltration. (hematoxylin and eosin stain, 20X and 200X). (C) Congo red staining (200X) revealed orange-red amyloid deposition in the submucosa under bright field microscopy, and (D) apple-green birefringence under polarized microscopy (400X). (E) Immunohistochemistry stain revealed an increased expression of immunoglobulin light chain kappa (200X).

she agreed to undergo a tongue biopsy, while refusing a bronchoscopic biopsy. The pathologic diagnosis of the tongue biopsy was amyloidosis (Figures 4A and 4B), with orange-red amyloid depositions infiltrating the submucosa seen through bright field microscopy (Figure 4C), and apple-green birefringence under polarized light on Congo red stain (Figure 4D). Increased expressions of immunoglobulin light chain kappa (Figure 4E) over lambda in the immunohistochemistry (IHC) stains were also seen. Both serum and urine immunologic studies showed polyclonal hypergammaglobulinemia (IgG, 2424 mg/dL, reference range 635 to 1741), with increased levels of immunoglobulin kappa (735 mg/dL, reference range 170 to 379) and lambda (288 mg/dL, reference range 90 to 210). After hematologic and rheumatologic consultation, immunoglobulin light-chain amyloidosis, and Sjögren's syndrome with positive findings on a Schirmer's test and sialoscintigraphy, were respectively diagnosed. The patient was subsequently discharged on Day 9. She is currently regularly followed up at our hematologic outpatient clinic where she receives supportive care, but still refuses further invasive surveillance.

Discussion

The estimated incidence of systemic amyloidosis is 0.4 to 1.2 cases per 100,000 persons per year [8-9], while there is no available data on the incidence of pulmonary amyloidosis. Amyloidosis could be classified into more than 36 subtypes, based on various precursor proteins [1]. Different subtypes of amyloidosis have different tendencies with regard to the main organs involved. Baumgart JV, *et al*. [4] and Ussavarungsi K, *et al*. [6] reported that amyloidosis with respiratory tract involvement is most commonly caused by immunoglobulin light-chain amyloidosis (AL, 76-88.3%), followed by transthyretin-derived amyloidosis (ATTR, 9.8-22%), and lastly amyloid A (AA, 1-1.5%). Patients with amyloidosis of the respiratory system were diagnosed at around the median age of 70 years [4, 10], with men being more susceptible than women [2-6].

Most patients with respiratory amyloidosis were asymptomatic [2-6, 10]; otherwise, patients may present symptoms of dyspnea, chest pain, cough, hemoptysis, hoarseness, pleural effusion, pulmonary hypertension, and even diffuse alveolar hemorrhage [2-4, 6, 10, 11]. Similar to systemic amyloidosis, lung amyloidosis is associated with comorbidities, including monoclonal gammopathy of uncertain significance, Waldenström macroglobulinemia, multiple myeloma, and mucosa-associated lymphoid tissue lymphoma [2-3, 10]. Nevertheless, Milani P, *et al*. [2] and Yamada M, *et al*. [10] reported that Sjögren's syndrome was the most com-

mon connective tissue disease associated with pulmonary amyloidosis, rather than rheumatoid arthritis, in systemic amyloidosis [12].

Pulmonary amyloidosis is difficult to diagnose and may be underdiagnosed due to asymptomatic or nonspecific manifestations [2-7, 10]. In an analysis of 76 autopsy-derived cases during a 7-year period, Ussavarungsi K, *et al*. showed that only 1 patient with pulmonary amyloidosis was diagnosed ante-mortem [6]. The diagnosis of amyloidosis rests upon confirmation of amyloid deposits through a tissue biopsy involving apple-green birefringence under polarized light on Congo red staining. Tissue sampling could also be approached via a noninvasive biopsy, such as abdominal fat aspiration, or through an invasive biopsy of the affected organ [12].

Amyloidosis with respiratory system involvement is classified pathologically using 3 manifestations: nodular pulmonary amyloidosis, diffuse alveolar-septal amyloidosis, or tracheobronchial amyloidosis [2-3, 13-14].

Chest radiography can reveal the following: single or multiple pulmonary nodules, consolidations, calcifications of noduli or pleural lesions and pleural effusions [2-6, 10]. Based on a review of chest CT images, Czeyda-Pommersheim F, *et al*. [13] and de Almeida RR, *et al*. [14] described nodular pulmonary amyloidosis as being commonly characterized by multiple pulmonary nodules with slow growth, a peripheral or subpleural location, and having smooth, lobulated, or spiculated margins with or without calcification or lung cysts. Chest CT findings in diffuse alveolar-septal amyloidosis consist of interlobar septal thickening, well-defined micronodules with ground glass opacities, and confluent consolidations with a basal and peripheral predominance. In tracheobronchial amyloidosis, chest CT can reveal tumor-like nodules, or circumferential thickening involving the trachea, main bronchus and lobar or segmental bronchi [2-6, 10, 13, 14]. Baumgart JV, *et al*. [4], in a retrospective study of 32 patients with proven lung amyloidosis, found that 69% of patients had a nodular pattern, 6% had a diffuse alveolar septal pattern, 13% had a tracheobronchial pattern, and 13% of patients had a mixed pattern. Of note, the most common patterns of pulmonary amyloidosis on chest CT are lung nodules (78%), followed by consolidations (50%), and calcifications of noduli or pleural lesions (44%). In their study, de Almeida RR, *et al*. [14] found that calcifications were seen on HRCT in approximately 50% of patients. Lung cysts can have the appearance of Sjögren's syndrome with lymphocytic interstitial pneumonia, as well as that of pulmonary amyloidosis. Baqir M, *et al*. [15] reported 8 patients with Sjögren's syndrome manifesting cystic lung lesions who were diagnosed with pulmonary amyloidosis, as confirmed by lung biopsies at the Mayo Clinic from 1997 to 2010. However, the above findings involving chest radiography or CT were nonspecific, and may have mimicked other diseases, such as malignancies, infections, collagen vascular diseases, interstitial lung diseases, or granulomatous diseases [13-14].

Although different types of amyloidosis share similar clinical presentations, treatments differ based on the various amyloid precursor proteins involved. Hence, identification of amyloid fibril types and evaluation of underlying amyloidogenic diseases are important. For instance, therapies targeting clonal plasma cells, including chemotherapy, monoclonal antibodies, proteasome inhibitors, and autologous stem cell transplants, are all aimed at AL amyloidosis. Treatments for AA amyloidosis

focus on any underlying infectious or inflammatory diseases. The exact treatment for ATTR amyloidosis remains uncertain, but the primary management for it is transplantation of the failing organ [12].

In conclusion, amyloidosis has been recognized as a benign disorder, but the clinical manifestations of pulmonary amyloidosis can mimic multiple lung metastases. A combination of signs, comparing the findings from a series of chest CT scans, and most importantly, encouraging the patient to undergo a tissue biopsy, are the keys to patient diagnosis in the future.

References

1. Benson MD, Buxbaum JN, Eisenberg DS, *et al*. Amyloid nomenclature 2020: update and recommendations by the International Society of Amyloidosis (ISA) nomenclature committee. Amyloid 2020; 27(4): 217-222.
2. Milani P, Basset M, Russo F, *et al*. The lung in amyloidosis. Eur Respir Rev 2017; 26(145): 170046.
3. Khoor A, Colby TV. Amyloidosis of the lung. Arch Pathol Lab Med 2017; 141(2): 247-254.
4. Baumgart JV, Stuhlmann-Laeisz C, Hegenbart U, *et al*. Local vs. systemic pulmonary amyloidosis-impact on diagnostics and clinical management. Virchows Arch 2018; 473(5): 627-637.
5. Utz JP, Swensen SJ, Gertz MA. Pulmonary amyloidosis. The Mayo Clinic experience from 1980 to 1993. Ann Intern Med 1996;124(4): 407-13.
6. Ussavarungsi K, Yi ES, Maleszewski JJ, *et al*. Clinical relevance of pulmonary amyloidosis: an analysis of 76 autopsy-derived cases. Eur Respir J 2017; 49(2): 1602313.
7. Ihne S, Morbach C, Sommer C, *et al*. Amyloidosis -- the diagnosis and treatment of an underdiagnosed disease. Dtsch Arztebl Int 2020; 117(10): 159-166.
8. Pinney JH, Smith CJ, Taube JB, *et al*. Systemic amyloidosis in England: an epidemiological study. Br J Haematol 2013; 161(4): 525-32.
9. Wisniowski B, McLeod D, Adams R, *et al*. The epidemiology of amyloidosis in Australia. Amyloid 2019; 26(sup1): 132-133.
10. Yamada M, Takayanagi N, Yamakawa H, *et al*. Amyloidosis of the respiratory system: 16 patients with amyloidosis initially diagnosed ante mortem by pulmonologists. ERJ Open Res 2020; 6(3): 00313-2019.
11. Shenin M, Xiong W, Naik M, *et al*. Primary amyloidosis causing diffuse alveolar hemorrhage. J Clin Rheumatol 2010; 16(4): 175-7.
12. Wechalekar AD, Gillmore JD, Hawkins PN. Systemic amyloidosis. Lancet 2016; 387(10038): 2641-2654.
13. Czeyda-Pommersheim F, Hwang M, Chen SS, *et al*. Amyloidosis: modern cross-sectional imaging. Radiographics 2015; 35(5): 1381-92.
14. de Almeida RR, Zanetti G, Pereira E, *et al*. Respiratory tract amyloidosis. State-of-the-art review with a focus on pulmonary involvement. Lung 2015; 193(6): 875-83.
15. Baqir M, Kluka EM, Aubry MC, *et al*. Amyloid-associated cystic lung disease in primary Sjögren's syndrome. Respir Med 2013;107(4): 616-21.

Interstitial lung Disease in Systemic Sclerosis and Dermatomyositis Overlap Syndrome: A Case Report

Pi-Hung Tung[1], Chen-Yiu Hung[1], Ning-Hung Chen[1,2,4], Shu-Min Lin[1,2,3]

Connective tissue diseases (CTDs) are frequently associated with interstitial lung disease (ILD), which significantly impacts morbidity and mortality. Organizing pneumonia is a clinical, radiological and histological entity that is classified as an ILD. We report a 68-year-old woman who presented bilateral lower lung consolidation on radiologic imaging, that later progressed to respiratory failure. The lung tissue biopsy pathology showed organizing pneumonia. In addition, the patient had progressive muscle weakness in all 4 limbs. Further investigation revealed a high antinuclear antibodies titer and a positive finding on the myositis panel. Steroid and immunosuppressive agents were used to treat the CTD-ILD; extubation was performed after the patient's clinical condition improved. This report focused on the characteristics of radiological findings and our experience in treating CTD-ILD. ***(Thorac Med 2022; 37: 223-229)***

Key words: Connective tissue disease, interstitial lung disease, systemic sclerosis, dermatomyositis

Introduction

Connective tissue diseases (CTDs) are systemic disorders typically characterized by circulating autoantibodies and varying degrees of autoimmune-mediated multiple organ damage [1]. Interstitial lung disease (ILD) is one of the most serious complications associated with CTDs, and results in significant morbidity and mortality [2]. Although ILD often occurs in patients with a known CTD, it can also be the first and only manifestation of a previously unrecognized CTD [3]. The management of CTD-ILD is challenging, largely due to significant heterogeneity in disease behavior between CTD-ILD subtypes, and the lack of a standard management guideline [4].

[1]Department of Thoracic Medicine, Chang Gung Memorial Hospital, Chang Gung University College of Medicine, Taipei, Taiwan, [2]Department of Respiratory Therapy, Chang Gung Memorial Hospital, Chang Gung University, School of Medicine, Taipei, Taiwan, [3]School of Medicine, Chang Gung University, Taoyuan, Taiwan, [4]School of Traditional Chinese Medicine, Chang Gung University, Taoyuan, Taiwan.
Address reprint requests to: Dr. Pi-Hung Tung, Department of Thoracic Medicine, Chang Gung Memorial Hospital, Chang Gung University College of Medicine, Mailing address: No.5, Fusing St., Gueishan Township, Taoyuan County 333, Taiwan (R.O.C.).

Case Report

A 68-year-old female had a history of subarachnoid hemorrhage that occurred 23 years ago. This time, she presented to the chest medicine outpatient department (OPD) with shortness of breath and non-productive cough for 3 months. On examination, the patient appeared chronically ill with mildly labored breathing, and bilateral coarse breathing sounds were heard on auscultation. Chest radiography showed increased infiltration in bilateral lung fields with left pleural effusion (Figure 1). Physical examination showed she had a body temperature of 37℃, a heart rate of 90 beats per minute, a respiratory rate of 20 breaths per minute, and blood pressure of 107/65 mmHg. Laboratory data revealed a white blood cell count of 8400/μL, a high C-reactive protein level of 65.4 mg/dl, and normal renal and liver functioning. The pleural fluid study results were exudative in nature with lymphocytes predominant (neutrophils 17%, lymphocytes 63%). The clinical course of the case is presented in Figure 2.

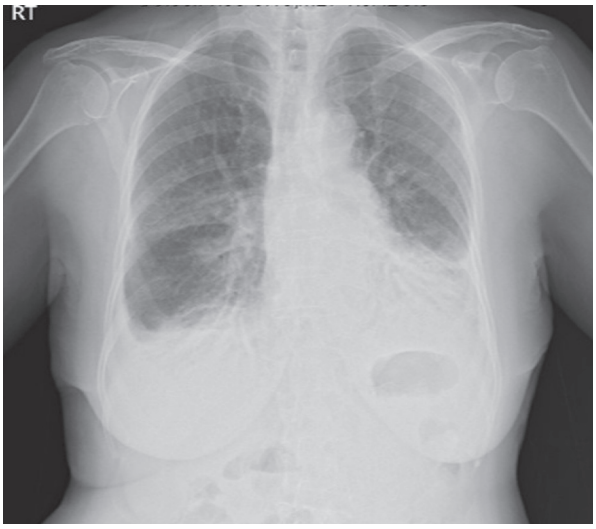

Fig. 1. Chest radiograph reveals left lower lung patchy consolidation and pleural effusion.

After admission, empirical antibiotic treatment with moxifloxacin was administered for infection control. Although the patient had persistent dyspnea on exertion and delayed resolution of the bilateral lung consolidation (Figure 3), she had no more fever and had a negative sputum bacterial culture. She then underwent video-assisted thoracoscopic wedge resection of the left upper lung for tissue proof. The pathological report of the left upper lung biopsy revealed multiple nodular lesions exhibiting interstitial fibrosis with mild infiltration of plasma cells and lymphocytes, which was compatible with organizing pneumonia (Figure 4). At this time, the patient had progressive muscle weakness, especially of the proximal limb muscles associated with arthralgia, as well as hand joints stiffness, puffy fingers, and skin thickness of both hands. The electromyography and motor and sensory nerve conduction velocity showed a small amplitude and a short duration of motor

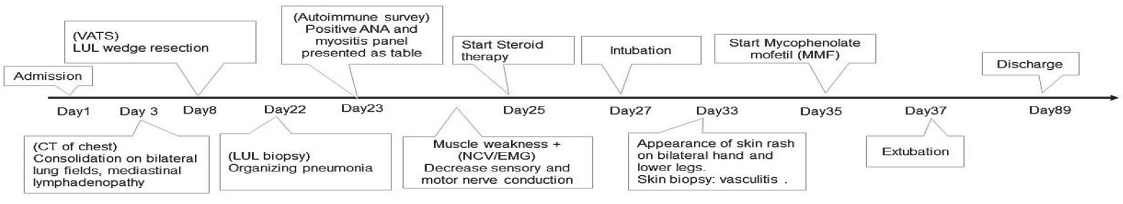

Admission day/ Ventilator support	Day27/MV day1	Day31/MV day5	Day 35/MV day9	Day37/ MV Day 11 (before extubation)
PaO2/FiO2	236/0.6	112/0.35	117/0.35	124/0.35
P/F ratio	393	320	334	354
Airway resistance/Compliance	11/44.8	6/36	6/46	6/63

Fig. 2. Timeline (clinical course) of the case.

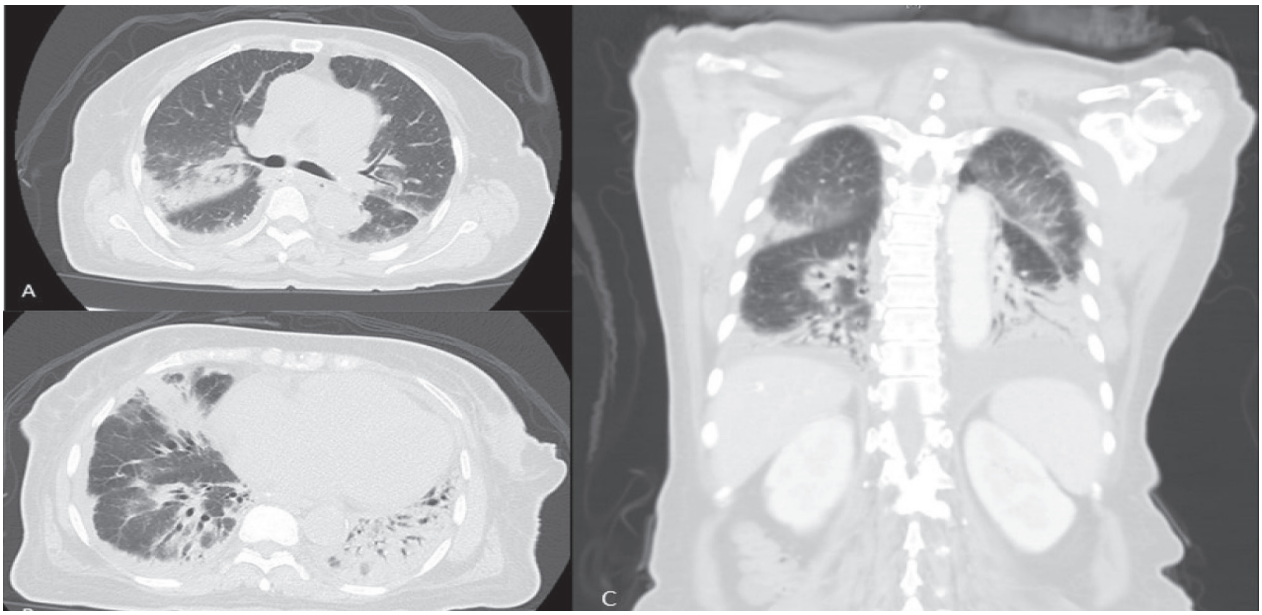

Fig. 3. Chest computed tomography shows ill-defined consolidation with bronchograms in the bilateral lower lung fields.

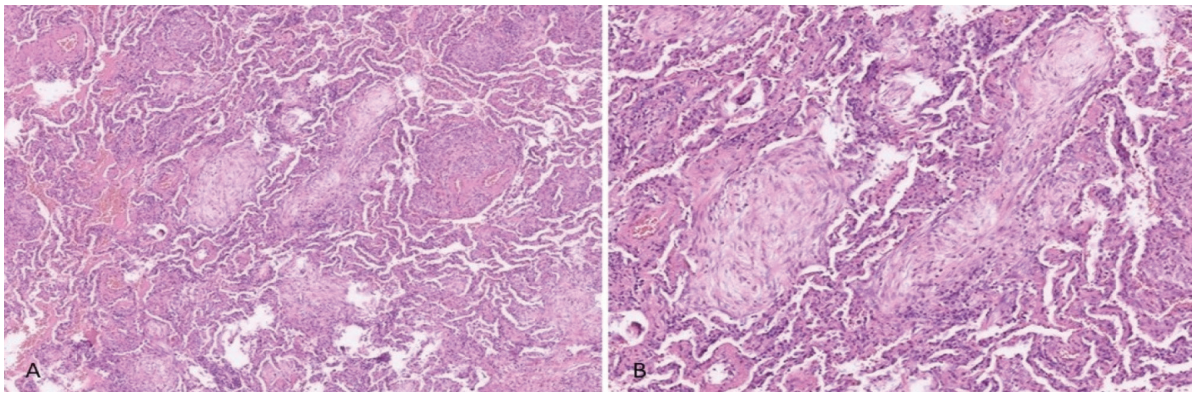

Fig. 4. Histologic section of specimens obtained from a left upper lung wedge resection shows multiple nodular lesions exhibiting interstitial fibrosis with mild infiltration of plasma cells and lymphocytes (hematoxylin and eosin stain).

unit potential with asymmetric motor- and axonal-predominant polyneuropathy. The autoimmune survey showed a high titer of antinuclear antibodies and a positive myositis panel (positive PM-Scl 75 and PM-Scl 100), in association with idiopathic inflammatory myositis, including systemic sclerosis overlap syndrome (OS) (Table 1). There were also elevated muscle enzymes. Scleroderma and inflammatory myositis OS were diagnosed based on the clinical (skin and musculoskeletal manifestation) and laboratory features (positive myositis panel and elevated muscle enzymes). At that point, intravenous methylprednisolone 2 mg/kg/day was used as a bridging therapy.

Unfortunately, the patient developed fever with progressive dyspnea, and arterial blood gas showed respiratory acidosis with carbon dioxide retention under a non-rebreathing mask, with an oxygen flow of 15 L/minute (pH 7.29,

Table 1. Results of the Serological Autoimmune Marker and Myositis Panel

Laboratory Data		
Autoimmune survey		Normal reference value
ANA	1:120 nucleolar pattern	< 1:80
A-DsDNA	Negative 28.9	<92.6WHOunit/ml
RF	<9.69 IU/ml	<15 IU/ml
C3	127 mg/ml	90-180 mg/dl
C4	24.3 mg/ml	20-50 mg/dl
Myoglobin	172 ng/ml	25-72 ng/ml
CPK	224 IU/L	26-192 U/L
Myositis panel		
Anti-CCP	<4.6AU/ml	<20 CU
Ro-52	-	-
OJ	-	-
EJ	-	-
PL-12	-	-
PL-7	-	-
SRP	-	-
Jo-1	-	-
Ku	-	-
PM-Scl75	++	-
PM-Scl100	+++	-
SAE1	-	-
NXP2	-	-
MDA5	-	-
TIF1γ	-	-
Mi-2β	+-	-
Mi-2α	-	-
Anti-Scl-70	31 AU/ml	<100 AU/ml

ANA: Antinuclear antibodies; A-DsDNA: Anti-double stranded DNA; Anti-CCP: Anti-cyclic citrullinated peptides; RF: Rheumatoid factor; CPK: Creatinine phosphokinase.

pCO_2 65.1, pO_2 236.7, HCO_2 31, SaO_2 99) on admission day 28. Endotracheal intubation was performed for acute respiratory failure, and the patient was subsequently admitted to the medical intensive care unit. Bronchoalveolar lavage (BAL) was performed from the right upper bronchus (RB2). The BAL fluid was lymphocyte-predominant (CD4/CD8: 0.9), but no microorganism was isolated from the BAL fluid culture. On day 6 of intubation (during ICU admission), multiple erythematous wheal-like plaques with a central dusky red hue or violaceous lesions appeared on the patient's back, bilateral thighs and knees (Figure 5). The skin

Fig. 5. Multiple erythematous wheal-like plaque lesions on the bilateral lower limbs.

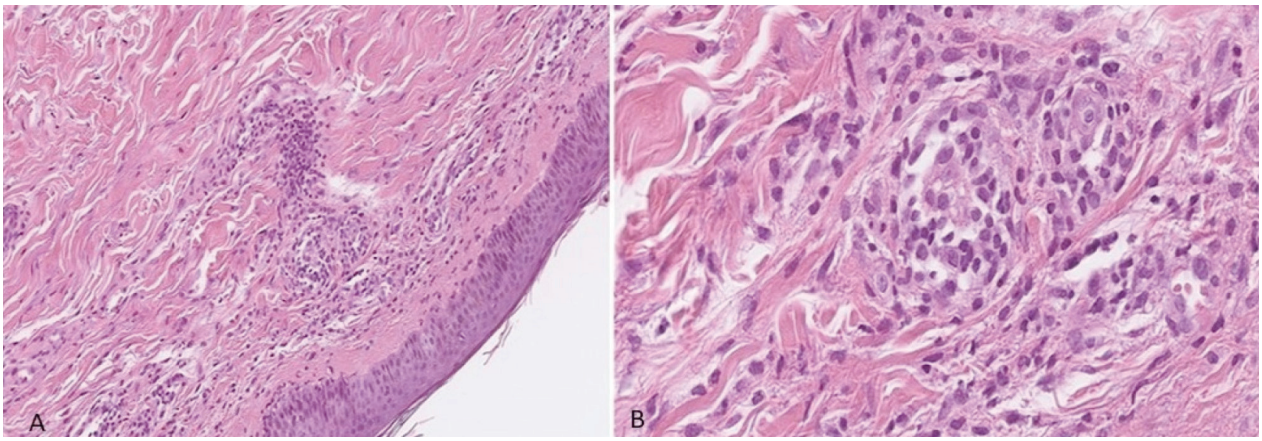

Fig. 6. Histology of a specimen obtained from a lower leg skin biopsy showed scanty necrotic keratinocytes and superficial perivascular lymphocytic infiltrates with some neutrophils and focally extravasated erythrocytes, compatible with urticarial vasculitis.

biopsy showed basal cell vacuolization with scanty necrotic keratinocytes and superficial perivascular lymphocytic infiltrates with some neutrophils and focally extravasated erythrocytes, which was compatible with urticarial vasculitis (Figure 6).

We continued steroid therapy. The clinical symptoms and chest X-ray showed improvement under treatment. Thereafter, self-paid mycophenolate mofetil (MMF) 750 mg twice a day was added. As her clinical condition had improved, the patient was extubated on admission day 37 (post-intubation day 10). The patient's post-extubation arterial blood gas showed no hypoxemia or hypercapnia (pH 7.46, $pCO_2$49.1, pO2 144.8, HCO3 34, SaO_2 98). Nevertheless, muscle weakness, especially of the bilateral lower limbs, persisted, and myopathic changes with polyneuropathy were shown in the follow-up electromyography. A rehabilitation program was arranged for the myopathy, and the patient was then discharged with an OPD follow-up plan.

Discussion

All patients with CTD have the risk of developing ILD, and those with systemic sclerosis (SSc), polymyositis/dermatomyositis (PM/DM), or rheumatoid arthritis are at particularly high risk [5]. In this report, we described a 68-year-old female who presented with dyspnea with dry cough for 2 months. Imaging and pathology revealed organizing pneumonia, but no evidence of interstitial lung fibrosis at first. Even though the high-resolution computed tomography (HRCT) pattern was atypical, the diagnosis of scleroderma and inflammatory myositis OS was made, as there was a cutaneous scleroderma manifestation together with sufficient clinical skeletal manifestations and laboratory features.

HRCT is a valuable diagnostic test and is used to evaluate patients with possible CTD-ILD [3]. Up to 90% of CTD patients will have some degree of ILD when they are screened randomly with HRCT [1]. The HRCT pattern of ILD in scleroderma is generally nonspecific interstitial pneumonia (NSIP), and the second

most common pattern is usual interstitial pneumonia [7], which yields a worse prognosis than NSIP [8]. The most common CT finding in lung disease associated with inflammatory myositis is organizing pneumonia, which has irregular linear opacities with areas of consolidation and ground-glass attenuation [10]. Organizing pneumonia is a common pattern of ILD found on lung biopsy in patients with inflammatory myositis [3].

Patients with SSc/PM had an anti-PM/Scl antibody in 33.1% of cases [17]. However, this antibody is not disease-specific, and may be associated with another CTD or OS in 17% of cases [17]. The diagnosis of CTD-ILD is based mainly on clinical findings, including history and physical examination, pulmonary function testing, and data from lung imaging and lung biopsy, along with histopathologic studies [1,16]. Lung biopsy may be obtained in some ILD cases, especially those without a clear diagnosis of CTD or atypical features on clinical or radiologic presentation [11]. The distinguishing features in the clinical, radiographic, and histopathologic findings of CTD-ILD subsets can predict prognosis and treatment response [12].

Corticosteroid remains the mainstay treatment for inflammatory myositis. Corticosteroid monotherapy is generally avoided due to a lack of consistency in the data available for efficacy. Caution is required with scleroderma patients and doses of prednisolone of more than 10–15 mg are avoided due to an increased risk of a scleroderma renal crisis. For scleroderma ILD, MMF and cyclophosphamide are most commonly used as first-line therapy. The efficacy of mycophenolate is comparable to that of cyclophosphamide, but with a better tolerability profile and fewer side effects [13]. In our case, MMF was prescribed for respiratory failure and urticaria vasculitis. Previous studies reported that immunosuppressant drugs such as cyclophosphamide, MMF, azathioprine and intravenous immunoglobulin improved the stabilization of lung function when combined with steroid [4, 14]. However, there is no published data to guide clinical decision-making regarding how long to continue immunomodulatory therapy in patients with CTD-ILD.

Lung transplant remains an option and should be considered for patients who do not respond to conventional medical management [15]. The proportion of lung transplant recipients among patients with ILD has increased in recent years. Also, pulmonary rehabilitation in patients with ILD has yielded significant improvement in 6-minute walking distance, dyspnea, muscle strength, and health-related quality of life. It is unclear whether patients with CTD-ILD benefit as much as those with idiopathic pulmonary fibrosis or other forms of ILD, due to comorbid conditions and therapy (such as corticosteroids), musculoskeletal pain and weakness, or other factors [16]. Because of the challenges in the diagnosis and management of patients with CTD-ILDs, a multidisciplinary approach involving relevant specialties, including pulmonology, rheumatology, radiology, pathology, and rehabilitation is necessary for optimal care [11].

However, our report has some limitations. First, we did not perform muscle biopsy or a pulmonary function test due to the patient's critical illness with ventilator use and a poor performance status. Second, we need to observe the influence of OS on a patient's long-term outcome (decline of lung function and quality of life). Nevertheless, we now are more experienced in seeking ILD in OS of CTDs in the future.

Conclusion

AILD is one of the most serious complications of CTD, and HRCT plays an important role in the diagnosis of CTD-ILD. In this case, we found that the diagnosis of OS was challenging if there were atypical features on clinical or HRCT imaging of CTD. The management of CTD-ILD is complex due to the heterogeneity of CTDs, the lack of recommended management guidelines, and the requirement of long-term follow-up.

Acknowledgment

We thank all staff members working in the Division of Pulmonary and Critical Care Medicine, Department of Thoracic Medicine, Chang Gung Memorial Hospital for their effort.

References

1. Solomon JJ, Fischer A. Connective tissue disease-associated interstitial lung disease: a focused review. J Intensive Care Med 2015; 30(7): 392-400.
2. Wallace B, Vummidi D, Khanna D, *et al*. Management of connective tissue diseases-associated interstitial lung disease: a review of the published literature. Curr Opin Rheumatol 2016; 28(3): 236-45.
3. Mathai SC, Danoff SK. Management of interstitial lung disease associated with connective tissue disease. BMJ 2016; 352: h6819.
4. Jee AS, Corte TJ. Current and emerging drug therapies for connective tissue disease-interstitial lung disease (CTD-ILD). Drugs 2019; 79(14): 1511-1528.
5. Fischer A, Brown KK, Du Bois RM, *et al*. Mycophenolate mofetil improves lung function in connective tissue disease-associated interstitial lung disease. J Rheumatol 2013; 40(5): 640-6.
6. Ahuja J, Arora D, Kanne JP, *et al*. Imaging of pulmonary manifestations of connective tissue diseases. Radiol Clin North Am 2016; 54(6): 1015-1031.
7. Solomon JJ, Olson AL, Fischer A, et al. Scleroderma lung disease. Eur Respir Rev 2013; 22(127): 6-19.
8. Ruano CA, Lucas RN, Leal CI, *et al*. Thoracic manifestations of connective tissue diseases. Curr Probl Diagn Radiol 2015; 44(1): 47-59.
9. Shimizu Y, Tsukagoshi H, Nemoto T, *et al*. Recurrent bronchiolitis obliterans organizing pneumonia in a patient with limited cutaneous systemic sclerosis. Rheumatol Int 2002; 22(5): 216-218.
10. Douglas WW, Tazelaar HD, Hartman TE, *et al*., Polymyositis-dermatomyositis-associated interstitial lung disease. Am J Respir Crit Care Med 2001; 164(7): 1182-5.
11. Mira-Avendano I, Abril A, Burger CD, *et al*. Interstitial lung disease and other pulmonary manifestations in connective tissue diseases. Mayo Clin Proc 2019; 94(2): 309-325.
12. Demoruelle MK, Mittoo S, Solomon JJ, *et al* . Connective tissue disease-related interstitial lung disease. Best Pract Res Clin Rheumatol 2016; 30(1): 39-52.
13. Das A, Kumar A, Arrossi AV, *et al*. Scleroderma-related interstitial lung disease: principles of management. Expert Rev Respir Med 2019; 13(4)357-367.
14. Silver KC, Silver RM. Management of systemic-sclerosis-associated interstitial lung disease. Rheum Dis Clin North Am 2015; 41(3): 439-457.
15. Lund LH, Khush KK, Cherikh WS, *et al*. The Registry of the International Society for Heart and Lung Transplantation: Thirty-fourth Adult Heart Transplantation Report-2017; Focus Theme: Allograft ischemic time. J Heart Lung Transplant 2017; 36(10): 1037-1046.
16. Ozerkis DA, Hinchcliff M. Connective tissue disease-associated interstitial lung disease: evaluation and management. Clin Chest Med 2019; 40(3): 617-636.
17. Pakozdi A, Nihtyanova S, Moinzadeh P, *et al*. Clinical and serological hallmarks of systemic sclerosis overlap syndromes. J Rheumatol 2011; 38(11): p.2406-9.

Primary Lung Cancer Presenting as Diffuse Tiny Pulmonary Nodules: A Case Report

Ming-Hung Chang[1], Kuo-Hwa Chiang[1]

Primary lung cancer seldom appears as a radiologic pattern with diffuse tiny pulmonary nodules, which may mimic miliary tuberculosis or other malignancies of hematogenous metastatic origin. We report the case of a 57-year-old female patient who was a non-smoker. The initial radiologic image study showed diffuse tiny pulmonary nodules, and the final pathologic study revealed primary lung adenocarcinoma with an epidermal growth factor receptor mutation. This unique radiologic pattern is a diagnostic challenge and further histologic evidence is important for the definitive diagnosis. ***(Thorac Med 2022; 37: 230-235)***

Key words: Lung cancer, adenocarcinoma, miliary metastasis, miliary intrapulmonary carcinomatosis

Background

Diffuse tiny pulmonary nodules with a chronic clinical course usually arise from atypical infections such as miliary tuberculosis, pneumoconiosis, sarcoidosis, malignancy, or other interstitial lung disease [1]. Primary lung cancer seldom appears with this unique radiologic pattern, which may mimic miliary tuberculosis or other malignancies of hematogenous metastatic origin. Histologic and microbiologic evidence that we acquired through further intervention played an important role in the definitive diagnosis.

Case Report

This 57-year-old female patient without systemic disease suffered from chronic cough with blood-tinged sputum for 1 month. She complained of dyspnea on exertion, lasting for weeks, but denied fever, chest pain, nausea, poor appetite or body weight loss. She was a retired teacher and denied a smoking history. Due to a poor response to treatment in a local medical department, she came to our chest outpatient department. Physical examination showed bilateral diffuse rhonchi, and pulse oximetry revealed oxyhemoglobin saturation of 93 percent. Chest X-ray showed diffuse tiny nodules in bilateral lung fields, with a nodular opacity at the left retro-cardiac area (Figure 1). She then was admitted for further evaluation. Laboratory data showed leukocytosis with neutrophil predominance, and an elevation of tumor markers, such as carbohydrate antigen 19-9 (CA 19-9) and

[1]Department of Internal Medicine, Division of Chest Medicine, Chi Mei Hospital, Tainan City, Taiwan.
Address reprint requests to: Dr. Kuo-Hwa Chiang, Division of Chest Medicine, Department of Internal Medicine, Chi Mei Hospital, No.901, Zhonghua Rd., Yongkang Dist., Tainan City 710, Taiwan (R.O.C.)

carcinoembryonic antigen (CEA). Chest computed tomography (CT) showed multiple bilateral lung nodules and ground glass opacities (Figure 2a, b, c), 2.2 cm in size and more dominant in the left lower lobe (Figure 2d, e), as well as a small amount of bilateral pleural effusion and pericardial effusion, lymphadenopathy at the mediastinum and bilateral hilar area, and expansile and osteolytic change at the right 9th rib. Multiple hypovascular tumors at the right lobe of the liver and right adrenal nodule were also found on chest CT. A gynecologist was consulted for an evaluation of the origin of the multiple metastases; however, no gynecological

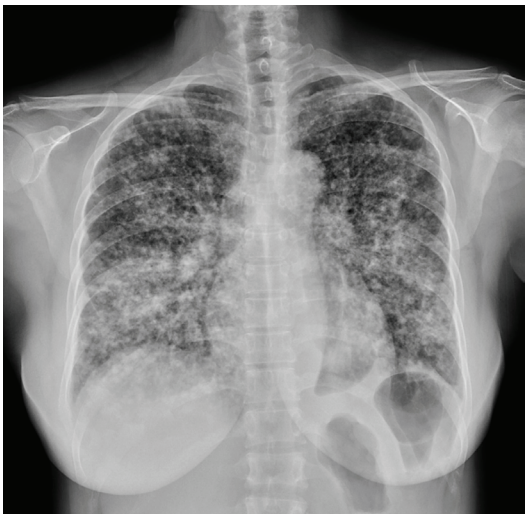

Fig. 1. Chest radiography at the initial presentation showed diffuse tiny nodules with ground glass opacities in bilateral lung fields and a nodular opacity at the left retro-cardiac area.e.

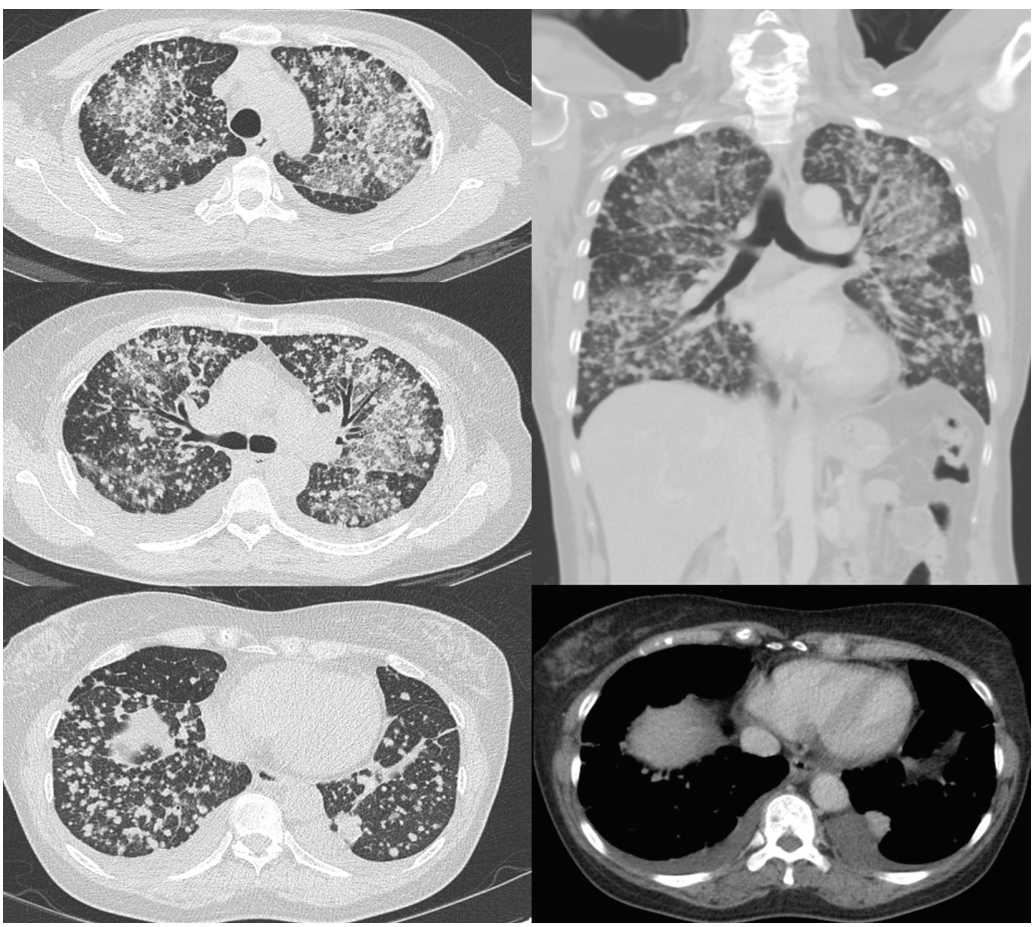

Fig. 2. Chest CT scan at the initial diagnosis showed multiple bilateral lung nodules and ground glass opacities (a,b,c), relatively dominant in the left lower lobe and 2.2 cm in size, with a small amount of bilateral pleural effusion (d,e); lymphadenopathy was also seen at the mediastinum and bilateral hilar area.

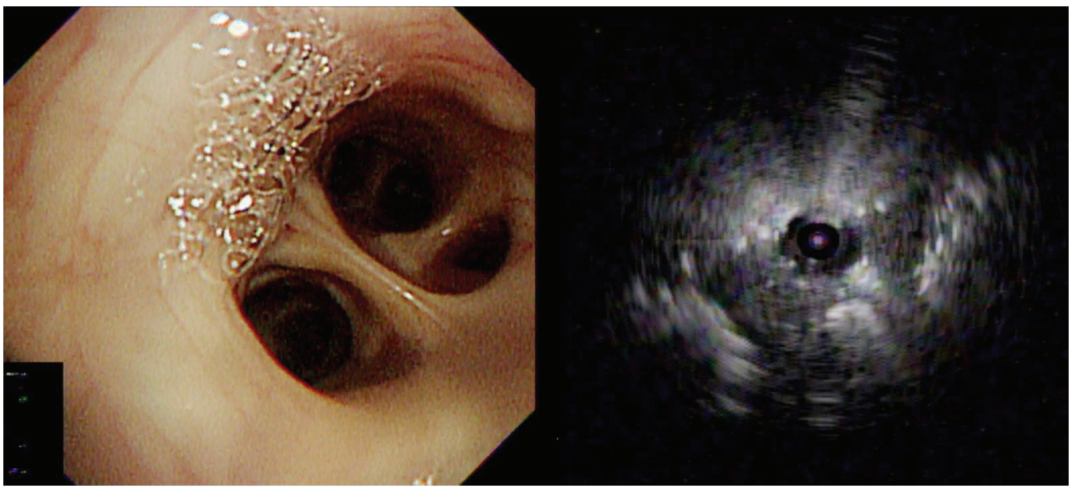

Fig. 3. Bronchoscopy showed no endobronchial lesion, lumen stenosis or mucosal change within visible range (a), but endobronchial ultrasonography revealed an atypical bronchus sign with partial consolidation at a 3 cm depth from the orifice of LB10a (b).

tumor was detected. Sputum cytology revealed atypical epithelial cells with a high nuclear-to-cytoplasmic ratio, coarse granular nuclear chromatin, and prominent nucleoli, which were suspicious of malignancy. Left-side diagnostic thoracentesis was also performed, and cytology of the pleural effusion showed malignant cells, similar to the result of the sputum cytology (Figure 4). Bronchoscopy was arranged later and revealed no endobronchial lesion, lumen stenosis or mucosal change within visible range (Figure 3a). However, endobronchial ultrasonography showed an atypical bronchus sign with partial consolidation at a 3-cm depth from the orifice of LB10a (Figure 3b).

Transbronchial biopsy was performed via LB10a, and pathology showed adenocarcinoma with hyperchromatic tumor cells in glandular structures and micropapillary groups, which were immunoreactive to thyroid transcription factor-1 (TTF-1) stain (Figure 5). Brain magnetic resonance imaging and bone scan showed diffuse brain and bony metastasis. Later, epidermal growth factor receptor (EGFR) was

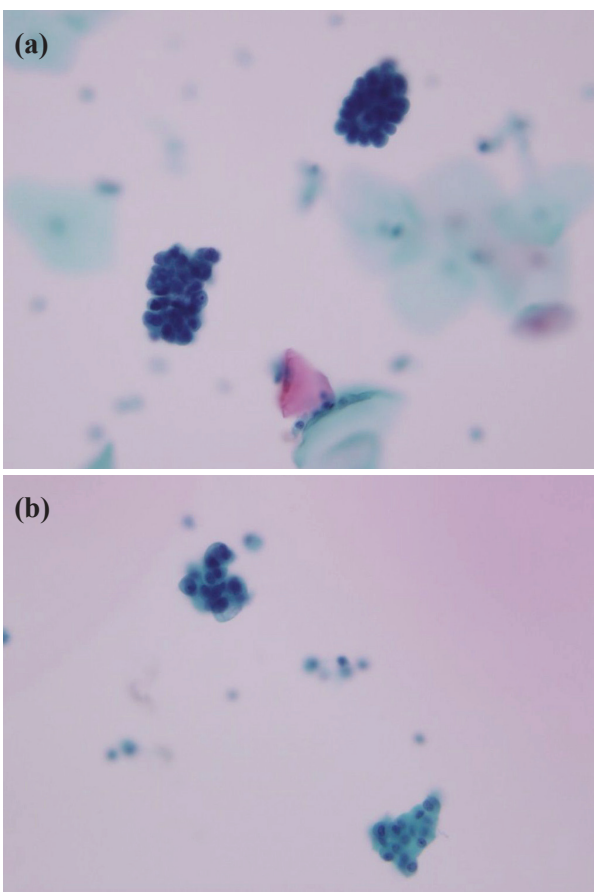

Fig. 4. Cytology of sputum (a) and pleural effusion (b) revealed some ball-like or glandular clusters of atypical epithelial cells with a high nuclear-to-cytoplasmic ratio, coarse granular nuclear chromatin and prominent nucleoli, all of which favored malignancy.

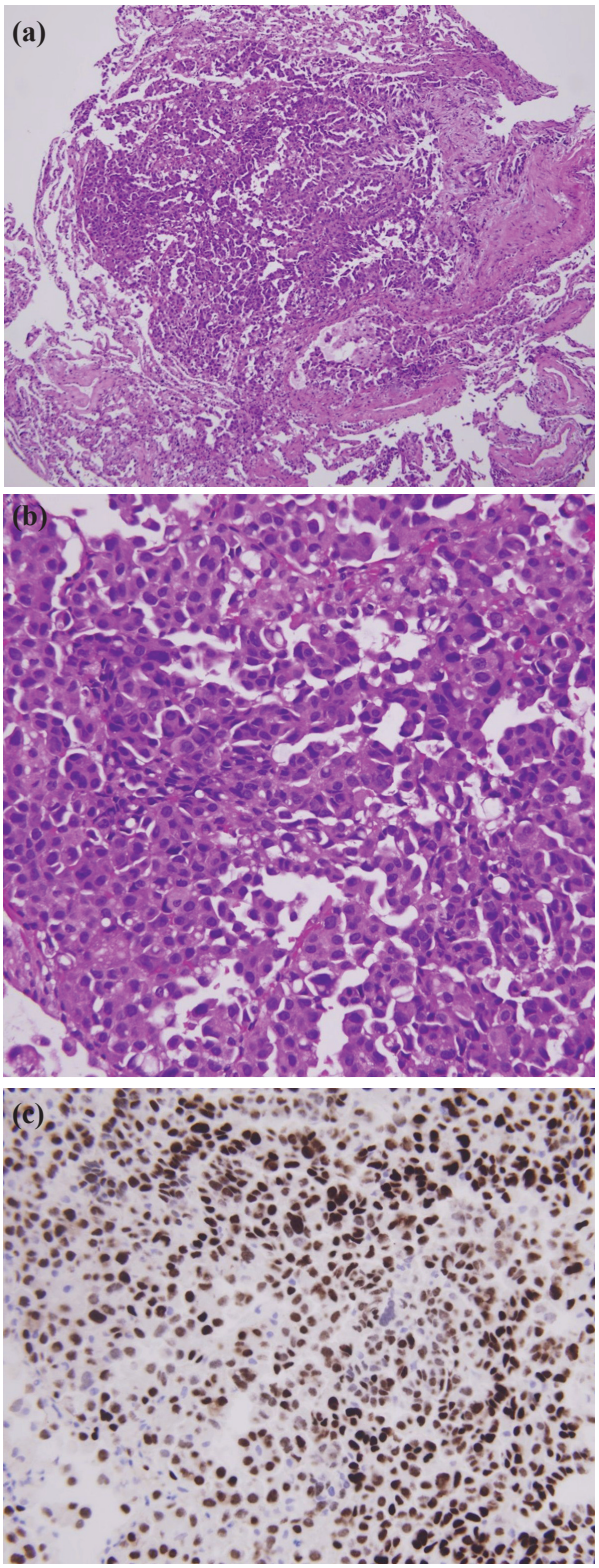

Fig. 5. Histological examination of the transbronchial biopsy via LB10a showed lung tissue infiltrated by hyperchromatic tumor cells arranged in glandular structures and micropapillary groups (a,b), which were immunoreactive to TTF-1 stain (c)

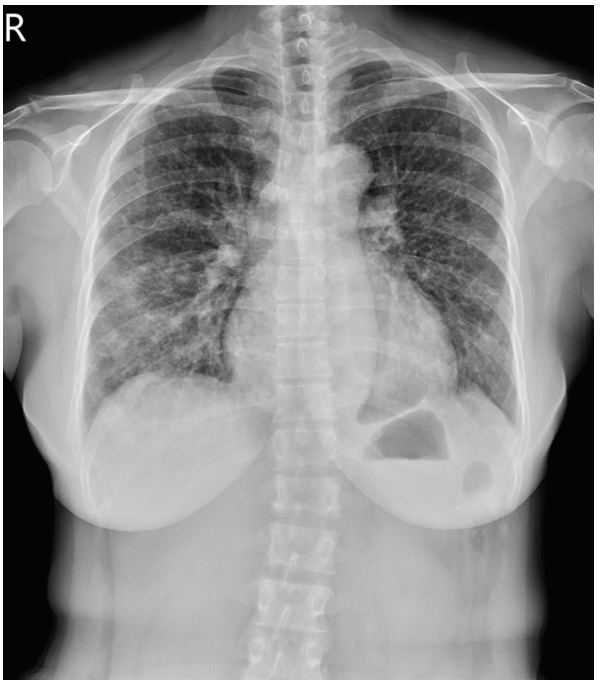

Fig. 6. Chest radiography after a 1-month TKI treatment showed interval regression of lung metastasis compared with the previous image.

found to be positive for an exon 21 L858R mutation. With the diagnosis of lung adenocarcinoma with multiple lung-to-lung, liver, brain and bony metastases, cT4N3M1c, stage IVB, the tyrosine kinase inhibitor (TKI) afatinib was prescribed. Spectacular improvement in the follow-up radiologic image was found 1 month later (Figure 6).

Discussion

Lung cancer is the most common cause of cancer-related deaths, accounting for 19% of all cancer deaths in Taiwan [2]. The lung is frequently a metastatic source of cancer, and chest radiography presents several different patterns, including multiple pulmonary nodules, interlobular septal thickening, pleural effusions and enlarged lymph nodes [3-4]. In some cases, nu-

merous diffuse tiny nodules appear in the pattern, and some investigators have termed this miliary intrapulmonary carcinomatosis (MIPC). The micronodules (<5 millimeter in size) seen on chest CT with diffuse distribution throughout the bilateral lungs, also known as a snowstorm sign, indicate a hematogenous dissemination of malignancy, and differ from cannonball metastases [5]. About 2 percent of patients with stage IV non-small cell lung cancer presented with an MIPC pattern at initial diagnosis [6]. Hematogenous dissemination as miliary intrapulmonary carcinomatosis also presents a high likelihood of distant organ metastasis, with the most frequent sites being bone (64%), brain (37%) and liver (27%) [6]. The most common lung cancer presenting this radiologic pattern was adenocarcinoma, and it was highly associated with an EGFR mutation [6-8]. Compared with wild-type EGFR, more cases (about 70-80%) with a pattern of miliary pulmonary metastasis revealed mutated EGFR [6-7]. Our case's EGFR showed an exon 21 L858R mutation, while the most frequent EGFR mutation reported in other studies was a deletion in exon 19 [6,9,10-11]. Some studies reported a somatic complex heterozygous EGFR mutation [12]. A high rate of adenocarcinoma and an EGFR mutation imply that a TKI is a better choice of treatment than chemotherapy [6,13-14]. A common mutation of EGFR such as an exon 19 deletion and L858R point mutation, and other rare mutations, such as an exon 19 insertion and point mutations of S768I, L861Q and G719X, are associated with responsiveness to EGFR-TKI therapy. Otherwise, some EGFR mutations, including an exon 20 insertion and T790M mutation, predict a lack of responsiveness [15]. Response to TKI in mutated EGFR metastatic lung adenocarcinoma was associated with a maximum standardized uptake value (SUVmax) of the primary tumor in an 18F-fluorodeoxyglucose positron emission tomography (18F-FDG-PET) exam, the serum CEA level, gender and smoking history [16]. Hsu et al. found that the presence of miliary metastases did not predict a poor overall survival [8]. However, other studies reported a poorer prognosis in patients with miliary pulmonary dissemination, especially in those harboring EGFR mutations, under first-generation TKI (gefitinib, erlotinib) treatment. Progression-free survival was 8-9 months and 13-14 months in patients with and without miliary pulmonary metastases [9,17-18]. Some studies reported a second-generation TKI (afatinib) prescription, but there were inadequate data for analysis [9,13]. Yang Fu et al. reported that a switch to a third-generation TKI (osimitinib) after treatment failure with first-generation TKIs yielded a shorter progression-free survival in a diffuse intrapulmonary metastases group than in a non-diffuse group (5.2 versus 14.6 months) [18]. There is a lack of data on the outcome of EGFR-mutated non-small cell lung cancer with miliary carcinomatosis with the use of different generations of TKIs. In conclusion, lung cancer with diffuse tiny nodular metastasis in both lungs is an uncommon phenomenon and deserves more attention in clinical practice. Diagnostic tissue proof with molecular and biomarker analysis in the early period is important in determining further treatment and predicting the prognosis.

References

1. Boitsios G, Bankier AA, Eisenberg RL. Diffuse pulmonary nodules. AJR Am J Roentgenol 2010 May; 194(5):W354-66. doi: 10.2214/AJR.10.4345. PMID: 20410379.

2. 108年國人死因統計結果. 衛生福利部統計處109-06-16. https://www.mohw.gov.tw/dl-61912-c189168f-f107-4a4b-9b10-b18789a2a4e9.html
3. Marom EM, Patz EF Jr, Swensen SJ. Radiologic findings of bronchogenic carcinoma with pulmonary metastases at presentation. Clin Radiol 1999 Oct; 54(10):665-8. doi: 10.1016/s0009-9260(99)91088-7. PMID: 10541392.
4. Quinn D, Gianlupi A, Broste S. The changing radiographic presentation of bronchogenic carcinoma with reference to cell types. Chest 1996 Dec; 110(6):1474-9. doi: 10.1378/chest.110.6.1474. PMID: 8989064.
5. Chiarenza, A., Esposto Ultimo, L., Falsaperla, D. *et al*. Chest imaging using signs, symbols, and naturalistic images: a practical guide for radiologists and non-radiologists. Insights Imaging 2019 Dec 4; 10(1):114. doi: 10.1186/s13244-019-0789-4. PMID: 31802270; PMCID: PMC6893008.
6. Wu SG, Hu FC, Chang YL, *et al*. Frequent EGFR mutations in non-small cell lung cancer presenting with miliary intrapulmonary carcinomatosis. Eur Res J 2013; 41(2):417-424. doi: 10.1183/09031936.00006912. Epub 2012 Apr 20. PMID: 22523351.
7. Togashi Y, Masago K, Kubo T, *et al*. Association of diffuse, random pulmonary metastases, including miliary metastases, with epidermal growth factor receptor mutations in lung adenocarcinoma. Cancer 2011; 117(4):819-825. doi: 10.1002/cncr.25618. Epub 2010 Sep 30. PMID: 20886633.
8. Hsu F, Nichol A, Toriumi T, *et al*. Miliary metastases are associated with epidermal growth factor receptor mutations in non-small cell lung cancer: a population-based study. Acta Oncol 2017 Sep; 56(9):1175-1180. doi: 10.1080/0284186X.2017.1328128. Epub 2017 May 19. PMID: 28521651.
9. Kim HJ, Kang SH, Chung HW, *et al*. Clinical features of lung adenocarcinomas with epidermal growth factor receptor mutations and miliary disseminated carcinomatosis. J Thoracic Cancer 2015; 6(5):629–635. doi: 10.1111/1759-7714.12234. Epub 2015 Feb 14. PMID: 26445612; PMCID: PMC4567009.
10. Li L, Zhou L, Zhang J. Lung adenocarcinomas with pulmonary miliary metastases: a case report and literature review. Zhongguo Fei Ai Za Zhi 2019 Dec 20; 22(12):798-804. Chinese. doi: 10.3779/j.issn.1009-3419.2019.12.11. PMID: 31874677; PMCID: PMC6935038.
11. Laack E, Simon R, Regier M, *et al*. Miliary never-smoking adenocarcinoma of the lung: strong association with epidermal growth factor receptor exon 19 deletion. J Thorac Oncol 2011 Jan; 6(1):199-202. doi: 10.1097/JTO.0b013e3181fb7cf1. PMID: 21178715.
12. Schaller A, Beau-Faller M, Mennecier B, *et al*. Lung adenocarcinoma with pulmonary miliary metastases and complex somatic heterozygous EGFR mutation. Case Rep Oncol 2014 Nov 19; 7(3):769-73. doi: 10.1159/000369526. PMID: 25722667; PMCID: PMC4322700.
13. Beck TN, Kharin LV, Kit OI, *et al*. Miliary adenocarcinoma of the lung responds to gefitinib and afatinib. J Thorac Oncol 2018 Jun; 13(6):e95-e97. doi: 10.1016/j.jtho.2018.01.018. PMID: 29793652.
14. Kobayashi M, Takeuchi T, Bandobashi K, *et al*. Diffuse micronodular pulmonary metastasis of lung adenocarcinoma predicts gefitinib response in association with epidermal growth factor receptor mutations. Anticancer Res 2006 Mar-Apr; 26(2B):1621-6. PMID: 16619582.
15. Ettinger DS, Wood DE, Aggarwal C, *et al*. NCCN Guidelines Insights: Non-Small Cell Lung Cancer, Version 1.2020. J Natl Compr Canc Netw 2019 Dec; 17(12):1464-1472. doi: 10.6004/jnccn.2019.0059. PMID: 31805526.
16. Ng KS, King Sun C, Boom Ting K, *et al*. Prognostic factors of EGFR-mutated metastatic adenocarcinoma of lung. Eur J Radiol 2020 Feb; 123:108780. doi: 10.1016/j.ejrad.2019.108780. Epub 2019 Dec 10. PMID: 31846863.
17. Okuma, Y., Kashima, J., Watanabe, K. *et al*. Survival analysis and pathological features of advanced non-small cell lung cancer with miliary pulmonary metastases in patients harboring epidermal growth factor receptor mutations. J Cancer Res Clin Oncol 2018 Aug; 144(8):1601-1611. doi: 10.1007/s00432-018-2681-x. Epub 2018 Jun 1. PMID: 29858682.
18. Fu Y, Tang Y, Zheng Y, *et al*. Imaging pattern of diffuse intrapulmonary metastases in lung cancer was associated with poor prognosis to epidermal growth factor receptor inhibitors. Cancer Manag Res 2020 Nov 17; 12:11761-11772. doi: 10.2147/CMAR.S261983. PMID: 33235504; PMCID: PMC7680171.

Rapid Pulmonary Fibrosis Induced by Oxaliplatin: An Unexpected but Serious Side Effect in Treating Colorectal Cancer

Chieh-Lung Chen[1], Wei-Chih Liao[1,2,3], Shinn-Jye Liang[1], Chih-Yu Chen[1], Chih-Yen Tu[1,3], Wu-Huei Hsu[1]

Drug-induced pulmonary fibrosis is a rare but serious side effect caused by chronic administration of certain drugs, and its actual incidence is unknown. There is an increasing number of reports in the literature on the association of oxaliplatin with pulmonary toxicity. Discontinuation of oxaliplatin often results in clinical and radiological improvement of mild disease. However, most cases of oxaliplatin-induced pulmonary fibrosis had a rapid and fatal course. The efficacy of systemic corticosteroids, antioxidant agents, or anti-fibrotic agents remains unclear. Herein, we present a rare case of rapid pulmonary fibrosis induced by oxaliplatin in a patient who received 11 courses of chemotherapy with 5-fluorouracil, leucovorin, and oxaliplatin (FOLFOX) as adjuvant treatment for resected colorectal cancer, and review the literatureis. ***(Thorac Med 2022; 37: 236-241)***

Key words: Pulmonary fibrosis, oxaliplatin, FOLFOX, colorectal cancer

Introduction

Pulmonary fibrosis is a chronic progressive interstitial lung disease characterized by repeated injury to the alveolar epithelium and dysregulated repair [1]. Although most cases of pulmonary fibrosis are idiopathic [2], a comprehensive medical history that includes comorbidities, medications, environmental exposure, and occupational and family history should be considered to identify a secondary etiology [3]. The most common symptoms on examination include dyspnea, nonproductive cough, and crackles. The diagnosis is reached through combination of clinical features, chest radiography, pulmonary function testing, high-resolution computed tomography, and histopathology in selected cases.

Drug-induced pulmonary fibrosis can be caused by chronic administration of certain drugs such as bleomycin, amiodarone, and cyclophosphamide [4]. The true incidence of

[1]Division of Pulmonary and Critical Care Medicine, Department of Internal Medicine, China Medical University Hospital, Taichung, Taiwan, [2]Department of Internal Medicine, Hyperbaric Oxygen Therapy Center, China Medical University Hospital, Taichung, Taiwan, [3]School of Medicine, China Medical University, Taichung, Taiwan.
Address reprint requests to: Dr. Chih-Yu Chen, Department of Internal Medicine, China Medical University Hospital, No. 2, Yude Road, Taichung, Taiwan

drug-induced pulmonary fibrosis is unknown. In a systematic review evaluating drug-induced interstitial lung disease, anti-neoplastic agents were the leading cause of the disease in most studies, accounting for 23–51% of cases, followed by disease-modifying anti-rheumatic drugs (6–72%), antibiotics (6–26%), non-steroidal anti-inflammatory agents (0–23%), psychiatric medications (0–9%), and anti-arrhythmic agents (0–9%) [5].

The combination of 5-fluorouracil (5-FU), leucovorin, and oxaliplatin, the so-called FOLFOX regimen, has become a well-established treatment for patients with advanced colorectal cancer [6]. The major side effects of oxaliplatin generally include gastrointestinal, hematologic, hepatic, and neurologic toxicities. Although there is an increasing number of reports in the literature on the association of oxaliplatin with pulmonary toxicity, there have been few reports on oxaliplatin-induced pulmonary fibrosis.

Case Report

A 58-year-old non-smoking male computer engineer presented with a 2-week history of dyspnea on exertion. Six months prior to this, he underwent laparoscopic anterior resection for colorectal adenocarcinoma with surgical stage T3N2M0. He subsequently received 11 cycles of FOLFOX chemotherapy with bi-weekly leucovorin (400 mg/m2), 5-FU (2400 mg/m2), and oxaliplatin (85 mg/m2). During treatment, no complaints were noted, and he receive no follow-up chest radiographs. Unfortunately, the 12th cycle of chemotherapy was postponed due to dyspnea.

Chest radiograph and computed tomography revealed reticulation, traction bronchiectasis, and volume loss in the upper lobes and perihilar regions (Figure 1), which were suggestive of pulmonary fibrosis. The serological markers of autoimmune disease were all nega-

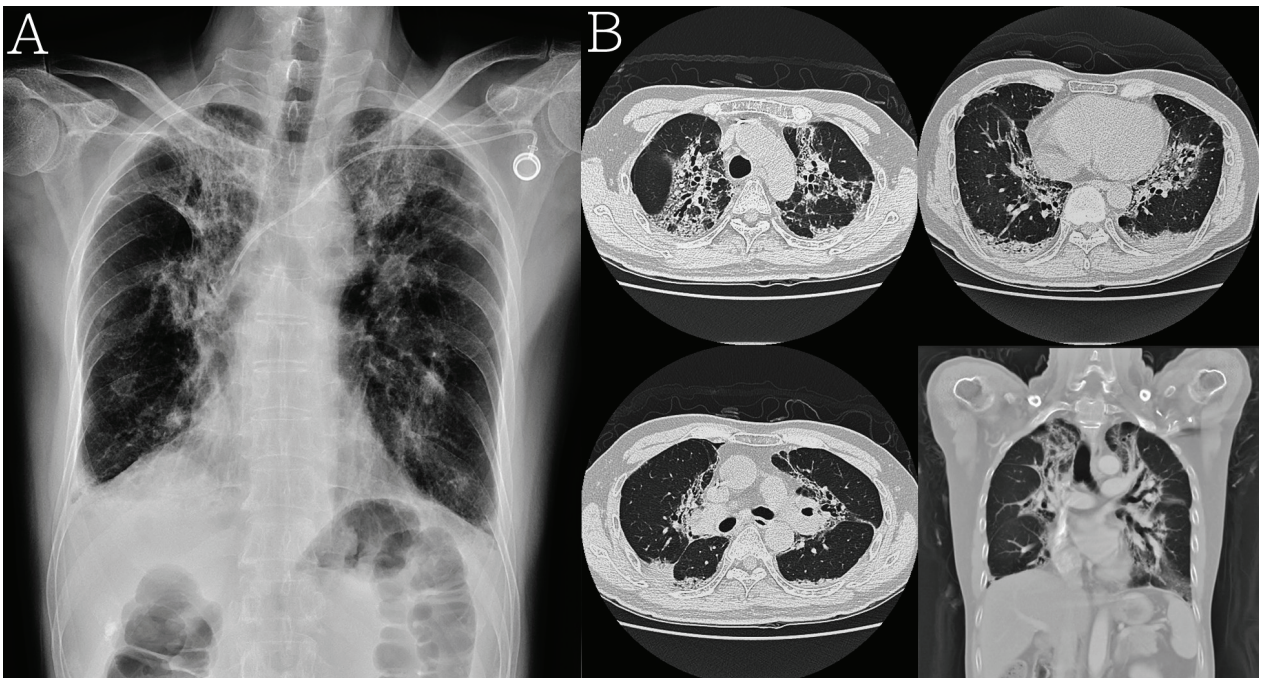

Fig. 1. (A) Chest radiography showing a radiopaque are with volume reduction of upper lungs. (B) Computed tomography of the chest showing reticulation, traction bronchiectasis and volume loss in the upper lobes and perihilar regions, suggestive of pulmonary fibrosis.

tive. Transbronchial lung biopsy via a flexible bronchoscope revealed chronic inflammation with focally increased lymphocytic infiltration, and no microorganisms (e.g., bacteria, mycobacteria, fungi, viruses, Pneumocystis jiroveci polymerase chain reaction, or aspergillus galactomannan antigen) were detected by bronchoalveolar lavage. We discontinued FOLFOX chemotherapy due to a suspicion of oxaliplatin-induced pulmonary fibrosis, and intravenous methylprednisolone (20 mg every 8 hours) was begun. With improvement in his symptoms and radiological abnormalities after treatment, he was discharged on the 20th admission day. However, the patient experienced progressive respiratory distress 2 weeks after discharge and presented to our clinic with acute respiratory failure. The patient died due to refractory respiratory deficiency 2 weeks later.

Discussion

Pulmonary toxicity in conjunction with FOLFOX therapy is uncommon (≤1.5%) [7]. It occurs late in the course of therapy [8-9], at a median of 8 cycles of FOLFOX therapy (ranging from 1 to 22 cycles) [10]. FOLFOX therapy-related pulmonary toxicity reportedly includes acute interstitial pneumonia [11], bronchiolitis obliterans organizing pneumonia, cryptogenic organizing pneumonitis, diffuse alveolar damage, eosinophilic pneumonia [10], and pulmonary fibrosis (Table 1).

An important consideration is determining oxaliplatin as the culprit of pulmonary toxicity. There has only been 1 report of pulmonary toxicity accompanying the administration of 5-FU as monotherapy [12]. In other reports, respiratory symptoms presented during FOLFOX therapy did not recur after re-challenging with a chemotherapy regimen containing 5-FU and leucovorin, but without oxaliplatin [9, 11, 13-15].

Pulmonary fibrosis is a rare but serious side effect of oxaliplatin treatment and resulted in patient death in most reported cases (Table 1). However, it is believed that the actual incidence of this side effect is probably higher. Cases with mild symptoms remain unrecognized or are under-reported. Most reported patient were older than 60 years and the majority were male (Table 1). The temporal evolution of interstitial pneumonia after initiation of treatment varies between studies. It may occur soon after treatment initiation, or it may develop several months after adjuvant treatment, as seen in our patient. Early initiation of monitoring of pulmonary toxicity is thus warranted.

The precise pathophysiological mechanism of this phenomenon has not been clarified yet. There are data suggesting that oxaliplatin may cause the depletion of glutathione, a small antioxidant molecule, which may be involved in the pathogenesis of liver damage caused by the drug [16]. In the lung, glutathione plays a significant role as a protector against oxidative damage. The depletion caused by oxaliplatin may be the factor triggering the pulmonary inflammation, leading to interstitial pneumonitis and subsequent pulmonary fibrosis [17].

Discontinuation of oxaliplatin often results in clinical and radiological improvement in patients with oxaliplatin-induced pulmonary toxicity [18]. Most cases of oxaliplatin-induced pulmonary fibrosis had a rapid and fatal course and systemic corticosteroid is the most commonly used treatment, other than drug withdraw (Table 1). However, the efficacy of systemic corticosteroids with mild or more severe disease, the optimal corticosteroids dose and

Table 1. Summary of Reported Cases of Oxaliplatin-induced Pulmonary Fibrosis

Year	Author [Reference]	Age (years) / sex	Oncologic diagnosis	Cycles of OX-based chemotherapy	Total dose OX (mg/m2)	Presumed lung disease (Radiology/Laboratory)	Pathology	Treatment other than discontinuation of OX	Outcome
2005	Hernández Yagüe *et al.* [19]	68/F	Colorectal cancer	6	510	PF	LB: IP + DAD	Corticosteroids	Death
2006	Ruiz-Casado *et al.* [20]	67/M	HCC	NA	1100	PF	NA	None	Improvement
2006	Pasetto *et al.* [21]	74/m	Colorectal cancer	6	510	PF	NA	Corticosteroids	Death
2007	Mundt *et al.* [22]	66/M	Colorectal cancer	12	1020	Infectious pneumonia	Necropsy: DAD + PF	Corticosteroids	Death
2008	Arevalo Lobera *et al.* [23]	73/F	Colorectal cancer	4	340	PF	Necropsy: DAD	Corticosteroids	Death
2008	Arevalo Lobera *et al.* [23]	71/M	Colorectal cancer	4	NA	Infectious pneumonia	Necropsy: IP + PF	Corticosteroids	Death
2008	Wilcox *et al.* [24]	71/M	Colorectal cancer *	5	900	PF	NA	Corticosteroids	Death
2008	Wilcox *et al.*[24]	69/M	Colorectal cancer *	6	NA	PF	NA	N-acetylcysteine	Improvement
2009	Arpan Shah *et al.* [17]	76/M	Colorectal cancer	2	260	PF	NA	Corticosteroids	Death
2010	Han Lim *et al.* [25]	64/M	Gastric cancer	8	680	ILD/PF	NA	Corticosteroids	Death
2011	Ryu *et al.* [26]	55/M	Colorectal cancer	13	1105	PF	NA	Corticosteroids	Death
2011	Ryu *et al.* [26]	73/M	Colorectal cancer	9	765	PF/HP	NA	Corticosteroids	Death
2011	Chan *et al.* [27]	66/M	Colorectal cancer	4	340	PF	NA	Corticosteroids N-acetylcysteine	Improvement
2012	Pontes *et al.* [28]	73/F	Colorectal cancer	11	935	PF	DAD + COP	Corticosteroids	Death
2012	Pontes *et al.* [28]	75/M	Gastric cancer	9	765	PF	NA	Corticosteroids	Death
2012	Pontes *et al.* [28]	64/M	Colorectal cancer	12	1020	PF	DAD + PF	Corticosteroids	Death
2020	Mirjana Pavlović *et al.* [29]	66/M	Colorectal cancer	11	935	ILD/PF	NA	Corticosteroids	Improvement
2020	Moreira *et al.* [18]	70/M	Colorectal cancer	8	1040	PF	NA	None	Improvement
2021	Present case	58/M	Colorectal cancer	11	935	PF	Chronic inflammation	Corticosteroids	Improvement, but died from respiratory deficiency 4 weeks later

** Patient had pre-existing mild ILD before oxaliplatin therapy.*

COP: cryptogenic organizing pneumonitis, DAD: diffuse alveolar damage, HCC: hepatocellular carcinoma, HP: hypersensitivity pneumonitis, ILD: interstitial lung disease, IP: interstitial pneumonia, LB: lung biopsy, OX: oxaliplatin, PF: pulmonary fibrosis, NA: not available

treatment duration, and the role of anti-fibrotic agents in oxaliplatin-induced pulmonary fibrosis remain to be further investigated. There are no adequate data suggesting whether treatment with antioxidant agents, such as N-acetylcysteine, may be beneficial.

In conclusion, as a possible offending agent, pulmonary fibrosis should be considered in patients receiving oxaliplatin. Regular follow-up chest radiography is warranted, and early recognition is of great importance because it allows prompt cessation of chemotherapy and initiation of systemic corticosteroids, which may improve patient outcome.

Disclosure

This case report was presented as a poster in the 2018 American Thoracic Society International Conference.

Consent for Publication

All authors have reviewed and approved the manuscript for publication.

Funding

There is no funding to report.

Conflicts of Interest

The authors report no conflicts of interest for this work.

References

1. Sgalla G, Iovene B, Calvello M, *et al*. Idiopathic pulmonary fibrosis: pathogenesis and management. Respir Res 2018; 19(1): 32.
2. Sauleda J, Nunez B, Sala E, *et al*. Idiopathic pulmonary fibrosis: epidemiology, natural history, phenotypes. Med Sci (Basel). 2018;6(4).
3. Kalchiem-Dekel O, Galvin JR, Burke AP, *et al*. Interstitial lung disease and pulmonary fibrosis: a practical approach for general medicine physicians with focus on the medical history. J Clin Med 2018; 7(12).
4. Daba MH, El-Tahir KE, Al-Arifi MN, *et al*. Drug-induced pulmonary fibrosis. Saudi Med J. 2004;25(6): 700-6.
5. Skeoch S, Weatherley N, Swift AJ, *et al*. Drug-induced interstitial lung disease: a systematic review. J Clin Med 2018; 7(10).
6. Ruzzo A, Graziano F, Loupakis F, *et al*. Pharmacogenetic profiling in patients with advanced colorectal cancer treated with first-line FOLFOX-4 chemotherapy. J Clin Oncol 2007; 25(10): 1247-54.
7. Shimura T, Fuse N, Yoshino T, *et al*. Clinical features of interstitial lung disease induced by standard chemotherapy (FOLFOX or FOLFIRI) for colorectal cancer. Ann Oncol 2010; 21(10): 2005-10.
8. Hannan LM, Yoong J, Chong G, *et al*. Interstitial lung disease in a patient treated with oxaliplatin, 5-fluorouracil and leucovorin (FOLFOX) for metastatic colorectal cancer. Radiol Oncol 2012; 46(4): 360-2.
9. Muneoka K, Shirai Y, Sasaki M, *et al*. Interstitial pneumonia arising in a patient treated with oxaliplatin, 5-fluorouracil, and, leucovorin (FOLFOX). Int J Clin Oncol 2009; 14(5): 457-9.
10. De Weerdt A, Dendooven A, Snoeckx A, *et al*. Prognosis and treatment of FOLFOX therapy-related interstitial pneumonia: a plea for multimodal immune modulating therapy in the respiratory insufficient patient. BMC Cancer 2017; 17(1): 586.
11. Homma T, Kurokawa M, Yamamoto Y, *et al*. Oxaliplatin-induced lung injury with allergic reaction. Chin J Cancer Res 2011; 23(3): 232-5.
12. Andou H, Itoh K, Tsuda T. [A case of fluorouracil-induced pneumonitis]. Nihon Kyoubu Shikkan Gakkai Zasshi 1997;35: 1080-1083
13. Wildner D, Boxberger F, Wein A, *et al*. Granulomatous lung disease requiring mechanical ventilation induced by a single application of oxaliplatin-based chemotherapy for colorectal cancer: a case report. Case Rep Oncol Med 2013; 2013: 683948.
14. Prochilo T, Abeni C, Bertocchi P, *et al*. Oxaliplatin-induced lung toxicity. Case report and review of the

literature. Curr Drug Saf 2012; 7(2): 179-82.
15. Garrido M, O'Brien A, Gonzalez S, *et al*. Cryptogenic organizing pneumonitis during oxaliplatin chemotherapy for colorectal cancer: case report. Chest 2007; 132(6): 1997-9.
16. Rubbia-Brandt L, Audard V, Sartoretti P, *et al*. Severe hepatic sinusoidal obstruction associated with oxaliplatin-based chemotherapy in patients with metastatic colorectal cancer. Ann Oncol 2004; 15(3): 460-6.
17. Shah A, Udwadia ZF, Almel S. Oxaliplatin-induced lung fibrosis. Indian J Med Paediatr Oncol 2009; 30(3): 116-8.
18. Moreira AC, Portela J, Couto C, *et al*. Pulmonary fibrosis secondary to oxaliplatin treatment: from rarity to reality: a case study and literature review. Oncol Ther 2020; 8(2): 183-90.
19. Yague XH, Soy E, Merino BQ, *et al*. Interstitial pneumonitis after oxaliplatin treatment in colorectal cancer. Clin Transl Oncol 2005; 7(11): 515-7.
20. Ruiz-Casado A, Garcia MD, Racionero MA. Pulmonary toxicity of 5-fluoracil and oxaliplatin. Clin Transl Oncol 2006; 8(8): 624.
21. Pasetto LM, Monfardini S. Is acute dyspnea related to oxaliplatin administration? World J Gastroenterol 2006; 12(36): 5907-8.
22. Mundt P, Mochmann HC, Ebhardt H, *et al*. Pulmonary fibrosis after chemotherapy with oxaliplatin and 5-fluorouracil for colorectal cancer. Oncology 2007; 73(3-4):270-2.
23. Arevalo Lobera S, Sagastibeltza Marinelarena N, Elejoste Echeberria I, et al. Fatal pneumonitis induced by oxaliplatin. Clin Transl Oncol 2008; 10(11):764-7.
24. Wilcox BE, Ryu JH, Kalra S. Exacerbation of pre-existing interstitial lung disease after oxaliplatin therapy: a report of three cases. Respir Med 2008; 102(2): 273-9.
25. Lim JH, Kim H, Choi WG, *et al*. Interstitial lung disease associated with FOLFOX chemotherapy. J Cancer Res Ther 2010; 6(4): 546-8.
26. Ryu CG, Jung EJ, Kim G, *et al*. Oxaliplatin-induced Pulmonary Fibrosis: Two Case Reports. J Korean Soc Coloproctol 2011; 27(5): 266-9.
27. Chan AK, Choo BA, Glaholm J. Pulmonary toxicity with oxaliplatin and capecitabine/5-Fluorouracil chemotherapy: a case report and review of the literature. Onkologie 2011; 34(8-9): 443-6.
28. Pontes LB, Armentano DP, Soares A, *et al*. Fatal pneumonitis induced by oxaliplatin: description of three cases. Case Rep Oncol. 2012;5(1): 104-9.
29. Mirjana Pavlović RŠ, Silovski T, Vuger AT, *et al*. Oxaliplatin-induced pulmonary fibrosis: a case report. Acta Clin Croat 2020; 59.(4.): 761-764.

Total Laparoscopic Cruroplasty with Gastropexy Using Unidirectional Barbed Suture for a Giant Hiatal Hernia

Xu-Heng Chiang[1], Shun-Mao Yang[2], Huan-Jang Ko[2]

The interrupted knot-tying suture is conventionally used in formal hiatal hernia repair, which consists of cruroplasty and gastropexy. The use of the unidirectional barbed suture is still uncommon in this field. Despite the limited data, barbed suture has been reported as safe and effective in cruroplasty. Here, we describe a case of giant hiatal hernia treated with total laparoscopic reduction of the hiatal hernia, followed by cruroplasty and gastropexy using unidirectional barbed suture. Use of a unidirectional barbed suture during the procedure is completely feasible and time-efficient. ***(Thorac Med 2022; 37: 242-247)***

Key words: Barbed suture, V-Loc, hiatal hernia, cruroplasty, gastropexy

Introduction

Hiatal hernia refers to a protrusion of elements other than the esophagus from the abdominal cavity into the thoracic cavity through an esophageal hiatus of the diaphragm. It is a relatively common condition, with an incidence rate of approximately 10–15% [1]. Most hiatal hernias are sliding hernias, or type I hiatal hernias, which account for 95% of cases. The remaining 5% of hiatal hernias are paraesophageal hiatal hernias (PEHs). Many patients with hiatal hernia show no symptom or only vague symptoms, and usually need no further surgical treatment. However, surgical intervention is indicated for symptomatic patients [2].

Laparoscopic hernia reduction is generally the surgical treatment of choice. Cruroplasty after hernia sac reduction is traditionally performed with an interrupted suture. Although experience is still limited, running barbed suture for cruroplasty has been reported to be effective and safe, and allows surgeons to perform more throws with better tissue approximation

[1]Division of Thoracic Surgery, Department of Surgery, National Taiwan University Hospital, Yun-Lin Branch,
[2] Division of Thoracic Surgery, Department of Surgery, National Taiwan University Hospital, Hsin-Chu Branch.
Address reprint requests to: Dr. Shun-Mao Yang, Department of Surgery, National Taiwan University Hospital

than does the interrupted suture [3]. Here, we describe the case of a giant hiatal hernia treated with total laparoscopic reduction, followed by cruroplasty and gastropexy with unidirectional barbed suture.

Case Presentation

The patient was an 85-year-old woman with a medical history of hypertension and type II diabetes mellitus for more than 20 years. Her surgical history was a left inguinal herniorrhaphy 1 year prior and left total knee arthroplasty 20 years prior. She presented to the emergency department with right back pain with radiation to the right chest for 3 days. She denied dyspnea, abdominal pain, dysphagia, vomiting, reflux, recent trauma history, or any similar episode before. The initial chest plain film showed a shadow above the left diaphragm. Computed tomography revealed a giant hiatal hernia, approximately 9.5 cm in diameter, with stomach and bowel loop incarceration (Figure 1).

The patient then was referred to the chest surgeon for advanced management. A barium contrast upper gastrointestinal study (Figure 2) was performed and also confirmed the diagnosis. Under the impression of type IV hiatal hernia, the chest surgeon successfully performed laparoscopic hiatal hernia repair with biologic mesh reinforcement 1 week after diagnosis. Abdominal inspection during the operation showed that the stomach, transverse colon, and omentum were incarcerated in the hernia sac (Figure 3). A type IV hiatal hernia was diagnosed during the operation, so the surgeon reduced the transverse colon and omentum, and also dissected the hernial sac. Then, the diaphragmatic defect was repaired with running barbed suture (V-Loc), after reduction of the contents in the

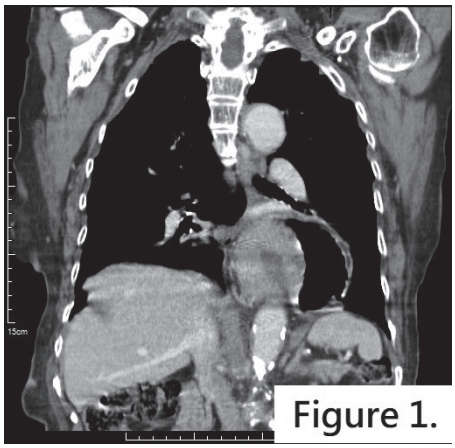

Fig. 1. Herniation of bowel loops in the thoracic cavity was revealed on chest computed tomography.

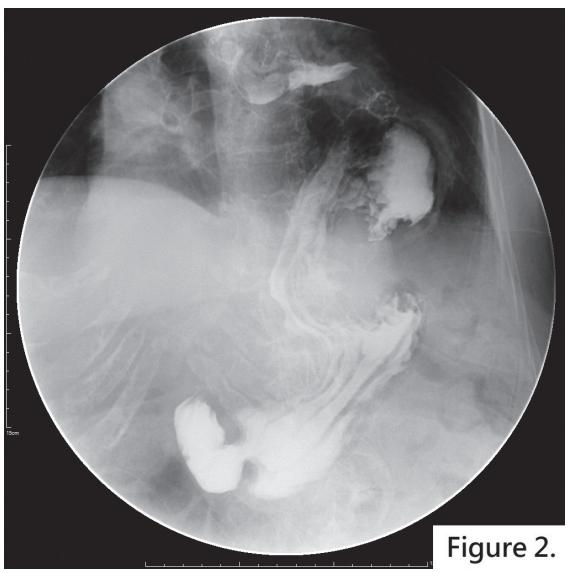

Fig. 2. Preoperative barium contrast study showed hiatal hernia.

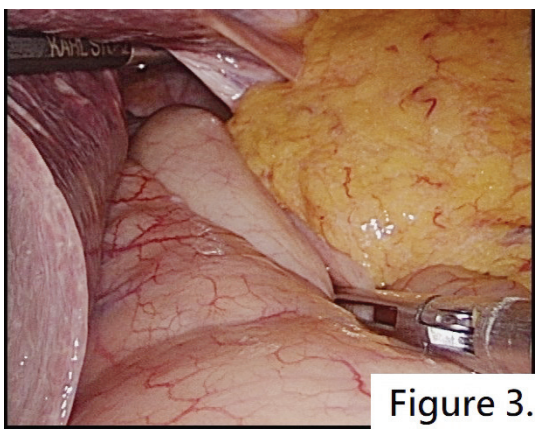

Fig. 3. The stomach, transverse colon, and greater omentum were incarcerated in the hernia sac.

hernial sac (Figure 4). Reinforcement with Biodesign mesh was performed to minimize the risks of recurrence (Figure 5). Finally, anterior gastropexy was performed with running barbed suture.

Another upper gastrointestinal barium study was performed on postoperative day 10, which revealed adequate reduction (Figure 6). The patient was discharged without an adverse event on postoperative day 12. No recurrence was observed during the 6-month outpatient follow-up.

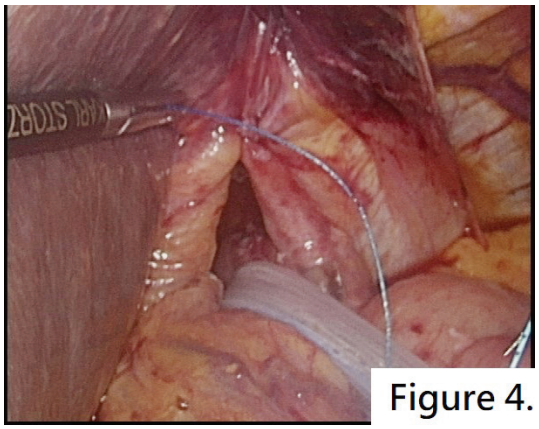

Fig. 4. Unidirectional running barbed suture was performed for cruroplasty.

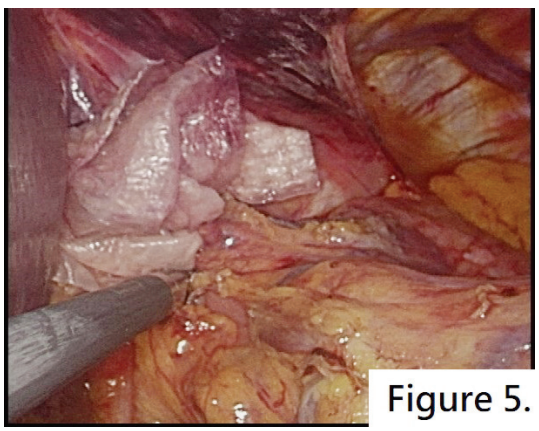

Fig. 5. Cruroplasty was reinforced with mesh.

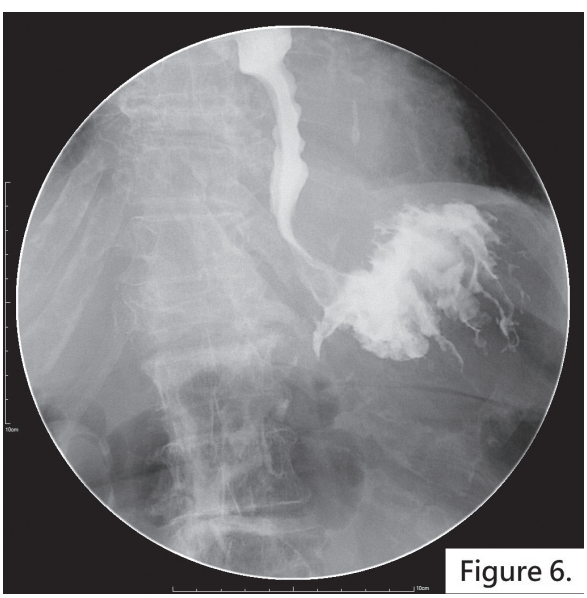

Fig. 6. Postoperative barium contrast study showed adequate reduction of the hiatal hernia.

Discussion

Once a symptomatic hiatal hernia is diagnosed, surgical intervention is indicated. The laparoscopic approach is currently the first choice to treat hiatal hernias. A previous study reported nearly comparable recurrence rates in procedures using the laparoscopic approach and the open approach [4]. Patients undergoing open hiatal hernia repair had longer hospital stay, longer surgical time, and higher postoperative ventilator dependence than those who underwent laparoscopic hiatal hernia repair [4]. In addition, morbidities such as pneumonia, thrombosis, hemorrhage, urinary tract infection, and wound infection were reported to be more frequent with the open approach. The only concern with the laparoscopic approach is the higher recurrence rate than with the open approach [5]. In the early 2000s, a case series of 94 patients who received PEH repair reported that the symptomatic recurrence rate was 12% and 0% with the laparoscopic and open approach, respectively [6]. Nevertheless, the recurrence rate has decreased with improvement in instruments, optimization of surgical techniques, and mesh reinforcement. In 2011, a retrospective

cohort that included 73 patients showed no significant difference in recurrence rates between the laparoscopic and open approaches [4]. The laparoscopic approach currently is considered as the first option for hiatal hernia repair.

Whether gastropexy should be performed is another issue in hiatal hernia repair. A prospective study series reported the use of gastropexy to reduce the recurrence rate after laparoscopic hiatal hernia repair. No recurrence was found during the 2-year follow-up period in 28 patients who underwent hernia reduction, sac excision, crural repair, an anti-reflux procedure, and routine anterior gastropexy [7]. In the elderly or high-risk patients, hernia reduction and gastropexy alone may be an effective option. In a case series, 11 patients received laparoscopic hernia reduction and anterior gastropexy without cruroplasty, and 8 of the 11 patients remained asymptomatic during the follow-up period (median, 10 months) [8]. Nevertheless, the radiological recurrence rate is relatively high in operations with gastropexy alone, compared with the formal procedure. Thus, cruroplasty combined with gastropexy is commonly recommended in routine hiatal hernia repair.

Both cruroplasty and gastropexy are usually performed with an interrupted knot-tying suture instead of a running barbed suture. The barbed suture was first applied for clinical use in the 1960s. As endoscopic surgery has become popular, these knotless sutures can make good use of a shorter operating time, and have a smoother training curve and perhaps a lower cost [9]. Although surgical knot-tying has been widely accepted and is thought to be safe, it has some disadvantages. The surgical knot is the weakest point throughout the suture line because of increased tension, and there may be more of an inflammatory reaction around the surgical knot [10]. The tying of a solid surgical knot is also more challenging to perform laparoscopically than hand sewing. Furthermore, a continuous barbed suture can attain a more even tension distribution than a knot-tying suture. Previous studies also demonstrated tensile strength equal to that of the traditional suture [9]. Many studies have verified that the barbed suture is a reliable, effective, and safe technique, even in comparison with the conventional suture [9, 11-12].

The barbed suture is commonly used in gynecology and urology. Most gynecologists and urologists have suggested that it requires less operative time, is safe, and provides even better anastomosis [11]. The barbed suture has also been applied widely in the field of general surgery. Laparoscopic gastrojejunostomy using the barbed suture has been reported with favorable outcomes [9]. Gastropexy, jejunopexy [12], esophagojejunostomy [13], and even repair of the bile duct [14] have been reported to be performed successfully with barbed suture. However, despite the shorter operative time, use of the barbed suture can still lead to surgical outcomes and complication rates comparable to those of the conventional suture.

The crural defect after reduction of a hiatal hernia is conventionally repaired with interrupted knot-tying sutures. A retrospective study compared immediate postoperative outcomes between running barbed and interrupted suture cruroplasty. The rate of recurrence identified on barium radiography was 16% in the interrupted suture group, but no recurrence was found in the running barbed suture group during a mean follow-up period of 72.6 and 291.4 days, respectively. The operative time per individual stitch was significantly shorter with the running barbed suture than with the interrupted suture.

Thus, surgeons could do more throws within the same operative period. Moreover, running sutures provide a more even distribution of tension between tissue approximations. Even though barbed sutures are more expensive, the reduced surgical time and other advantages can compensate for this [4].

In our experience, the use of barbed sutures in repairing crural defects and in gastropexy is feasible. Under a laparoscopic view, we had no difficulty in performing cruroplasty and gastropexy with continuous barbed suture. The running barbed suture is indeed more time-efficient than the knot-tying suture. Each throw should be performed carefully because barbed sutures cannot be removed once inserted. Only a few authors have reported postoperative gastrointestinal complications, such as secondary bowel obstruction, or torsion of the small bowels with the barbed suture. Nevertheless, no complication associated with using the barbed suture for cruroplasty has been reported.

Conclusion

The laparoscopic approach is effective and safe for the management of symptomatic hiatal hernia, and cruroplasty with gastropexy using an intracorporeal running barbed suture is a feasible and time-efficient technique.

Declarations

Ethics approval and consent to participate.

Consent for publication

Written informed consent was obtained from the patient for publication of this case report and accompanying images. A copy of the written consent is available for review by the Editor-in-Chief of the journal.

Availability of data and materials

Data sharing not applicable to this article.

Competing interests

All authors declare they have no conflict of interest.

Funding

No funding was obtained for this manuscript.

Authors' contributions

XHC prepared the first draft. SMY and HJK provided the study material. SMY has cautiously reviewed and drafted the manuscript until its final version. All authors read and approved the final manuscript.

References

1. Chory ET. Laparoscopic surgical treatment of paraesophageal hiatus hernia. J Lancast Gen Hospital 2007; 2(2).
2. Landreneau RJ, Del Pino M, Santos R. Management of paraesophageal hernias. Surg Clin North Am 2005; 85(3): 411-32.
3. Wade A, Dugan A, Plymale MA, *et al*. Hiatal hernia cruroplasty with a running barbed suture compared to interrupted suture repair. Am Surg 2016; 82(9): 271-4.
4. Zehetner J, Demeester SR, Ayazi S, *et al*. Laparoscopic versus open repair of paraesophageal hernia: the second decade. J Am Coll Surg 2011; 212(5): 813-20.
5. Draaisma WA, Gooszen HG, Tournoij E, *et al*. Controversies in paraesophageal hernia repair: a review of literature. Surg Endosc 2005; 19(10): 1300-8.

6. Smith GS, Isaacson JR, Draganic BD, *et al*. Symptomatic and radiological follow-up after para-esophageal hernia repair. Dis Esophagus 2004; 17(4): 279-84.
7. Ponsky J, Rosen M, Fanning A, *et al*. Anterior gastropexy may reduce the recurrence rate after laparoscopic paraesophageal hernia repair. Surg Endosc 2003; 17(7): 1036-41.
8. Agwunobi AO, Bancewicz J, Attwood SE. Simple laparoscopic gastropexy as the initial treatment of paraoesophageal hiatal hernia. Br J Surg 1998; 85(5): 604-6.
9. Ferrer-Márquez M, Belda-Lozano R, Soriano-Maldonado A. Use of barbed sutures in bariatric surgery. Review of the literature. Obes Surg 2016; 26(8): 1964-9.
10. Tera H, Aberg C. Tensile strengths of twelve types of knot employed in surgery, using different suture materials. Acta Chir Scand 1976; 142(1): 1-7.
11. Ferrer-Márquez M, Belda-Lozano R. Barbed sutures in general and digestive surgery. Review. Cir Esp 2016; 94(2): 65-9.
12. Yang SM, Hsiao WL, Lin JH, *et al*. Laparoscopic percutaneous jejunostomy with intracorporeal V-Loc jejunopexy in esophageal cancer. Surg Endosc. 2017 Jun;31(6): 2678-2686.
13. Son SY, Cui LH, Shin HJ, *et al*. Modified overlap method using knotless barbed sutures (MOBS) for intracorporeal esophagojejunostomy after totally laparoscopic gastrectomy. Surg Endosc 2016.
14. Takahashi Y, Yokoyama N, Matsuzawa N, *et al*. Effectiveness of a barbed suture in the repair of bile duct injury during laparoscopic cholecystectomy: report of two cases. Int J Surg Case Rep 2016; 26: 183-6.

An Unusual Radiographic Pattern of Organizing Pneumonia: A Case Report

Shu-Hung Kuo[1,2], Chen-Tu Wu[3], Chao-Chi Ho[1]

Organizing pneumonia (OP) is classified as an interstitial lung disease characterized by intra-alveolar granulation tissue. Common clinical presentations of OP include shortness of breath, non-productive cough, fever, malaise, and other nonspecific symptoms, but some cases of OP can be totally asymptomatic. Typical radiographic findings of OP on chest radiographs and computed tomography (CT) scans are multifocal consolidations at the bilateral and peripheral lungs, which are sometimes migratory. Distinguishing OP from other differential diagnoses, such as malignancy or infection, is quite challenging.

We report the case of a 78-year-old man with productive cough for several months. His chest radiograph showed patchy consolidations with a central distribution in the bilateral hilar area. Chest CT demonstrated peribronchovascular consolidations in the bilateral central lungs with enlarged mediastinal lymph nodes. Based on the imaging findings, the first impression was lung cancer or lymphoma. The histopathologic diagnosis of OP was finally confirmed using surgical biopsy. The patient was treated as having cryptogenic OP because no obvious secondary cause was found. There was almost complete remission of the bilateral lesions after corticosteroid therapy. ***(Thorac Med 2022; 37: 248-255)***

Key words: Organizing pneumonia, bilateral patchy pulmonary consolidations, video-assisted thoracoscopic surgery

Introduction

Organizing pneumonia (OP) is classified as an interstitial lung disease, and is characterized by polypoid granulation tissue in the alveolar ducts and alveoli [1-3].

Approximately two-thirds of OP cases are "cryptogenic"(idiopathic form) [4-6]; the others are considered to be "secondary" to various etiologies, such as infections, aspiration, drug toxicities, malignancies, and connective tissue diseases [7]. Cryptogenic organizing pneumonia (COP), which was previously known as "bronchiolitis obliterans organizing pneumonia (BOOP)", was first described as a clinicopathological entity in the early 1980s [8]. However, previous studies have shown there are no significant differences between COP and secondary

[1]Division of Pulmonary and Critical Care Medicine, Department of Internal Medicine, National Taiwan, [2]University Hospital and College of Medicine, National Taiwan University, Taipei, Taiwan, [3]Department of Pathology, National Taiwan University Hospital and College of Medicine, National Taiwan University, Taipei, Taiwan.
Address reprint requests to: Dr. Chao-Chi Ho, Division of Pulmonary and Critical Care Medicine, Department of Internal Medicine National Taiwan University Hospital, No. 7, Chung-Shan South Road, Taipei 100, Taiwan

OP [6-7, 9].

Typical clinical presentations of OP include shortness of breath, non-productive cough, weight loss, fever, malaise, and other nonspecific symptoms, but some cases can be totally asymptomatic [6-7]. The diagnosis of OP depends on the characteristic clinical history, imaging findings, and histopathological examination, which is necessary for some ambiguous cases. Corticosteroids are the cornerstone of treatment for OP, while underlying conditions should be managed in case of secondary OP [6, 10].

Here, we describe a case of histopathologically confirmed OP, with an unusual radiographic pattern (bilateral consolidation with a central distribution in the bilateral hilar area and multiple enlarged mediastinal lymph nodes) that was initially considered a malignancy.

Case Presentation

A 78-year-old man with a past medical history of hypertension, chronic hepatitis B infection, and bilateral knee osteoarthritis presented at another hospital with cough and a small amount of whitish sputum for several months. He also complained of shortness of breath and unintentional weight loss (18 kg, or 22% in 6 months). There was no history of fever, chills, hemoptysis, leg swelling, or chest pain. He was a non-smoker and worked as a cementer. Chest radiography showed patchy consolidations with a central distribution in the bilateral hilar areas (Figure 1). The main radiographic manifestation on chest computed tomography (CT) was peribronchovascular consolidations in the bilateral central lungs with multiple enlarged mediastinal lymph nodes (Figure 2A, B, C, D).

Based on the clinical and imaging findings, the patient was referred to our pulmonology clinic and was admitted to our hospital 3 weeks later due to the differential diagnosis of lung cancer or lymphoma.

During admission, a radial-probe endobronchial ultrasound (EBUS)-guided transbronchial biopsy was performed for the peribronchial lesion in the left upper lobe (LUL), and EBUS-guided transbronchial needle aspiration (TBNA) was performed for the mediastinal lymph nodes (groups 4R and 7). However, the pathology reports of the transbronchial biopsy and EBUS-TBNA showed no evidence of malignancy. Later, the patient underwent video-assisted thoracoscopic surgery (VATS) for an LUL tumor biopsy and group 5/6 lymph node biopsy.

The microscopic examination revealed OP with multiple foci of fibroblast proliferation filling airspaces, accompanied by dense lymphoplasma cell infiltration (Figure. 3A) and

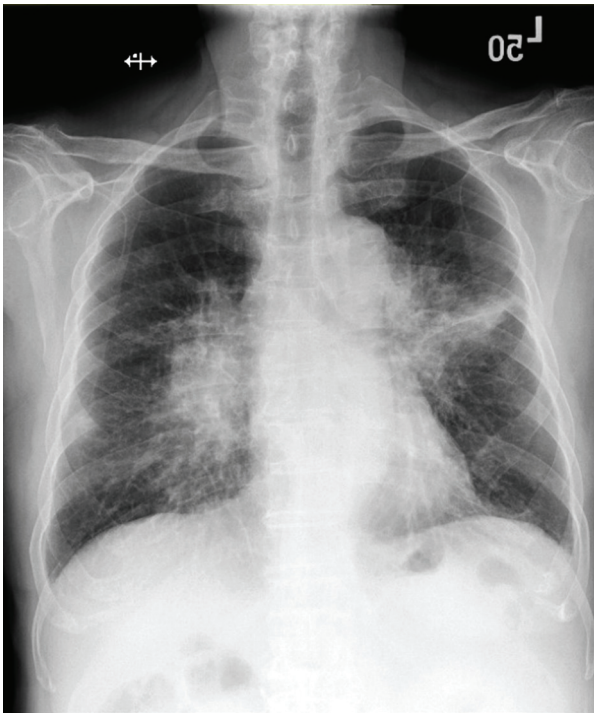

Fig. 1. The first chest radiograph in our hospital showed patchy consolidations with a central distribution in the bilateral hilar area.

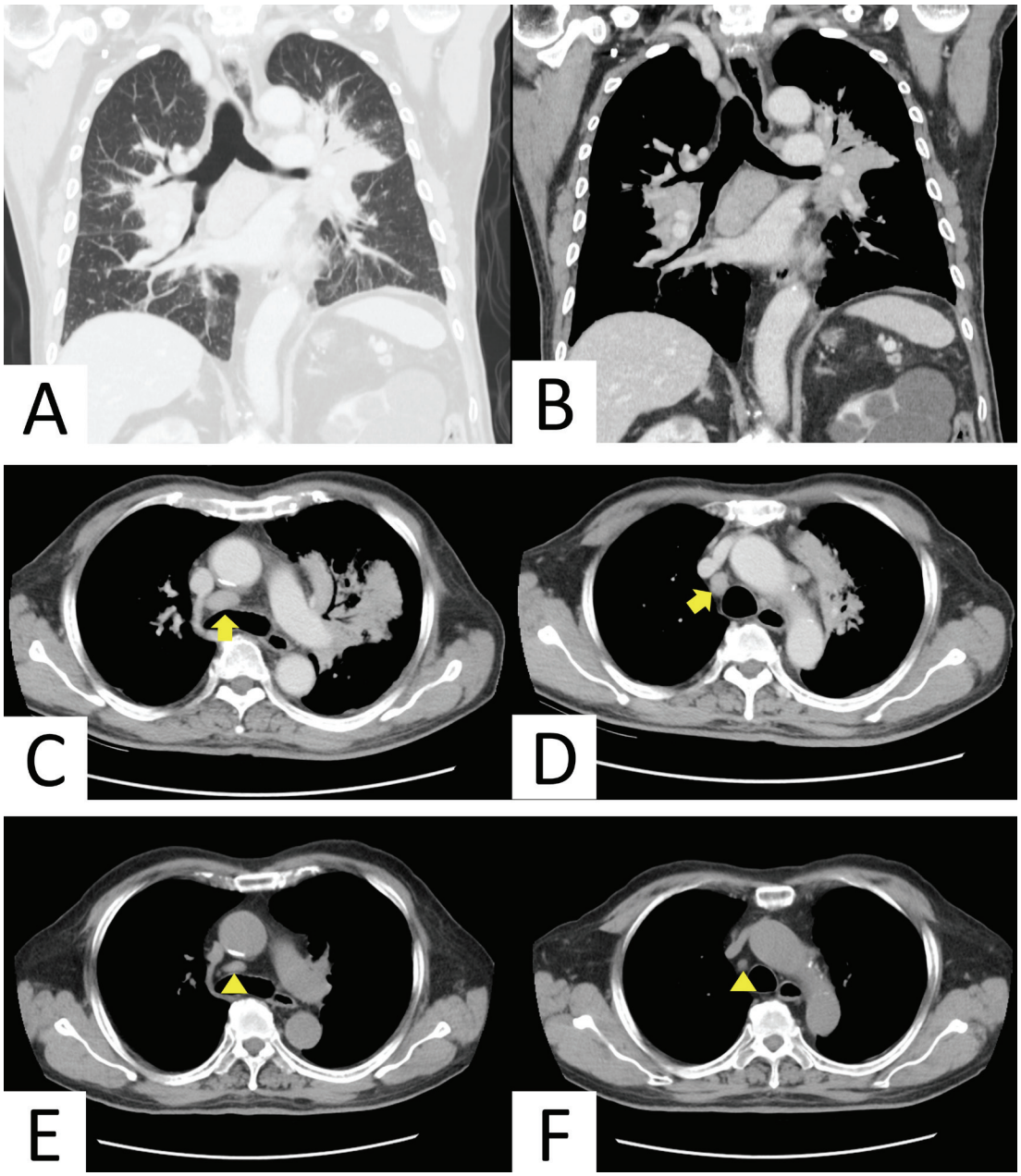

Fig. 2. (A)&(B) The initial chest CT demonstrated peribronchovascular consolidations of the bilateral central lungs. (C)&(D) The initial chest CT showed multiple enlarged mediastinal lymph nodes (arrows). (E)&(F) The 6-month follow-up CT revealed that the bilateral lung parenchymal lesions had resolved, and the mediastinal lymph nodes had become much smaller (arrow heads).

variable inflammation in fibroblast plugs (Figure 3B). IgG4-related disease was less likely based on the inadequate number of IgG4-positive plasma cells and the absence of storiform fibrosis. Special stains for infection demonstrated negative results.

To survey the secondary etiologies of OP, more laboratory tests were performed. The patient's hemogram, liver, and renal function tests were within normal limits. The level of C-reactive protein was low (0.44 mg/dL). Autoimmune profiles revealed an antinuclear antibody

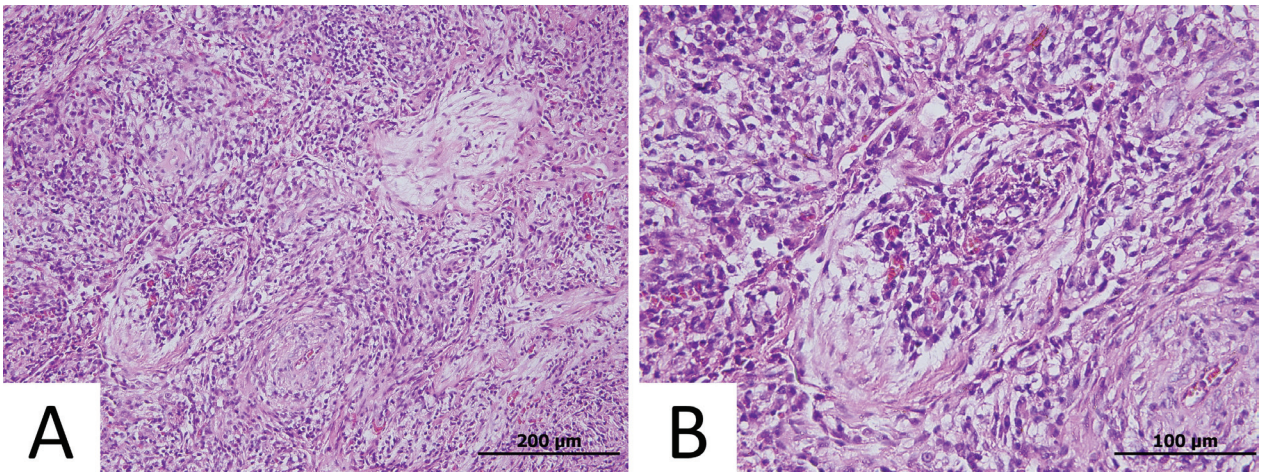

Fig. 3. (A) Hematoxylin and eosin (H&E) stain of left upper lobe lung tissue from the surgical biopsy: A few lightly stained fibroblast plugs filling airspaces and chronic inflammatory cell infiltration. (B) H&E stain of left upper lobe lung tissue from the surgical biopsy: Variable inflammation in fibroblast plugs.

(ANA) 1:80 positive, with a homogeneous nuclear pattern; however, other markers were unremarkable. Cultures obtained from biopsy tissue and bronchial washing yielded no growth of microorganisms.

Corticosteroid therapy with intravenous methylprednisolone (60 mg/day) was then administered. The patient's serial follow-up chest radiographs demonstrated rapid improvement, and then resolution of the bilateral consolidations (Figure 4A, B, C) within 3 weeks thereafter. Afterwards, the dosage of corticosteroid was tapered gradually, and was switched to oral prednisolone (30 mg/day) 11 days after treatment initiation. The dose of oral prednisolone was titrated during the months following the patient's discharge from the hospital. The 6-month follow-up CT revealed that the bilateral lung parenchymal lesions had resolved, and the mediastinal lymph nodes had regressed in size. While the patient was maintained on a very low dose of prednisolone (5 mg/day), his chest radiograph findings remained stable at the one-year follow-up (Figure 4D).

Discussion

OP is a rare lung disorder. A nationwide retrospective study in Iceland for suspected or proven OP during the period 1984–2003 revealed that the mean incidence rate of OP was 1.97/100,000 people per year, and the mean age at diagnosis was 67 (15-87) years [5]. Another regional study from Minnesota, in the the United States of America, showed an age- and sex-adjusted incidence rate of 0.85/100,000 people per year [11]. There is currently no available data on the incidence rate of OP (cryptogenic or secondary) in Taiwan, but, we know the incidence rate of idiopathic pulmonary fibrosis (IPF) in Taiwan was 0.9-1.6/100,000 people per year [12]. Meanwhile, several registries of interstitial lung diseases indicated that the incidence rate of IPF was approximately 3.6~7.6 times more than that of COP [13]. Thus, we indirectly estimate that the incidence rate of COP in Taiwan could be less than 0.5/100,000 people per year.

The mean age at onset of OP is 50-60 years, with no significant sex predominance [5, 6, 8].

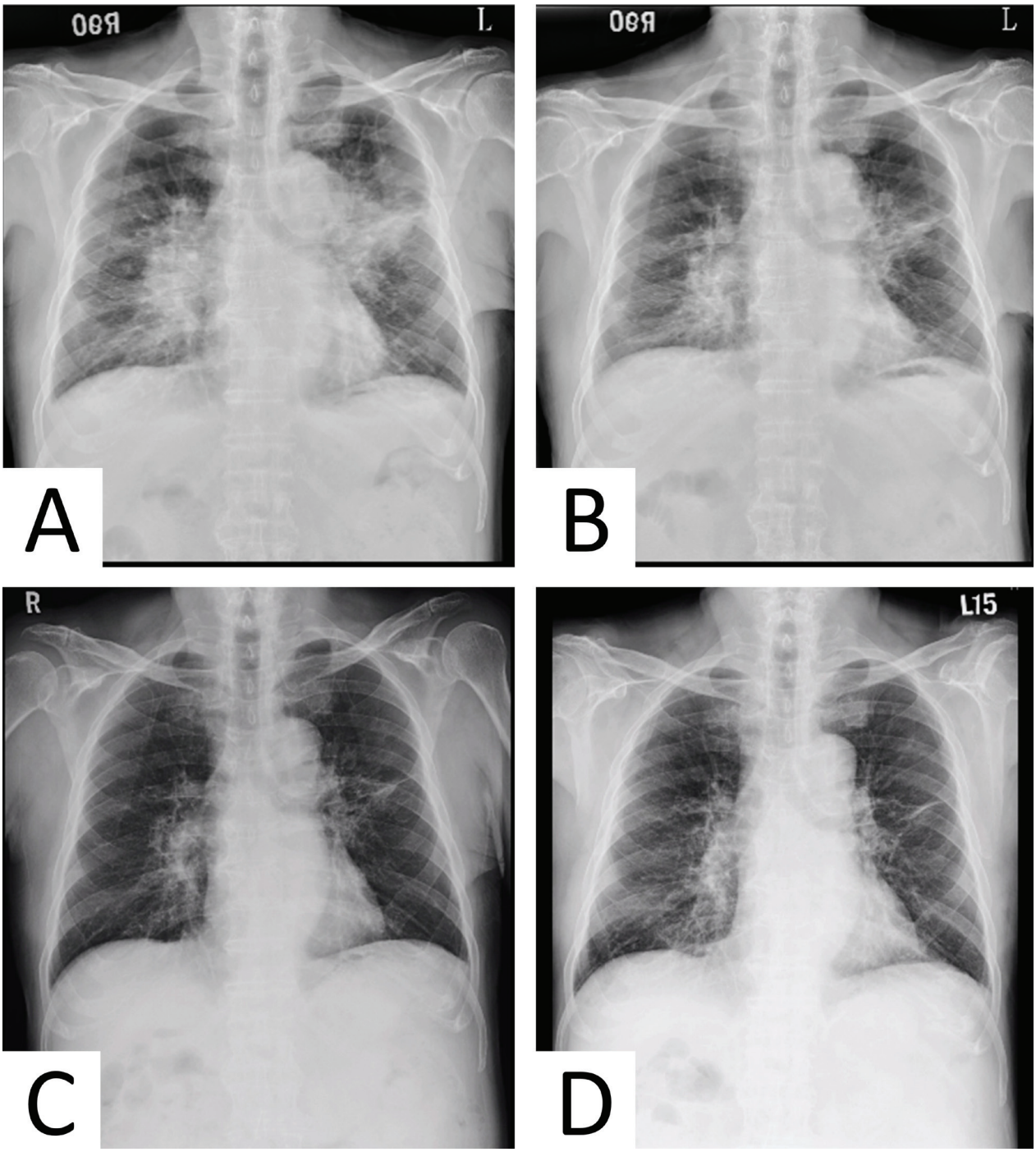

Fig. 4. Serial chest radiographs of this 78-year-old man showed a rapid response to corticosteroid therapy, with long-lasting effects. (A) On day 1, a chest radiograph just prior to the corticosteroid therapy showed patchy consolidations with a central distribution in the bilateral hilar area. (B) After completion of a 7-day course of intravenous methylprednisolone (60 mg/day), the chest radiograph showed rapid improvement. (C) Three weeks after initiation of corticosteroid therapy, the chest radiograph revealed near complete resolution of bilateral central pulmonary consolidations. (D) The one-year follow-up chest radiograph showed stable results with low-dose oral prednisolone (5 mg/day) treatment.

According to recent data from the population-based national cancer registration system in Taiwan, the age-standardized incidence rate for males during the period 2013–2016 was 44.23/100,000 people per year for lung cancer (mean age: 68 years) and 8.47/100,000 people per year for non-Hodgkin lymphoma (mean age: 62 years), respectively.[14] Thus, the first tentative diagnosis of pulmonary malignancy, which was based on chronic cough, weight loss, and an unusual radiographic pattern, including consolidations with a central distribution and enlarged mediastinal lymph nodes, was quite reasonable for this elderly male patient.

For patients with OP, the classic findings on chest radiographs are multifocal consolidations in the bilateral and peripheral lungs; migration or spontaneous regression of the consolidations within weeks are seldom noted [6-7]. On CT scan, bilateral patchy consolidations with a predominant subpleural or peribronchial distribution in the middle and lower lung and ground-glass opacities (GGO), and randomly distributed small nodular opacities, are the most common radiographic features of OP [15-17]. Ground-glass attenuation and nodules, which are usually with a random distribution pattern, are commonly seen in imaging [15-17]. Reticulation, bronchiectasis, and interlobular septal thickening are less common findings [16-17]. In our case, chest radiographs showed bilateral patchy consolidations with a central distribution, mainly affecting the middle zone of the lungs. Chest CT revealed peribronchovascular consolidations of the bilateral central lungs. Only minimal GGO were noted around the consolidations. These lesions persisted for at least 3 weeks without obvious regression or migration before diagnosis and treatment.

Enlarged mediastinal lymph nodes were also found on the CT scans of this patient (Figure 2C, D); thus, the differential diagnosis mainly included lung cancer, lymphoma, sarcoidosis, and pulmonary tuberculosis. However, the sample obtained by TBNA showed no evidence of malignant cells or infection. In addition to the parenchymal lesions, the mediastinal lymph nodes also showed a good response to corticosteroid therapy thereafter (Figure 2E, F). Previous studies reported that mildly enlarged mediastinal lymph nodes (1.0-1.5 cm in size) associated with parenchymal infiltration were a common finding on chest CT in patients with cryptogenic OP [18-19].

Histopathological examination is critical for OP patients with unusual clinical or radiographic presentations. To obtain adequate samples and volumes of lung tissue for histopathologic diagnosis, surgical lung biopsy using VATS is preferred over conventional transbronchial biopsy [10]. In recent years, transbronchial lung cryobiopsy, a new technique, has become an alternative in selected patients with interstitial lung disease [20-21]. In our case, the radial-probe EBUS-guided transbronchial biopsy yielded inconclusive findings, which might be due to the small sample size.

The complete review and examinations showed no obvious cause of secondary OP, so this case was regarded as COP and was treated with corticosteroid therapy alone. The patient showed clinical and radiographic improvements within weeks and was discharged with oral prednisolone therapy.

The majority of patients with OP have a good and rapid response to corticosteroid therapy, although relapse or recurrence is also common, especially while tapering the dose of corticosteroid or after cessation of corticosteroid therapy [6, 10, 22]. Nevertheless, the

prognosis of patients with clinical relapses or recurrences seems to be the same as for those without relapse or recurrence [10, 22]. The ideal duration of corticosteroid therapy has not been established, but one year is often suggested [10, 22]. Several previous studies have tried to identify the potential predictive factors for relapse of COP, such as an elevated serum KL-6 level [23], a high neutrophil percentage in the bronchoalveolar lavage (BAL) fluid and the amount of fibrin deposition in lung biopsy specimens [24], and a particular CT scan pattern (bilateral shadow pattern, traction bronchiectasis) [25]. However, further studies with more cases are needed to confirm these findings. In addition, if the patient with OP had poor responses to systemic corticosteroid therapy, some immunosuppressive and anti-inflammatory agents, such as macrolides, cyclophosphamide, and cyclosporine, seem to be effective when used as adjuvant therapy [26].

A large retrospective study of biopsy-proven OP in a single center in China revealed that about 15% of OP cases that were initially identified as COP were subsequently found to be secondary OP during the follow-up; thus, long-term follow-up is essential to exclude secondary etiologies [27]. To date, this case has been followed for approximately 1 year after confirming the diagnosis of OP, and the serial chest images showed a sustained response even when the dose of oral prednisolone was tapered to 5 mg/day.

As OP usually presents with non-specific symptoms, it could be difficult to distinguish OP from other diagnoses such as neoplasm, fungal infection, or pulmonary tuberculosis [2], particularly when the radiographic features are not typical. Clinicians should be alert if the diagnosis cannot be made straightforwardly, and surgical biopsy may be indicated to determine the final diagnosis.

References

1. Cordier JF. Organising pneumonia. Thorax 2000; 55(4): 318-28.
2. Baque-Juston M, *et al*. Organizing pneumonia: what is it? A conceptual approach and pictorial review. Diagn Interv Imaging 2014; 95(9): 771-7.
3. Drakopanagiotakis F, Polychronopoulos V, Judson MA. Organizing pneumonia. Am J Med Sci 2008; 335(1): 34-9.
4. Cazzato S, *et al*. Bronchiolitis obliterans-organizing pneumonia: an Italian experience. Respir Med 2000; 94(7): 702-8.
5. Gudmundsson G, *et al*. Epidemiology of organising pneumonia in Iceland. Thorax 2006; 61(9): 805-8.
6. Drakopanagiotakis F, *et al*. Cryptogenic and secondary organizing pneumonia: clinical presentation, radiographic findings, treatment response, and prognosis. Chest 2011; 139(4): 893-900.
7. Roberton BJ, Hansell DM. Organizing pneumonia: a kaleidoscope of concepts and morphologies. Eur Radiol 2011; 21(11): 2244-54.
8. Epler GR, *et al*. Bronchiolitis obliterans organizing pneumonia. N Engl J Med 1985; 312(3): 152-8.
9. Basarakodu KR, *et al*. Differences in treatment and in outcomes between idiopathic and secondary forms of organizing pneumonia. Am J Ther 2007; 14(5): 422-6.
10. Bradley B, *et al*. Interstitial lung disease guideline: the British Thoracic Society in collaboration with the Thoracic Society of Australia and New Zealand and the Irish Thoracic Society. Thorax 2008; 63 Suppl 5: v1-58.
11. Lohr RH, *et al*. Organizing pneumonia. Features and prognosis of cryptogenic, secondary, and focal variants. Arch Intern Med 1997; 157(12): 1323-9.
12. Lai CC, *et al*. Idiopathic pulmonary fibrosis in Taiwan - a population-based study. Respir Med 2012; 106(11): 1566-74.
13. Kreuter M, *et al*. Exploring clinical and epidemiological characteristics of interstitial lung diseases: rationale, aims, and design of a nationwide prospective registry--the EXCITING-ILD Registry. Biomed Res Int 2015; 2015: 123876.

14. Huang YC, Chen YH. Cancer incidence characteristic evolution based on the National Cancer Registry in Taiwan. J Oncol 2020; 2020:1408793.
15. Lee KS, *et al*. Cryptogenic organizing pneumonia: CT findings in 43 patients. AJR Am J Roentgenol 1994; 162(3): 543-6.
16. Faria IM, *et al*. Organizing pneumonia: chest HRCT findings. J Bras Pneumol 2015; 41(3): 231-7.
17. Cho YH, *et al*. Chest CT imaging features for prediction of treatment response in cryptogenic and connective tissue disease-related organizing pneumonia. Eur Radiol 2020; 30(5): 2722-2730.
18. Greenberg-Wolff I, *et al*. Cryptogenic organizing pneumonia: variety of radiologic findings. Isr Med Assoc J 2005; 7(9): 568-70.
19. Niimi H, *et al*. CT of chronic infiltrative lung disease: prevalence of mediastinal lymphadenopathy. J Comput Assist Tomogr 1996; 20(2): 305-8.
20. Raghu G, Lederer DJ, Rabe KF. Cryobiopsy for Interstitial Lung Disease: The Heat Is On. Am J Respir Crit Care Med 2019; 199(10): 1183-1184.
21. Ravaglia C, *et al*. Diagnostic yield and risk/benefit analysis of trans-bronchial lung cryobiopsy in diffuse parenchymal lung diseases: a large cohort of 699 patients. BMC Pulm Med 2019; 19(1): 16.
22. Cordier JF. Cryptogenic organising pneumonia. Eur Respir J 2006; 28(2): 422-46.
23. Okada F, *et al*. Comparison of pulmonary CT findings and serum KL-6 levels in patients with cryptogenic organizing pneumonia. Br J Radiol 2009; 82(975): 212-8.
24. Onishi Y, *et al*. Factors associated with the relapse of cryptogenic and secondary organizing pneumonia. Respir Investig 2017; 55(1): 10-15.
25. Saito Z, *et al*. Predictive factors for relapse of cryptogenic organizing pneumonia. BMC Pulm Med 2019; 19(1): 10.
26. Radzikowska E, *et al*. Cryptogenic organizing pneumonia-Results of treatment with clarithromycin versus corticosteroids-observational study. PLoS One 2017; 12(9): e0184739.
27. Zhang Y, *et al*. Analysis of the clinical characteristics of 176 patients with pathologically confirmed cryptogenic organizing pneumonia. Ann Transl Med 2020: 8(12): 763.